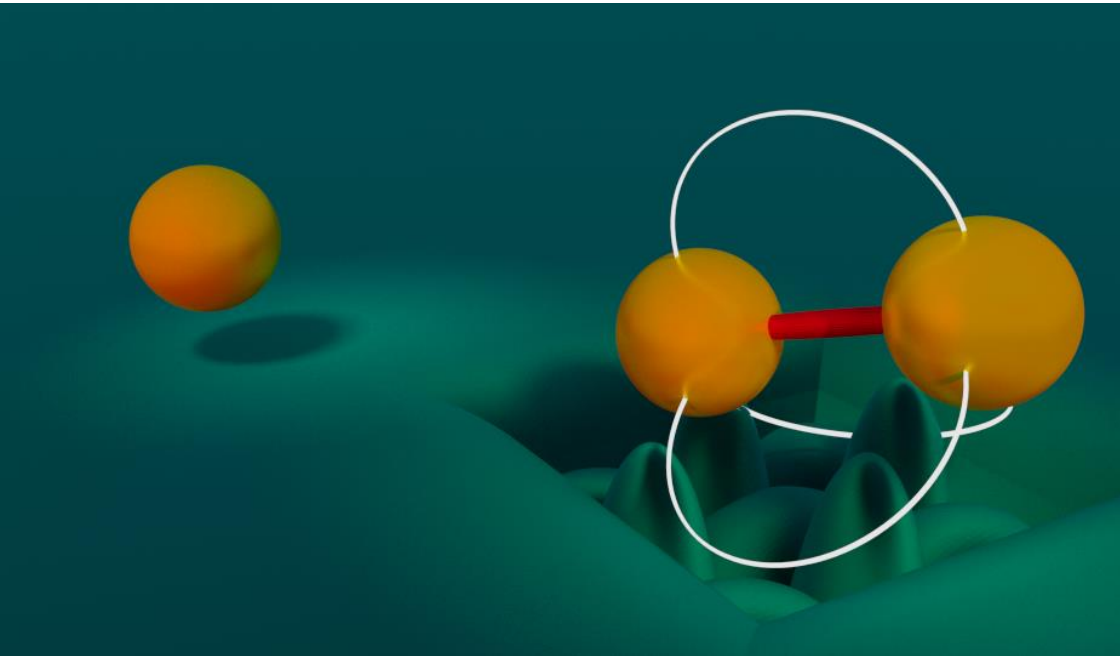


# WCEEN 2016

June 20-22

Conferencia Española de Nanofotónica  
Spanish Nanophotonics Conference



Organisers



Centro de Tecnología Nanofotónica de Valencia



UNIVERSITAT  
POLITÈCNICA  
DE VALÈNCIA



UNIVERSITAT  
DE VALÈNCIA



UNIVERSITAT DE  
BARCELONA



CSIC

CONSEJO SUPERIOR DE INVESTIGACIONES CIENTÍFICAS



Institut  
de Ciències  
Fotòniques



UNIVERSITAT  
ROVIRA I VIRGILI



Universidad  
del País Vasco



Euskal Herriko  
Unibertsitatea



UNIVERSIDAD  
DE CANTABRIA



# Index

Foreword	<u>Page 5</u>
Organisers/ Sponsors/ Exhibitors	<u>Page 6</u>
Committees	<u>Page 7</u>
Index (Contributions)	<u>Page 8</u>
Abstracts	<u>Page 13</u>



---

## Foreword

---

Following the spirit initiated by the first four editions of the "Conferencia Española de Nanofotónica", held respectively in Tarragona in 2008, Segovia in 2010, Carmona-Sevilla 2012 and Santander 2014, we launch the 5th edition that will be conducted in Valencia (Spain) during June 20-22, 2016. The Conference aims to gather all the groups carrying out research in Nanophotonics in Spain (as well as somewhere else with interest in the research in Nanophotonics performed here). It intends to spread the research results achieved by all the different Spanish groups and to promote the establishment or reinforcement of contacts between them, as a mean to help the community to become more visible and dynamic.

The Conference technical program aspires to address a wide area of research related to nanophotonics, metamaterials and subwavelength optics. Topics will include all aspects of the research, ranging from fundamental science to nanofabrication or applications.

The Conference will be organized in thematic sessions composed of Keynotes / invited talks and contributed scientific communications (oral and poster).

The meeting will be structured in the following thematic lines, but interactions among them will be promoted:

1. Magnetoplasmonics and Optomechanical systems
2. Novel synthetic routes: materials aspects of photonic nanostructures
3. Colloidal nanophotonics and nanoplasmonics
4. Photonic nanostructures for energy efficient optoelectronic devices
5. Graphene and silicon photonics
6. New concepts and metamaterials
7. Near Field Optics: nanospectroscopy and nanoimaging
8. Nanophotonics for sensing

We are indebted to the following Scientific Institutions for their financial support: Universidad Politécnica de Valencia and Centro de Tecnología Nanofotónica de Valencia.

We would also like to thank the following companies for their participation: LOT Quantum Design, Nanoscribe and VLC Photonics.

Finally, thanks must be directed to the staff of all organising institutions whose hard work has helped the smooth organisation and planning of this conference.

THE ORGANISING COMMITTEE

## Organisers



## Sponsors



## Exhibitors



[www.nanoscribe.de](http://www.nanoscribe.de)

**Nanoscribe** provides maskless lithography and additive manufacturing on the nano- and micrometer scale in one device. The underlying technique of these outstanding 3D printers, Photonic Professional GT, is based on direct laser writing into photoresists: Empowered by their unprecedented 3D nano-/micro-fabrication capabilities, the two-photon polymerization driven systems set new standards in a multitude of applications, e.g. photonics, micro-optics, and metamaterials. Furthermore, Nanoscribe, market and technology leader in the field of 3D laser lithography, serves solutions as well as processes for specific applications to its scientific and industrial customers.



[www.lot-qd.com](http://www.lot-qd.com)

**LOT-QuantumDesign** group is a leading European distributor of high-quality scientific instruments and components supplying academic and industrial scientific research customers. The group offers components and systems used in material sciences, imaging, spectroscopy, photonics, nanotechnology and life science research. The group was founded almost 45 years ago and now employs more than highly-qualified 140 staff across Europe. The headquarters are in Darmstadt, Germany, further offices are located in Paris, London, Rome und Lausanne. Together with the parent company Quantum Design International Inc. and sister companies in North America, Asia and South America LOT-QuantumDesign offers the only global distribution network for high-tech instruments.



[www.vlcp Photonics.com](http://www.vlcp Photonics.com)

**VLC Photonics** is a company providing all kind of services related to photonic integration: from initial engineering studies, to optical chip design support, outsourced chip fabrication and packaging, and in-house testing. VLC has worked for more than 12 years in this field, with an extensive network of +20 foundry partners for the main technology platforms (silicon photonics, silica/PLC, silicon nitride or InP/GaAs), and can support any optical integration project with its stand alone services or turn-key solutions.

## Committees

### Chair

**Alejandro Martínez** (NTC-UPV)  
**Pablo Sanchís** (NTC-UPV)

### Organizing Committee

**Antonio Correia** (Fundación Phantoms)  
**Javier Aizpurua** (EHU)  
**Alvaro Blanco** (ICMM-CSIC)  
**Antonio García Martín** (IMM-CSIC)  
**Lluís Marsal** (URV)  
**Sol Carretero** (ICMS-CSIC)  
**Juan José Sáenz** (DIPC)  
**Blas Garrido** (UB)  
**Isabel Pastoriza-Santos** (UV)  
**María García-Parajo** (ICFO)  
**Fernando Moreno** (UC)

### Technical Committee

**José Luis Roldan** (Fundación Phantoms)  
**Saturnino Castillo Oñate** (NTC-UPV)

### Scientific Committee

**Ramón Alcubilla** (UPC)  
**Pablo Aitor Postigo** (IMM-CSIC)  
**Gonçal Badenes** (ICFO)  
**Salvador Balle** (UIB)  
**José M. Calleja** (UAM)  
**Enrique Calleja** (UPM)  
**Francesc Díaz** (URV)  
**Concepción Domingo** (IEM-CSIC)  
**Francisco J. García-Vidal** (UAM)  
**Cefe López** (ICMM-CSIC)  
**Javier Marti** (CTN-UPV)  
**Juan Martínez-Pastor** (ICMUV)  
**Jordi Martorell** (ICFO)  
**Francisco Meseguer** (UPV-CSIC)  
**Hernán Míguez** (ICMS-CSIC)  
**Josep Pallarés** (URV)  
**Jose Sánchez-Dehesa** (UPV)  
**José A. Sánchez Gil** (IEM-CSIC)  
**Rosalía Serna** (IO-CSIC)  
**Jan Siegel** (IO-CSIC)  
**Clivia Sotomayor** (ICN-CIN2)  
**María Ujué** (IMM-CSIC)  
**Luis Viña** (UAM)

# Contributions



# Index alphabetical order

K: Keynote Speakers  
I: Invited Speakers  
O: Oral Presentation  
P: Poster Presentation

	<b>Page</b>
<b>Ricardo Martin Abraham Ekeroth</b> (Instituto de Microelectrónica de Madrid, Spain) Optical forces exerted on nanowire dimers: New characterization of Plasmons	O <b>13</b>
<b>Laura Karen Acosta Capilla</b> (Universitat Rovira i Virgili, Spain) Rugate filters in nanoporous anodic alumina for photonic applications: fabrication, design and analysis	P <b>14</b>
<b>Pablo Alonso</b> (CIC nanoGUNE, Spain) Ultra-confined acoustic THz graphene plasmons	I <b>15</b>
<b>Estela Baquedano Peralvarez</b> (Instituto de Microelectrónica de Madrid, Spain) Fabrication of low-cost and high aspect ratio nanowires and 2D nanostructures by soft lithography for nanophotonic devices	O/P <b>16</b>
<b>Ángela I. Barreda Gómez</b> (Universidad de Cantabria, Spain) Using linear polarization for sensing with core-shell nanostructures	O/P <b>17</b>
<b>Francesc Bertó Roselló</b> (Universitat Rovira i Virgili, Spain) Nanoporous anodic alumina 3d-fddd modelling optical behaviour for long interpore distance	P <b>18</b>
<b>Mauro Brotóns i Gisbert</b> (ICMUV, Universidad de Valencia, Spain) Morphological manipulation of the luminescent response of atomically thin Indium Selenide nanosheets	O/P <b>19</b>
<b>Blanca Caballero</b> (Instituto de Microelectrónica de Madrid, Spain) Boosting Sensing Performance Using Hybrid Magnetoplasmonic Nanohole Arrays	O <b>20</b>
<b>Raffaele Caroselli</b> (Nanophotonics Technology Center (NTC - UPV), Spain) Biosensors based on nanoporous silicon multilayer structures	O/P <b>21</b>
<b>Pau Castera</b> (Nanophotonics Technology Center (NTC - UPV), Spain) Optimization of a hybrid BaTiO <sub>3</sub> /Si Waveguide Structure for Electro-optic Modulation	O/P <b>22</b>
<b>Rafael Cichelero</b> (Institut de Ciència de Materials de Barcelona ICMAB-CSIC, Spain) Dual plasmon excitation imaged by leakage radiation microscopy	P <b>23</b>
<b>Antonio Consoli</b> (Instituto de Ciencia de Materiales de Madrid - CSIC, Spain) Emission regimes of random lasers with spatially localized feedback	O <b>24</b>
<b>Federic Cortés Juan</b> (Nanophotonics Technology Center (NTC - UPV), Spain) Ferroelectric-semiconductor heterostructures for photovoltaic applications	P <b>25</b>
<b>Juan Carlos Cuevas</b> (UAM, Spain) Near-field radiative heat transfer at the nanoscale	K <b>26</b>
<b>David Domenech Gomez</b> (VLC Photonics, Spain) Open access to low cost photonic integrated circuits prototyping in a generic Silicon Nitride foundry	P <b>27</b>
<b>Chris Eckstein</b> (Universitat Rovira i Virgili, Spain) Fluid Imbibition-Coupled Laser Interferometry: a highly sensitive optical technique for nanometrology	O/P <b>28</b>
<b>Felix Eltes</b> (IBM Research – Zurich, Switzerland) Low-loss, Nonlinear BaTiO <sub>3</sub> -Si-Photonic Waveguide Structures	O <b>29</b>
<b>Alba Espinosa-Soria</b> (Nanophotonics Technology Center (NTC - UPV), Spain) Experimental and numerical demonstration of a plasmonic nanoantenna embedded in a silicon waveguide gap	O/P <b>30</b>

	<b>Page</b>
<b>Alba Espinosa-Soria</b> (Nanophotonics Technology Center (NTC - UPV), Spain) Beam polarimetry using silicon nanoantennas	P <b>31</b>
<b>Victoria Esteso</b> (Instituto de Ciencia de Materiales de Sevilla (ICMS) - Universidad de Sevilla, Spain) Theoretical prediction of levitation due to Casimir force of plane-parallel systems made of realistic materials	O/P <b>32</b>
<b>Roberto Fenollosa</b> (CSIC, Spain) The influence of the internal structure in the resonant properties of poly-crystalline silicon microspheres	O <b>33</b>
<b>Anna Fontcuberta i Morral</b> (EPFL, Switzerland) Photonics and applications with semiconductor nanowires	K <b>34</b>
<b>Zeev Fradkin</b> (Sami Shamoan college of Engineering, Israel) An RCE based NIR PD using a resonant cavity with dual grating mirrors	O <b>35</b>
<b>Francisco Gallego-Gómez</b> (Instituto de Ciencia de Materiales de Madrid - CSIC, Spain) Photonic colloidal crystals as nano-sand: lab-on-a-chip to study water in granular media	O <b>36</b>
<b>Sonia García-Blanco</b> (University of Twente, The Netherlands) High-index contrast waveguides in potassium double tungstates: towards rare-earth ion doped on-chip integrated photonics	I <b>37</b>
<b>David García Rodríguez</b> (Universitat Politècnica de Valencia, Spain) Silicon Photonic Integrated Mode Converter and Multiplexer for Few-Mode Fiber at 1550 nm	P <b>38</b>
<b>John Jaiber González-Murillo</b> (Universitat de Barcelona, Spain) Optical response of PMMA+Au <sub>2</sub> nanostructured metasurface composite over Silicon substrate	P <b>40</b>
<b>Yael Gutiérrez Vela</b> (Universidad de Cantabria, Spain) Rhodium Nanocubes for plasmonics in the UV range	O/P <b>41</b>
<b>Beatriz Hernández Juárez</b> (IMDEA Nanociencia / UAM, Spain) Synthesis and optical trapping of colloidal quantum dot-based structures	I <b>42</b>
<b>Alberto Jiménez-Solano</b> (ICMSE-CSIC, Spain) Nanosources shine on demand thanks to a deterministic control of the local density of states	O/P <b>43</b>
<b>Juerg Leuthold</b> (ETH Zürich, Switzerland) The Ultimate Limit of Photonic Scaling	K <b>44</b>
<b>José Manuel Llorens</b> (Instituto de Microelectrónica de Madrid, Spain) Amplifying the zero-th order mode absorption in the ultra-thin film regime	O <b>46</b>
<b>Jorge Luis Hita</b> (Universidad Autónoma de Madrid, Spain) Arrested dimer's diffusion by self-induced back-action optical forces	O/P <b>47</b>
<b>Nicolò Maccaferri</b> (CIC nanoGUNE, Spain) Enhanced and tunable magneto-optical activity in magnetoplasmonic crystals	O/P <b>48</b>
<b>Manuel Marqués</b> (Universidad Autónoma de Madrid, Spain) Dynamics of electric dipoles in fluctuating random electromagnetic fields	O <b>49</b>
<b>Luis Martín-Moreno</b> (Instituto de Ciencia de Materiales de Aragón, Spain) Quantum nanophotonics in waveguides	K <b>50</b>
<b>Ángel Mateos Sánchez</b> (Instituto de Ciencia de Materiales de Madrid - CSIC, Spain) Coupled random laser resonators in DNA thin films: fabrication and characterization	O/P <b>51</b>
<b>Alberto Maulu</b> (ICMUV, Instituto de Ciencia de los Materiales, Univ. de Valencia, Spain) Solution-Processed QD Solid by Doctor Blading Based on PbS QD Nanoinks for the Fabrication of Photodetectors at Telecom Wavelengths	O/P <b>52</b>
<b>Agustín Mihi</b> (ICMAB-CSIC, Spain) Low Cost and Large Area Photonic Architectures for Enhanced Light Management in Optoelectronic Devices	I <b>53</b>
<b>José María Miranda Muñoz</b> (Instituto de Ciencia de Materiales de Sevilla, Spain) Tailoring disorder for absorption enhancement in bifacial dye-sensitized solar cells	O/P <b>54</b>

		<b>Page</b>
<b>Verónica Montes-García</b> (University of Vigo, Spain)		
Supramolecular mediated self-assembly of gold nanoparticles for selective SERS detection	O/P	<b>55</b>
<b>Daniel Navarro Urríos</b> (ICN2, Spain)		
Self-sustained coherent phonon generation in optomechanical crystals	I	<b>56</b>
<b>Camiel Op de Beeck</b> (Nanophotonics Technology Center (NTC - UPV), Spain)		
Integration of indium tin oxide on silicon for enabling electro-optical functionalities	P	<b>57</b>
<b>Jose Ángel Pariente</b> (Instituto de Ciencia de Materiales de Madrid - CSIC, Spain)		
Fano resonance reveals Percolation in photonic crystals	O/P	<b>58</b>
<b>Pablo Aitor Postigo</b> (Instituto de Microelectrónica de Madrid (IMM-CNM-CSIC), Spain)		
Near thresholdless laser operation at room temperature	O	<b>59</b>
<b>Pablo Aitor Postigo</b> (Instituto de Microelectrónica de Madrid (IMM-CNM-CSIC), Spain)		
Optical coupling of double L7 photonic crystal microcavities for applications in quantum photonics	P	<b>60</b>
<b>Pablo Aitor Postigo</b> (Instituto de Microelectrónica de Madrid (IMM-CNM-CSIC), Spain)		
Finite-difference time-domain optimization of organic thin-film solar cells using photonic crystal gratings	P	<b>61</b>
<b>Pablo Aitor Postigo</b> (Instituto de Microelectrónica de Madrid (IMM-CNM-CSIC), Spain)		
Enlargement of free spectral range by selective suppression of optical cavity modes	P	<b>62</b>
<b>Francisco Prats</b> (Nanophotonics Technology Center, Spain)		
Ultra-Fast Spectral Optical Analysis of Nanophotonic Structures	O/P	<b>63</b>
<b>Romain Quidant</b> (ICFO-ICREA, Spain)		
Heterogeneous nanoplasmonics for quantum optics and biosensing	K	<b>64</b>
<b>Andrés Raya Bejarano</b> (Instituto de Microelectrónica de Madrid, Spain)		
Towards a high degree of uniformity in the diameter and length of self-catalyzed GaAs nanowires on silicon by adjusting the growth temperature	P	<b>65</b>
<b>Isabelle Rodríguez</b> (Instituto de Tecnología Química and Centro de Tecnologías Físicas-CSIC/UPV, Spain)		
Kamikase silicon colloids as cancer cells killers	P	<b>66</b>
<b>Sofía Rodríguez</b> (Nanoscribe GmbH, Germany)		
3D Printing Sets New Standards in Microfabrication	O	<b>67</b>
<b>Francisco Rodríguez Fortuño</b> (King's College London, UK)		
Spin-orbit interactions of light in evanescent waves: from theory to experiments	I	<b>69</b>
<b>Ángela Ruiz Tórtola</b> (Universitat Politècnica de València, Nanophotonics Technology Center, Spain)		
Design and characterization of plasmonic nanostructures on silicon waveguides for sensing	P	<b>70</b>
<b>Ángela Ruiz Tórtola</b> (Universitat Politècnica de València, Nanophotonics Technology Center, Spain)		
Biosensing using photonic bandgap structures on silicon waveguides	P	<b>71</b>
<b>José Guadalupe Sánchez López</b> (Universitat Rovira i Virgili, Spain)		
Inverted BHJ solar cells based on PTB7:PC <sub>70</sub> BM using TiO <sub>x</sub> as electron transport layer	O/P	<b>72</b>
<b>Nuno Miguel Santos Teixeira de Sousa</b> (Universidad Autónoma de Madrid, Spain)		
Light Emission Statistics as a Local Probe for Structural Phase Switching	O	<b>73</b>
<b>Nuno Miguel Santos Teixeira de Sousa</b> (Universidad Autónoma de Madrid, Spain)		
Magneto-optical activity in high-index dielectric materials	P	<b>74</b>
<b>Aina Serrano</b> (Universitat Politècnica de València, Nanophotonics Technology Center, Spain)		
Photonic sensors based on molecular gates and plasmonic structures	P	<b>75</b>
<b>Mattia Signoretto</b> (ICMUV, University of Valencia, Spain)		
Integration of metal nanoparticles in polymer waveguides: enhancement and redirection of light in photonic structures	O/P	<b>76</b>
<b>Magdalena Solà García</b> (Universitat Politècnica de Catalunya, Spain)		
Periodic arrangements of Si quasi-spheres	P	<b>77</b>

	<b>Page</b>
<b>Mattin Urbieto</b> (FCT/ZTF, UPV/EHU; CFM-MPC, CSIC-UPV/EHU; DIPC, Spain) Optical spectroscopy of metallic nanoparticles: classical versus quantum description	P <b>78</b>
<b>Niek Van Hulst</b> (ICFO-ICREA, Spain) Femtosecond dynamics at the nanoscale: talking to antenna complexes one-by-one	K <b>79</b>
<b>Steven Van Roye</b> (Nanophotonics Technology Center, Spain) Influence of Annealing for Enhancing Second-Order Nonlinearity in Strained Silicon	P <b>80</b>
<b>Dries Van Thourhout</b> (Ghent University - IMEC, Belgium) New Materials for Multifunctional Photonic ICs	K <b>81</b>
<b>J. Enrique Vázquez-Lozano</b> (Nanophotonics Technology Center (NTC), Spain) Spin-dependent light interference	P <b>82</b>
<b>Elisabet Xifre-Perez</b> (Universitat Rovira i Virgili, Spain) Photoluminescent porous alumina particles for the development of label-free biomarkers	O <b>83</b>
<b>Nerea Zabala</b> (University of the Basque Country UPV/EHU, CFM and DIPC, Spain) Ultrafast control of plasmonic nanoantennas driven by hot-spot induced phase-transition in VO <sub>2</sub>	O <b>84</b>
<b>Mario Zapata Herrera</b> (Materials Physics Center CSIC-UPV/EHU and Donostia International Physics Center DIPC, Spain) Optical response and electron dynamics of charged plasmonic nanoparticles	O <b>85</b>

# Optical forces exerted on nanowire dimers: New characterization of Plasmons

<sup>1</sup>Instituto de Microelectrónica de Madrid, Isaac Newton 8 (PTM), Tres Cantos, Madrid, Spain

<sup>2</sup>Instituto de Física Arroyo Seco- Universidad Nacional del Centro de la Provincia de Buenos Aires, Tandil, Buenos Aires, Argentina

[martinabrahame@gmail.com](mailto:martinabrahame@gmail.com)

A new numerical study of the electromagnetic coupling between two metallic nanowires is realized under plane-wave incidence. Considered as near-field observables, the induced forces and torques can give a different point of view of the interaction [1-4].

Although several studies of the opto-mechanical inductions have been done [5-7], unexpected features of the movement are obtained. "Coordinated" spin for the wires are found, in addition to binding or repulsion forces between the wires and scattering forces. The rotations of the wires identify uniquely the surface plasmons. In particular, dark modes can be optically detected without using incidence with evanescent fields. The results could be applied to the real observation/detection of surface plasmons [8].

Also, the validity of the Newton's third law in the system is discussed. The action-reaction law is directly valid for the mechanical response in small dimers. However, for bigger systems, the law needs to be recovered by considering the momentum carried by the scattered light [9].

---

## References

---

- [1] Raziman T.V. and Martin O.J.F., *Optics Express* 23, 15 (2015) 20143.
- [2] Lamothe E., Lévêque G., and Martin O.J.F., *Optics Express* 15, 15 (2007) 9631.
- [3] Abraham Ekeroth R. M. and Lester M.F., *Journal of Optics* 17, 10 (2015) 1.
- [4] Abraham Ekeroth R. M. and Lester M.F., *Plasmonics* 10, 4 (2015) 989.
- [5] K. Dholakia and P. Zemánek, *Review of Modern Physics* 82, 2 (2010) 1767.
- [6] Maragò O.M. et al., *Nature nanotechnology* 8 (2013) 807.
- [7] Miljkovic V.D. et al, *Journal of Physical Chemistry C* 114 (2010) 7474.
- [8] Shu-Chun Yang et al., *Nano Letters* 10 (2010) 632.
- [9] S. Sukhov, A. Shalin, D. Haefner, and A. Dogariu, *Optics Express* 23, 1 (2015) 247.

Optical properties of nanoporous anodic alumina (NAA) are interesting in many photonic applications of this nanomaterial. Such optical properties can be modified in several ways [1] and applications such as optical biosensing have already been demonstrated [2]. One possible optical function is the rugate filter: a multilayer structure with continuous variation of refractive index along the pore. It can be produced in a quasi-galvanostatic regime with a sinusoidal perturbation of the current and leads to structures with a sharp stop band around the design wavelength. One advantage of such structures is the possibility to overlap several sinusoidal profiles resulting in several tunable stop bands in the same structure. This features permit to envision other applications such as colorimetric sensing or barcode labeling.

In this work, we present a complete study of the design parameters for sinusoidal-anodization rugate filters made of NAA. The complex porous structures obtained by the electrochemical anodization of aluminum present a set of unique optical properties, by the galvanostatic control of the anodization that provides an accurate control of the porosity and growth rate of the alumina. Our study establishes the principles for understanding the effect of the fabrication parameters (current amplitude, offset current, period length and number of periods) on the optical properties of the sinusoidal rugate filters. The obtained results reveal that the transmission and reflection spectrum of the rugate filters can be precisely tuned in the UV, visible and IR range by adjusting the different fabrication parameters (Figure 1).

**Acknowledgements:** This work was supported in part by the Spanish Ministry of Economy and competitiveness TEC2015-71324-R (MINECO/FEDER), the Catalan authority AGAUR 2014SGR1344, and ICREA under the ICREA Academia Award.

## References

- [1] J. Ferré-Borrull, E. Xifre-Perez, J. Pallares, L.F. Marsal. Optical properties of nanoporous anodic alumina and derived applications. In: D. Losic, A. Santos editors. Nanoporous Alumina. Fabrication, Structure, Properties and Applications, Springer Series in Materials Science Vol. 219 (2015) p. 185-217.
- [2] G. Macias, L.P. Hernández-Eguía, J. Ferré-Borrull, J. Pallares, L.F. Marsal, ACS Appl. Mater. Interfaces, 5 (2013) 8093.

## Figures

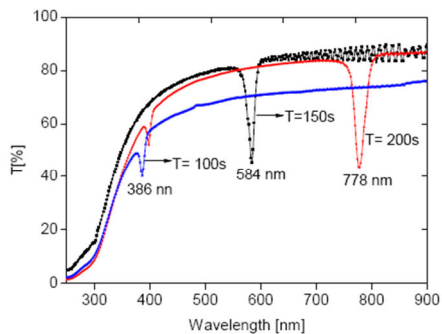


**Figure 1:** Transmission spectra of NAA sinusoidal rugate filters with different period lengths ( $T=100, 150$  and  $200$  s).

P. Alonso-González<sup>1,2</sup>, A. Y. Nikitin<sup>1,3</sup>, Y. Gao<sup>4</sup>, A. Woessner<sup>5</sup>, M. B. Lundeberg<sup>5</sup>, A. Principi<sup>6</sup>, N. Forcellini<sup>7</sup>, W. Yan<sup>1</sup>, S. Vélez<sup>1</sup>, A. J. Huber<sup>8</sup>, K. Watanabe<sup>9</sup>, T. Taniguchi<sup>9</sup>, L. E. Hueso<sup>1,3</sup>, M. Polini<sup>10</sup>, J. Hone<sup>4</sup>, F. H. L. Koppens<sup>5,11</sup> and R. Hillenbrand<sup>3,12</sup>

<sup>1</sup>CIC nanoGUNE, Spain

<sup>2</sup>Departamento de Física, Universidad de Oviedo, Spain

<sup>3</sup>IKERBASQUE, Basque Foundation for Science, Spain

<sup>4</sup>Department of Mechanical Engineering, Columbia Univ., USA

<sup>5</sup>ICFO-Institut de Ciències Fòtoniques, Spain

<sup>6</sup>Radboud University, Institute for Molecules and Materials, The Netherlands

<sup>7</sup>Department of Physics, Imperial College London, UK

<sup>8</sup>Neaspec GmbH, Germany

<sup>9</sup>National Institute for Materials Science, Japan

<sup>10</sup>Istituto Italiano di Tecnologia, Graphene labs, Italy

<sup>11</sup>ICREA – Institució Catalana de Recerca i Estudis Avançats, Spain

<sup>12</sup>CIC NanoGUNE and EHU/UPV, Spain

## Ultra-confined acoustic THz graphene plasmons

palonso@nanogune.eu

The interaction of terahertz (THz) radiation with graphene has a vast application potential in many technologies, including imaging, communications, sensing, or photo-detection, among others. Recently, it has been shown that the excitation of localized THz plasmons in graphene can strongly enhance light-matter interactions, opening the door to more efficient optoelectronic devices. Here, we will present on the first visualization of propagating graphene plasmons (GPs) at THz frequencies, which can also be controlled by metallic (split) gates. More importantly, due to the coupling of the GPs with the metal gate underneath we observe a linearization of the plasmon dispersion (thus revealing acoustic plasmons), which comes along with an extreme confinement of the plasmon fields [1]. These extraordinary GPs properties are very promising for sensing and communication technologies. To map the THz GPs, we introduce nanoscale-resolved THz photocurrent nanoscopy as a novel tool for studying fundamental and applied aspects of local THz photocurrent generation with a resolution of 50 nm, 3 orders of magnitude below the diffraction limit (Fig. 1).

### References

- [1] P. Alonso-González, A. Y. Nikitin, Y. Gao, A. Woessner, M. B. Lundeberg, A. Principi, N. Forcellini, W. Yan, S. Vélez, A. J. Huber, K. Watanabe, T. Taniguchi, L. E. Hueso, M. Polini, J. Hone, F. H. L. Koppens, and R. Hillenbrand, arXiv:1601.05753 [cond-mat.mes-hall], (2016).

### Figures

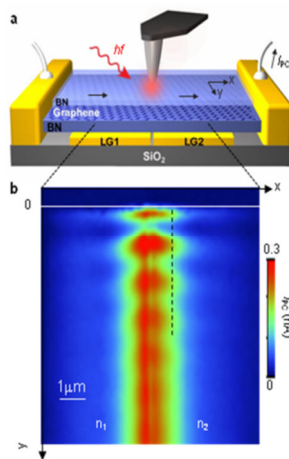


**Figure 1:** (a) Schematics of the experimental setup. The laser-illuminated metal tip of an AFM serves as a nanoscale near-field light source. The near-field induced photocurrent in the graphene (encapsulated by h-BN layers) is measured through the two metal contacts to the left and right. LG1 and LG2 represent the split gate (gold) used for controlling the carrier concentration in the graphene to the left and the right of the gap between them. (b) Experimental near-field photocurrent image,  $I_{PC}$ , recorded at  $f = 2.52$  THz.

# Fabrication of low-cost and high aspect ratio nanowires and 2D nanostructures by soft lithography for nanophotonic devices

E. Baquedano, R. Martinez and P.A. Postigo

Instituto de Microelectrónica de Madrid, CSIC, Tres Cantos, Madrid, Spain

estela.baquedano@csic.es

High aspect ratio nanostructures are needed for relevant photonic applications like light harvesting, light generation and amplification and optical sensing. High quality nanoimprint lithography (NIL) can be carried out using a low cost version called soft lithography. This method was introduced as a low-cost alternative to conventional lithography, and has been shown to be a powerful method to generate reproducible nanopatterns in wide areas (in the order of square cm) using elastomeric polymers like polydimethylsiloxane (PDMS) or others [1]. However, due to the low level of stiffness of PDMS, only limited aspect ratios are achievable. In this work, high aspect ratio silicon nanowires and nanostructures have been achieved by the combination of soft lithography and the careful optimization of the reactive ion etching (RIE) process used to transfer the nanopatterns to silicon. Using this procedure we have obtained linear nanopatterns in areas in the order of square cm with high aspect ratios around 1.2 and 1.6, which are among the best found in the literature. Furthermore, we have achieved this results using

low-cost commercial DVD and Blu-Ray as masters to obtain the PDMS stamp (Figure 1a). We have also fabricated 2D nanostructures (Figure 1b) and achieved high aspect ratios of 5.4. The reflectivity of these samples, which is critical for potential photonic applications, was measured. Figure 1(c) shows the reflectivity of silicon nanowires fabricated with different aspect ratio. Finally, the fabricated nanowires have been used for different applications like the enhanced generation of solar thermal energy [2] or new nanophotonic optical sensors [3].

## References

- [1] Y. Xia, G.M. Whitesides, *Soft lithography*, Annual review of materials science, 28 (1998) 153-184.
- [2] S. Núñez-Sánchez, E. Baquedano-Peralvarez, J. Pugh, P. A. Postigo, N.A. Fox and M. J. Cryan, *ECIO2016*.
- [3] E. Baquedano-Peralvarez et al, to be published.

## Figures

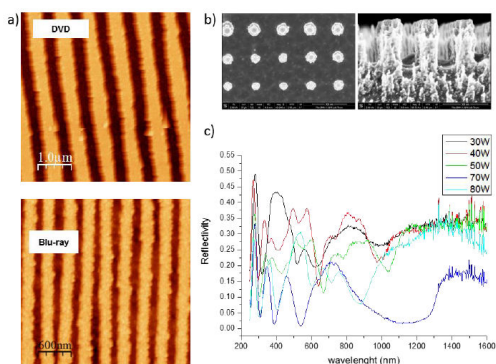


**Figure 1:** a) AFM images of patterns resultant for DVD and Blu-ray on silicon. b) SEM images of pattern 2D on silicon. c) Reflectivity for silicon nanowires with different aspect ratio obtained by different RIE etching powers.



# Using linear polarization for sensing with core-shell nanostructures

Ángela I. Barreda, Juan M. Sanz, Yael Gutiérrez, Andrea Fernández, Fernando Moreno, Francisco González

Grupo de Óptica, Departamento de Física Aplicada, Universidad de Cantabria, Facultad de Ciencias, Santander, Spain

barredaai@unican.es

The interaction of light with metallic nanoparticles (NPs) has been a very active field that has impacted many different areas. For instance, the development of new sensing techniques especially has attracted the attention of researchers in science and engineering [1]. However, in spite of the strong response of metallic NPs in infrared and visible spectral regions, their metallic nature is also the cause of their main disadvantage, ohmic losses. High Refractive Index (HRI) dielectric NPs have been proposed as a means to address this issue. Some of their most important advantages are they do not show losses and also they can show new scattering effects due to magnetic contributions even for non-magnetic ( $\mu = 1$ ) materials, [2]. This magneto-dielectric behavior is responsible for interesting directionality properties. Under certain conditions, proposed by Kerker et al [3], the forward and backward scattered intensity is almost null or null respectively. The spectral response depends on the NP size, its refractive index, its purity and the refractive index of the surrounding medium  $m_{\text{med}}$ . Due to this last dependence, dielectric NPs can be used for sensing purposes. In recent publications, the sensitivity of different semiconductor materials to changes in  $m_{\text{med}}$  has been studied attending to energy or polarimetric measurements, [4-5]. In this work, we propose to analyze the sensitivity to  $m_{\text{med}}$  of metallo-dielectric core-shell NPs through the measurement of the spectral linear polarization degree at right angle scattering,  $P_i(90^\circ)$ . The results of this study have been compared with those for a HRI dielectric NP in the same spectral range.

For particles much smaller than the incident wavelength, both directionality conditions are satisfied when  $P_i(90^\circ) = 0$ . In this work, using the Lorenz-Mie theory and focusing on the spectral shift of the  $P_i(90^\circ)$  at both Kerker's conditions as a function of  $m_{\text{med}}$ , we show the utility of  $P_i(90^\circ)$  spectral measurements for sensing applications. As an example, in Fig. 1 we show the sensitivity,  $\xi_m$ , of

$P_i(90^\circ)$  to  $m_{\text{med}}$  for the first (Zero-Backward) and second (near Zero-Forward) Kerker conditions for a core-shell Si-Ag spherical NP as a function of the core size [6]. The external (core+shell) radius was fixed to  $R_{\text{ext}} = 230\text{nm}$ .

## References

- [1] P. N. Prasad, Nanophotonics (John Wiley & Sons, Inc., 2004).
- [2] Y. H. Fu et al., Nat. Commun. 4:1527, (2013).
- [3] M. Kerker, D. S. Wang and C. L. Giles. J. Opt. Soc. Am. 6, (1983) 765.
- [4] B. García-Cámara, et al., Opt. Express 20, (2013) 23007.
- [5] A. I. Barreda, et al., Opt. Express 7, (2015) 9157.
- [6] A. I. Barreda, et al., Nanotechnology 23, (2016) 234002.

## Figures

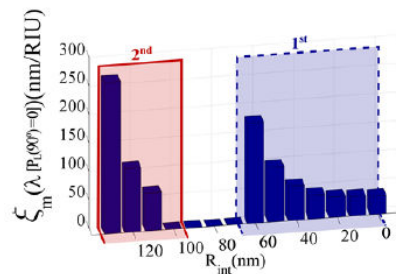


Figure 1: Sensitivity of  $P_i(90^\circ)$  to the refractive index of the surrounding medium,  $m_{\text{med}}$

Modeling the optical properties of nanoporous anodic alumina (NAA) is interesting in order to study and design photonics applications of this nanomaterial. The optical properties of NAA are related to their geometric characteristics (interpore distance, pore diameter, barrier layer thickness, etc.) which depend of the fabrication conditions (acid electrolyte, anodization voltage or current, pH and temperature) [1]. Numerical methods for optical modelling such as the transfer-matrix method are not adequate since cannot take into account features such as the texturization of the metal-oxide interface, the great range of interpore distances, or the inhomogeneities in the chemical composition of the oxide [2].

In this work we show that FDTD is an adequate method to solve these issues as it permits to take into account all the geometrical and composition characteristics. Figure 1 illustrates some of the results: it shows the comparison of the calculated reflectance spectra using TMM and FDTD with the spectrum of a real sample, for short-interpore distance (Figures 1a,c) and for long interpore distance (Figures 1b,c). It can be seen that FDTD, taking into account the texturization of the metal-oxide interface permits to simulate all the range of structures.

These results validate the method for the simulation of such structures, thus, we apply it to the evaluation of the sensitivity of a NAA-based nanostructure in detecting the binding of a biological-related molecule to the surface of the pores. Figure 2 shows the obtained results: the structure consists of a NAA thin film with a 5 nm thick conformal coating of gold (Figure 2a, inset). The bound molecule is modeled by considering a second 5 nm conformal coating with a refractive index slightly different than the medium filling the pores. The spectrum in figure 2a shows a sharp reflectance valley around 800 nm. This valley shifts with the refractive index of the second coating, as illustrated in Figure 2b, what demonstrates the possibility of using the structure as a sensor.

Acknowledgements: This work was supported in part by the Spanish Ministry of Economy and competitiveness TEC2015-71324-R, the Catalan authority AGAUR 2014SGR1344, ICREA under the ICREA Academia Award.

## References

- [1] T. Kumeria et al., *Sensors*, 14 (2014) 11878-11918.
- [2] W. Lee et al., *Chemical reviews*, 114 (2014) 7487-7556.

## Figures

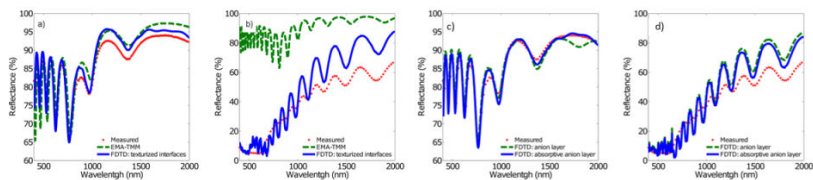


Figure 1: Comparison of the measured reflectances with the simulated ones for NAA structures.

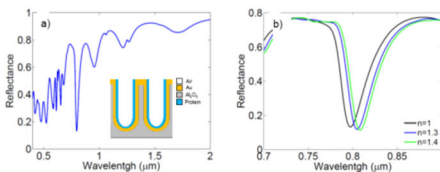


Figure 2: Study of sensing with a gold-coated NAA film.

# Morphological manipulation of the luminescent response of atomically thin Indium Selenide nanosheets

**Mauro Brotons-Gisbert**, Daniel Andres-Penares, Alfredo Segura, Juan P. Martínez-Pastor, Juan F. Sánchez-Royo

ICMUV, Instituto de Ciencia de Materiales, Universidad de Valencia, Valencia, Spain

Mauro.Brotons@uv.es

Many efforts have been devoted to manipulate the morphology of two-dimensional (2D) materials to tune and improve their functionalities. It is usually believed that morphological manipulation strategies, such as nanotexturing, reduce transport abilities of 2D systems whereas introduces or enhances other functionalities. It is the case, for instance, of graphene [1,2]. Single layers (SLs) of transition-metal dichalcogenides [3,4] offer unquestionable technological applications [5-8]. Nevertheless, tuning their properties for optoelectronic applications is challenging due to the intrinsically localized nature and orbital character of the d-states that dominate their valence and conduction bands. 2D forms of other layered semiconductors, as Indium Selenide, are less explored and may exhibit interesting and tunable properties [9-11]. First-principles calculations predicted that 2D InSe should produce a band-gap tuning window as large as 1.1 eV [10] and, experimentally, a blue shift of the optical band gap of 0.2 eV has been already observed in 5 nm thick InSe nanosheets [10,11]. Also, devices based on few-layer InSe have shown promising applications [12-14]. In this communication, we show the ability of nanotexturing strategies to enhance the luminescent response of atomically thin Indium Selenide nanosheets. Besides, quantum-size effects make this two-dimensional semiconductor to exhibit one of the largest band gap tunability ranges observed in a two-dimensional semiconductor: from 1.25 eV, in bulk, to 2.1 eV, in the single layer. These results are relevant for the design of new optoelectronic devices, including heterostructures of two-dimensional materials with optimized band gap functionalities and in-plane heterojunctions with minimal junction defect density.

---

## References

---

- [1] C. H. Lui, L. Liu, K. F. Mak, G. W. Flynn, and T. F. Heinz, *Nature*, 462 (2009), 339-341.
- [2] C. R. Dean, A. F. Young, I. Meric, C. Lee, L. Wang, S. Sorgenfrei, K. Watanabe, T. Taniguchi, P. Kim, K. L. Shepard, and J. Hone, *Nature Nanotech.* 5 (2010) 722-726.
- [3] K. F. Mak, C. Lee, J. Hone, J. Shan, and T. F. Heinz, *Phys. Rev. Lett.*, 105 (2010), 136805.
- [4] A. Splendiani, L. Sun, Y. B. Zhang, T. S. Li, J. Kim, C. Y. Chim, G. Galli, and F. Wang, *Nano Lett.*, 10 (2010) 1271-1275.
- [5] B. Radisavljevic, A. Radenovic, J. Brivio, A. V. Giacometti, and A. Kis, *Nature Nanotech.*, 6 (2011) 147-150.
- [6] F. K. Perkins, A. L. Friedman, E. Cobas, P. M. Campbell, G. G. Jernigan, and B. T. Jonker, *Nano Lett.*, 13 (2013) 668-673.
- [7] M. Bernardi, M. Palumbo, and J. C. Grossman, *Nano Lett.*, 13 (2013) 3664-3670.
- [8] Y. J. Zhang, T. Oka, R. Suzuki, J. T. Ye, and Y. Iwasa, *Science*, 344 (2014) 725-728.
- [9] M. Brotons-Gisbert, J. F. Sánchez-Royo, and J. P. Martínez-Pastor, *Appl. Surf. Sci.*, 354B, (2014) 453-458.
- [10] J. F. Sánchez-Royo, G. Muñoz-Matutano, M. Brotons-Gisbert, J. P. Martínez-Pastor, A. Segura, A. Cantarero, R. Mata, J. Canet-Ferrer, G. Tobias, E. Canadell, J. Marqués-Hueso, and B. D. Gerardot, *Nano Res.*, 7 (2014) 1556-1568.
- [11] G. W. Mudd, S. A. Svatek, T. Ren, A. Patanè, O. Makarovskiy, L. Eaves, P. H. Beton, Z. D. Kovalyuk, G. V. Lashkarev, Z. R. Kudrynskiy, and A. I. Dmitriev, *Adv. Mater.*, 25, (2013) 5714-5718.
- [12] W. Feng, W. Zheng, W. Cao, and P. Hu, *Adv. Mater.*, 26 (2014) 6587-6593.
- [13] W. Luo, Y. Cao, P. Hu, K. Cai, Q. Feng, F. Yan, T. Yan, X. Zhang, and K. Wang, *Adv. Opt. Mater.*, 3 (2015) 1418-1423.
- [14] G. W. Mudd, S. A. Svatek, L. Hague, O. Makarovskiy, Z. R. Kudrynskiy, C. J. Mellor, P. H. Beton, L. Eaves, K.S. Novoselov, Z. D. Kovalyuk, E. Vdovin, A. J. Marsden, N. R. Wilson, and A. Patanè, *Adv. Mater.*, 27 (2015) 3760-3766.

# Boosting Sensing Performance Using Hybrid Magnetoplasmonic Nanohole Arrays

<sup>1</sup>IMM-Instituto de Microelectrónica de Madrid (CNM-CSIC), Madrid, Spain

<sup>2</sup>Departamento de Física Teórica de la Materia Condensada and Condensed Matter Physics Center (IFIMAC), Universidad Autónoma de Madrid, Madrid, Spain

blanca.caballero@imm.cnm.csic.es

Plasmonic structures are widely used in low-cost, label-free biosensors, and the investigation of how to improve their sensitivity or to widen their range of applications is a central topic in the field of plasmonics.[1,2] The most commonly used plasmonic sensors are based on the concept of surface plasmon resonance (SPR) and, in particular, on the sensitivity of these resonances to changes in the refractive index of the medium surrounding a metallic structure.

In the search for an improved bulk sensitivity of SPR-based sensors, researchers have proposed different strategies. Thus, for instance, it has been shown that the use of the magneto-optical properties of layered systems containing magnetic materials can, in principle, enhance the sensitivity of these sensors.[3,4] Another possibility that is becoming increasingly popular is the use of nanohole arrays or perforated metallic membranes featuring arrays of subwavelength holes.[5,6] These sensors make use of the extraordinary optical transmission phenomenon, which originates from the resonant excitation of surface plasmons in these periodically patterned nanostructures.

We present here a theoretical study that shows how the use of hybrid magnetoplasmonic crystals comprising both ferromagnetic and noble metals leads to a large enhancement of the performance of nanohole arrays as plasmonic sensors. In particular, we propose using Au–Co–Au films perforated with a periodic array of subwavelength holes as transducers in magneto-optical surface-plasmon-resonance sensors, where the sensing principle is based on measurements of the transverse magneto-optical Kerr effect (TMOKE). We demonstrate that this detection scheme may result in bulk figures of merit that are two orders of magnitude larger than those of any other type of plasmonic sensor.[7] The sensing strategy put forward here can make use of the different

advantages of nanohole–based plasmonic sensors such as miniaturization, multiplexing, and its combination with microfluidics.

## References

- [1] O. Tokel, F. Inci, U. Demirci, *Chem. Rev.* 114, (2014) 5728
- [2] M.–C. Estevez, M. A. Otte, B. Sepulveda, L. M. Lechuga, *Anal. Chim. Acta* 806, (2014) 55
- [3] B. Sepulveda, A. Calle, L.M. Lechuga, G. Armelles, *Opt. Lett.* 31, (2006) 1085
- [4] M.G. Manera, et al., *Biosens. Bioelectron.* 58, (2014) 114
- [5] A.A. Yanik, et al., *Proc. Natl. Acad. Sci. U. S. A.* 108, (2011) 11784
- [6] A.E. Cetin, et al., *ACS Photonics* 2, (2015) 1167
- [7] B. Caballero, A. García–Martín, and J. C. Cuevas, *ACS Photonics* 3, (2016) 203

## Figures

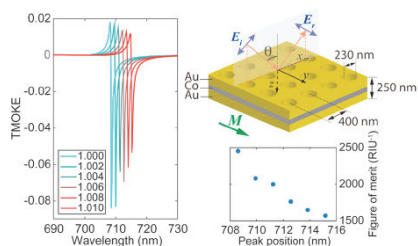


**Figure 1:** Left: TMOKE signal as a function of wavelength for varying values of the environment refractive index. Top–right: sketch of the structure used for the study. Bottom–right: figure of merit of obtained from the TMOKE curves.

In a traditional planar photonic sensing structure only its external surface is typically used for sensing purposes. In order to increase its sensitivity, its surface/volume ratio takes relevance. In this respect, porous silicon (PSi) multilayer structures allow to increase this ratio as well as offering the possibility to infiltrate the target analytes directly into the pores. The infiltration produces a variation of the effective refractive index of PSi layers, and a shift of the multilayer spectral response. This shift is much higher if the specific surface area increases. According to Fig. 1, it implies PSi layers with low diameters and high densities (high porosity). Because of that, in this work we present a PSi multilayer structure with a high refractive index contrast and pores with low average diameters.

One effective reflectivity optical sensor based on photonic structures is the Bragg reflector [1]. It consists of a periodic structure made of alternating layers of high ( $n_H$ ) and low ( $n_L$ ) refractive index. Their thicknesses,  $d$ , must satisfy the relation  $n_H \cdot d_H = n_L \cdot d_L = \lambda_B/4$ , being the stop band centered at  $\lambda_B$ . Taking into account the characteristics of our measurement setup, we have used ten periods of PSi layers with refractive indices of  $n_H \approx 2.5$  and  $n_L \approx 1.8$ , and thicknesses of  $d_H \approx 145$  nm and  $d_L \approx 200$  nm respectively. The average pore diameter is lower than 12 nm and 20 nm for the PSi layers with the high and low refractive index respectively. Taking into account the tendencies of the surface/volume ratio presented in Fig. 1, and respect to publications from other researchers [2], the available sensing area is higher in our case. Moreover and for sensing areas with millimeter dimensions, this multilayer structure has a higher mechanical stability than in cases where higher pore diameters are used. The reflectance spectrum of our Bragg reflector is presented in Fig. 2. As the refractive indices of the PSi layers change due to the infiltration of analytes, the bandgap will shift to longer wavelengths.

To carry out our experimental measurements, we have developed a fluidic cell that allows to flow different solutions over the sample and to illuminate perpendicularly the sample at the same time. An optical interrogator is used to analyze the spectrum of the light reflected in real-time. A LabVIEW

program has been implemented to examine the evolution of the reflectance spectrum. A highly sensitive photonic sensing interrogation method based on the continuous monitoring of the output power of a range of the reflectance spectrum, obtaining a real-time measurement.

The sensitivity of our sensing structure has been tested by flowing several ethanol concentrations in DIW. The limit of detection (LoD) of our sensor is in the range of  $10^{-6}$  RIU.

Funding of the Spanish Government through the TEC2013-49987-EXP project is acknowledged. Raffaele Caroselli also acknowledges the Generalitat Valenciana for the Doctoral Scholarship GRISOLIAP/2014/109.

## References

- [1] Snow et al., J. Appl. Phys., 86, pp. 1781 -1784, 1999
- [2] Mukherjee et al., Opt. Express, 21, pp. 17324 - 17339, 2013

## Figures

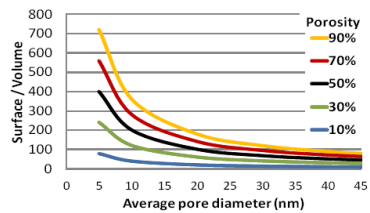


Figure 1: Surface/Volume ratio of a PSi layer respect to its porosity and its average pore diameter. It has been assumed that pores have cylindrical shapes.

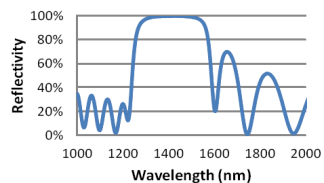


Figure 2: Reflectance spectrum of the PSi multilayer structure.

# Optimization of a hybrid BaTiO<sub>3</sub>/Si Waveguide Structure for Electro-optic Modulation

P. Castera<sup>†</sup>, A. Rosa, A. M. Gutierrez, D. Tulli, P. Sanchis\*

Nanophotonics Technology Center, Universitat Politècnica de València, Valencia, Spain

<sup>†</sup>pacasmo@ntc.upv.es

\*pabsanski@ntc.upv.es

Silicon photonics technology is currently one of the most promising platforms for enabling automated and low-cost volume manufacturing of highly integrated and complex photonic circuits, mainly because the fabrication processing steps are developed using standard CMOS (Complementary Metal Oxide Semiconductor) fabrication infrastructure. In this context, the integration of CMOS compatible active materials such as barium titanate (BaTiO<sub>3</sub> or BTO) has become a promising way to achieve electro-optic (EO) modulation by means of the Pockels effect [1,2]. In this work, a Mach-Zehnder Modulator in a hybrid BTO/Si optical waveguide is proposed for enabling EO modulation with high performance. A layer of amorphous silicon (a-Si) is deposited on top of the BaTiO<sub>3</sub>/SOI structure and then etched down to form the optical waveguide. The influence of waveguide parameters on the static EO performance has been previously reported [2]. Besides, a silicon oxide (SiO<sub>2</sub>) layer is deposited over the optical waveguide to protect the device and lateral windows are open to place the electrodes on top of the BaTiO<sub>3</sub> layer thus enhancing the modulation efficiency. The waveguide structure and parameters are shown in Fig. 1(a). The electrodes have been designed to achieve RF impedance matching and high EO bandwidth. Simulations have been carried out with COMSOL<sup>TM</sup>.

The high permittivity of BaTiO<sub>3</sub> ( $\epsilon_r \sim 56$ ,  $\epsilon_x \sim 2200$ ) reduces the RF impedance in comparison with

usually lower dielectric constant substrates or thin films with symmetric coplanar waveguides. In such a way, the electrode dimensions have been designed to overcome the high permittivity of BaTiO<sub>3</sub>. Asymmetric coplanar electrodes, as depicted in Fig. 1(a), have been chosen to achieve the matching impedance around 50Ω, maintaining a narrow gap in the optical waveguide with the aim of keeping the modulation efficiency as high as possible. Figures 1(b) and (c) show the RF impedance and losses and RF, effective and optical group indices as a function of the frequency. It can be seen that the impedance is quite well matched. On the other hand, an EO bandwidth higher than 40 GHz is ensured as a result of the velocity matching between the electrical and optical signals. The modulation efficiency variation with the RF frequency is shown in Fig. 1(d). The VrL is below 1V·cm in the 40 GHz frequency range.

To summarize, the RF electrodes in a hybrid BTO/Si waveguide structure have been designed for optimum EO performance. This work was supported by the European Commission under project FP7-ICT-2013-11-619456 SITOGA.

## References

- [1] C. Xiong et al., Nano Letters, vol. 14(2014), pp. 1419–1425.
- [2] P. Castera et al., Opt. Express, vol. 23(2015), pp. 15332–15342.

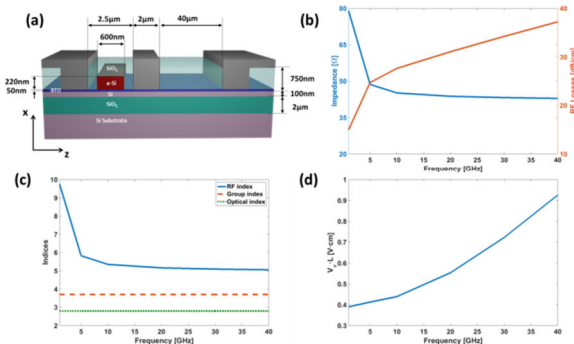


**Figure 1:** (a) Schematic of the waveguide cross-section. (b) RF impedance and losses, (c) RF, effective and optical group indices and (d) modulation efficiency as a function of the frequency.

# Dual plasmon excitation imaged by leakage radiation microscopy

Rafael Cichelero, Blai Casals and Gervasi Herranz

Institut de Ciència de Materials de Barcelona  
ICMAB-CSIC, Spain

richelero@icmab.es

Surface plasmons, originated by the collective oscillations of conduction electrons at a metal-dielectric interface, have attracted a lot of interest over the last decades. This research is motivated by the current trends for optical device miniaturization, associated with the plasmon-assisted enhancement of optical activity. One of the important features of the metal-dielectric interface is the capability to convert an incident electromagnetic wave with wavevector  $k_o$ , to a surface plasmon with wavevector  $k_{sp}$ , yet this conversion cannot be done directly by light. However, several strategies can be applied to perform the coupling between light and plasmons, based on the interaction of light with different structures, including gratings, cavities, slits or prisms.

In the present work we have adopted a prism-coupling strategy based on Kretschmann configuration, in which the role of the prism is played by an oil immersion objective. In our setup, the latter is able to collect the leakage radiation of plasmons that are converted back to light [1].

We have used the leakage radiation microscopy to image surface plasmons in real space. For that purpose, we have designed metallic nanostructures (slits, dots and gratings), by optical and e-beam lithography, allowing a dual surface plasmon excitation. A first kind of plasmons is generated by the Kretschmann configuration when the angle of incidence is higher than the critical angle and propagates along the plane of incidence. A second set of plasmons are generated by surface corrugation, with propagation modes determined by the corrugation geometry. The possibility of this dual plasmon excitation has enabled us to explore the interaction between them, either in real or in reciprocal space. The results may be of relevance for the development of methods to manipulate the propagation of surface plasmons in metal/dielectric nanostructures.

---

## References

---

- [1] A. Bouhelier and G.P. Wiederrecht. Phys. Rev. B, 2005.

# Emission regimes of random lasers with spatially localized feedback

We report the experimental results obtained with random lasers with spatially localized feedback [1], in which the active material, free of scatterers, is placed between two large scattering regions. Emission regimes with typical “resonant” and “non-resonant” random lasing spectra have been previously reported from large area devices [2]. Here, random lasing emission is investigated as a function of the illuminated area of the scattering regions, obtaining “resonant” and “non-resonant” spectral signatures, depending on the device geometry [3]. We propose a theoretical approach for the understanding of the observed phenomena, modelling the scattering elements with arbitrary spectral profiles in amplitude and phase and considering strong coupling between lasing modes. Good agreement between experiments and simulation results is obtained.

## References

- [1] A. Consoli and C.Lopez, *Sci. Rep.* 5, 16848 (2015).
- [2] A. Consoli, D. M. da Silva, N. U. Wetter and C. López *Opt. Express*, 23, 23 (2015) 29954-29963.
- [3] A. Consoli and C.Lopez, *Opt. Express*, accepted (2016).

## Figures

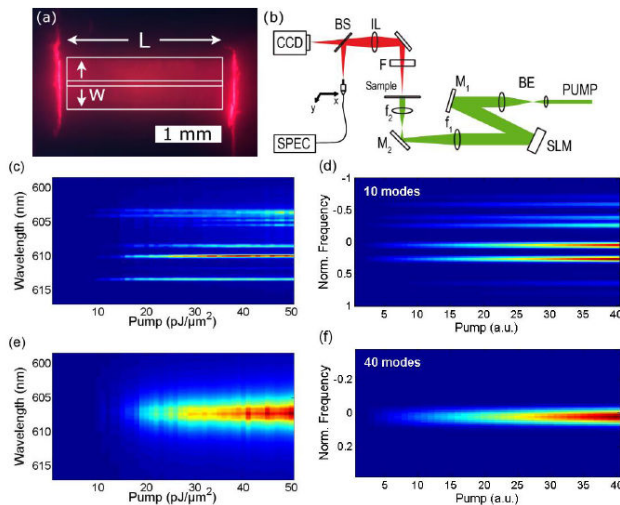


**Figure 1:** (a) Sample image with device geometry: length ( $L$ ) and variable width ( $W$ ). (b) Experimental set-up. Emission spectra for increasing pump energy with few modes in experiments (c) and simulations (d). Emission spectra for increasing pump energy with many modes in experiments (e) and simulations (f).



## Ferroelectric-semiconductor heterostructures for photovoltaic applications

Recently, ferroelectric materials have been considered as one of the most interesting materials for next-generation photovoltaic (PV) devices because of their outstanding advantages over conventional p-n junction based photovoltaic devices, such as their high output voltage and polarization controlled PV response [1]. However, the efficiency of light-to-electricity conversion in these materials is much less than that in the conventional solar cells due to the inefficient generation of e-h pairs [2]. One possible pathway to achieve the desired high photovoltaic efficiency is to insert a semiconductor layer in the metal-ferroelectric-metal structure, which combines advantage of the semiconductor in order to obtain a large short circuit current density ( $J_{sc}$ ), and the ferroelectric for high open circuit voltage ( $V_{oc}$ ) [2].

In this work, we report on the effect of the position of the ZnO layer on the photovoltaic response of the 0.5BZT-0.5BCT/ZnO heterostructure. To achieve this task, we study three types of heterostructures: Pt/0.5BCT (350 nm)/ZnO (10 nm)/ITO, Pt/ZnO

(10 nm)/0.5BCT (350 nm)/ITO and Pt/ZnO (10 nm)/0.5BCT (350nm)/ZnO (10 nm)/ITO. The presence of the 0.5BZT-0.5BCT perovskite phase and the ZnO wurtzite phase was confirmed by X-ray diffraction measurements. The enhanced ferroelectric photovoltaic effect was achieved for the Pt/ZnO/0.5BZT-0.5BCT/ITO heterostructure with the  $V_{oc} \approx 0.03$  V and the  $J_{sc} \approx 5.5$  mA.cm<sup>-2</sup>. The photovoltaic effect is explained in terms of the alignment of the internal electric fields and by the polarization-dependent interfacial coupling effect at the ZnO/0.5BZT-0.5BCT interface, which was confirmed by the presence of a hysteresis loop on the  $J_{sc}$  as a function of the poling voltage.

### References

- [1] S. Sharma, M. Tomar, A. Kumar, N. K. Puri, V. Gupta, *J. Appl. Phys.*, 118 (2015) 074103.
- [2] Z. Fan, K. Yao, J. Wang, *Appl. Phys. Lett.*, 105 (2014) 162903.

### Figures

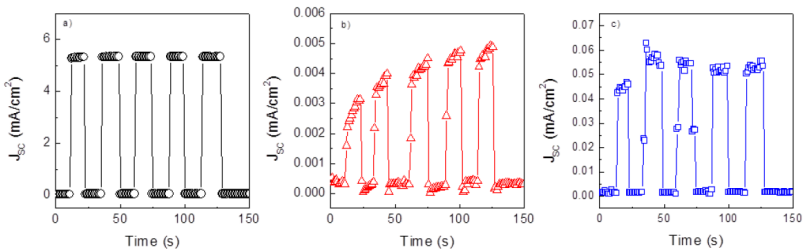


Figure 1:  $J_{sc}$  as a function of time in a) Pt/ZnO/BZT-BCT/ITO, b) Pt/BZT-BCT/ZnO/ITO and c) Pt/ZnO/BZT-BCT/ZnO/ITO heterostructures

## Near-field radiative heat transfer at the nanoscale

Radiative heat transfer between objects at different temperatures is of fundamental importance in applications such as energy conversion, thermal management, lithography, data storage, and thermal microscopy. It was predicted long ago that when the separation between objects is smaller than the thermal wavelength, which is of the order of  $10\ \mu\text{m}$  at room temperature, the radiative heat transfer can be greatly enhanced and it can even overcome the theoretical limit set by Stefan-Boltzmann law for black bodies. This is possible due to the contribution of the near field in the form of evanescent waves (or photon tunneling). In recent years, different experimental studies have confirmed this long-standing theoretical prediction. However, in spite of this progress, there are still many basic open questions in the context of near-field radiative heat transfer. In this talk, I will review our recent theoretical and experiment efforts to shed new light on the problem of thermal radiation exchange at the nanoscale. In particular, I will discuss the following two fundamental issues: (i) The enhancement of near-field radiative heat transfer in polar dielectric thin films [1] and (ii) the radiative heat transfer in the extreme near-field regime when objects are separated by nanometer-size distances [2].

### References

- [1] B. Song, Y. Ganjeh, S. Sadat, D. Thompson, A. Fiorino, V. Fernández-Hurtado, J. Feist, F.J. García-Vidal, J.C. Cuevas, P. Reddy, and E. Meyhofer, *Nature Nanotechnology* 10, 253 (2015).
- [2] K. Kim, B. Song, V. Fernández-Hurtado, W. Lee, W. Jeong, J. Feist, M.T.H. Reid, F.J. García-Vidal, J.C. Cuevas, E. Meyhofer, and P. Reddy, *Nature* 528, 387 (2015).

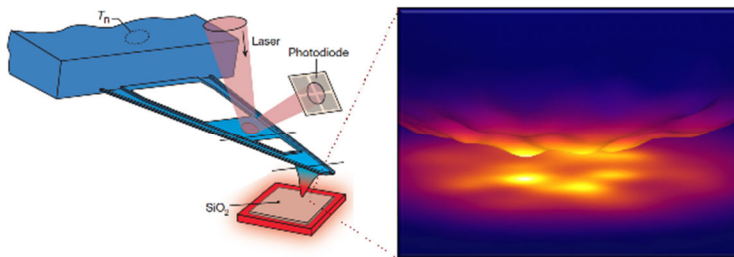


Figure 1: Radiative thermal radiation between an AFM tip and a surface both made of  $\text{SiO}_2$  and separated by a few nanometers.

# Open access to low cost photonic integrated circuits prototyping in a generic Silicon Nitride foundry

David Domenech<sup>1</sup>, Iñigo Artundo<sup>1</sup>, Bernardo Gargallo<sup>1</sup>, Rocio Baños<sup>1</sup>, Pascual Muñoz<sup>1,2</sup>, Carlos Dominguez<sup>3</sup>

<sup>1</sup>VLC Photonics S.L., Spain

<sup>2</sup>iTEAM Research Institute, Universitat Politècnica de València, Spain

<sup>3</sup>Institute of Microelectronics of Barcelona, IMB-CNM (CSIC), Spain

david.domenech@vlcphotonics.com

A Silicon Nitride ( $\text{Si}_3\text{N}_4$ ) waveguide platform [1] has been developed with very low propagation losses, low autofluorescence and a high level of integration to realize compact systems at low cost targeted from the visible spectrum to the infrared. Passive components are introduced here with best-in-class performance, including waveguides, splitters, filters, multiplexers and couplers based on optimized ultralow loss  $\text{Si}_3\text{N}_4$  material as shown in Fig. 1. In order to make efficient use of the fabrication runs and inspired by the cost sharing model that has been in use for ASICs and silicon photonics in the past, access to the fabrication platform is offered through Multi Project Wafer runs (MPW's) [2]. There are two different sizes that users can choose from: M with an area of  $5,5 \times 5,5 \text{ mm}^2$ , and L with an area of  $11 \times 5,5 \text{ mm}^2$  as shown in Fig. 2. The full wafer will be later diced in individual areas and several copies of the chips will be delivered to the users.

## References

- [1] Daldosso, N. et al. Comparison among various  $\text{Si}_3\text{N}_4$  waveguide geometries grown within a CMOS fabrication pilot line. IEEE J. Lightwave Technol. 22, 1734–1740 (2004).
- [2] M. Smit, X. Leijtens, E. Bente, J. Van der Tol, H. Ambrosius, D. Robbins, M. Wale, N. Grote and M. Schell, "Generic foundry model for InP-based photonics". IET Optoelectron, Vol. 5, pp. 187-194, 2011.

## Figures

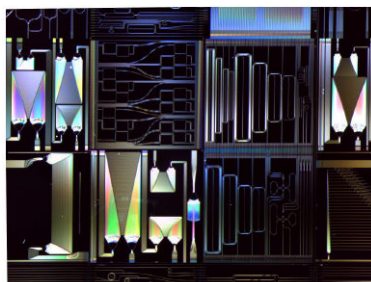


Figure 1: Multiple components fabricated in a  $\text{Si}_3\text{N}_4$  MPW.

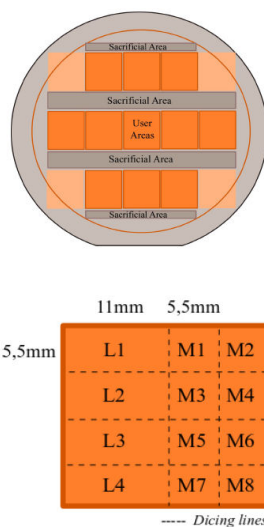


Figure 2: Wafer plan and reticle division for the CNM MPW run.

Fluid imbibition-coupled laser interferometry (FICLI) is a technique recently introduced [1] consisting of the registration of the interference pattern produced by a laser beam reflected off the two interfaces of a nanoporous anodic alumina (NAA) film, as it is being filled by a liquid front, Fig. 1. As the liquid interface within the nanopores moves, the optical path between the two reflected waves varies leading to successive intensity maxima and minima, Fig. 2. From the analysis of this time-resolved oscillation pattern, geometrical characteristics of the pores can be extracted. This analysis can be done in several different ways [1, 2]. In ref. [1], the radius at each side of the NAA pores can be estimated from the filling time from top ( $t_{Fill,Top}$ ) and from bottom ( $t_{Fill,Bottom}$ ) of the pores. However, the determination of such filling times is affected by a noticeable uncertainty, which propagates into the calculation of the pore radius. In this work, we propose an alternative method for the determination of the radius, based on the analysis of the succession of maxima and minima. Fig. 3 illustrates this procedure: the time differences between two consecutive extremes are plotted against the ordinal of each extremes pair. The slope of the linear regression is related to the radius of the pore, what provides a more robust estimate. In this work, we aim at evaluating the accuracy of the different pore radius determination procedures. Fig. 4 shows the estimated values of top and bottom radius for the two methods, together with the error bars corresponding to the uncertainty, for samples with increasing radius. As it can be seen, the new method provides better accuracy. Furthermore, in Fig. 4, the detection of the binding event of a protein (Bovine Serum Albumin, BSA) to the inner pore walls of the NAA is demonstrated as a reduction in pore radius.

This work was supported in part by the Spanish Ministry of Economy and competitiveness TEC2015-71324-R, the Catalan authority AGAUR 2014SGR1344, ICREA under the ICREA Academia Award.

References

- [1] R. Urteaga et al., Langmuir, 29 (2013) 2784.
- [2] E. Elizalde et al., Physical Review Letters, 112 (2014) 134502.

Figures

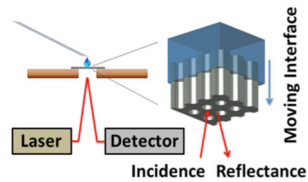


Figure 1: Scheme of the technique.

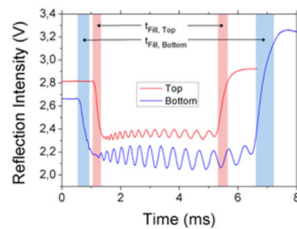


Figure 2: Example of the measured magnitude.

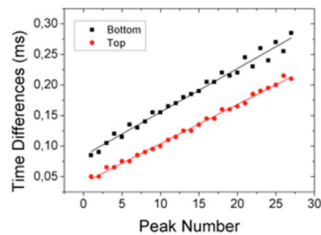


Figure 3: Fitting for radius determination.

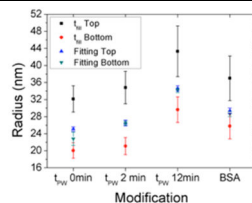


Figure 4: Comparison of the two techniques.

# Low-loss, Nonlinear BaTiO<sub>3</sub>-Si-Photonic Waveguide Structures

F. Eltes<sup>1</sup>, D. Caimi<sup>1</sup>, F. Fallegger<sup>1</sup>, M. Sousa<sup>1</sup>, E. O'Connor<sup>1</sup>, M. D. Rossell<sup>2</sup>, B. Offrein<sup>1</sup>, J. Fompeyrine<sup>1</sup> and S. Abel<sup>1</sup>

<sup>1</sup>IBM Research – Zurich, Switzerland

<sup>2</sup>Electron Microscopy Center, EMPA, Switzerland

fee@zurich.ibm.com

Barium titanate (BaTiO<sub>3</sub>) has become an attractive material to extend the functionalities of the silicon photonics platform because of its large Pockels coefficient of more than 1000 pm/V. BaTiO<sub>3</sub> integrated epitaxially on silicon-on-insulator (SOI) substrates, using SrTiO<sub>3</sub> seed layers, can be structured in active and passive silicon photonic devices using slot-waveguide geometries (Fig. 1a). However, all devices demonstrated so far suffer from high optical propagation losses of ~40 – 600 dB/cm [1,2,3], which limits their performance compared with state-of-the-art silicon photonics devices (< 2 dB/cm). Reported losses of 4 dB/cm in waveguides fabricated made from BaTiO<sub>3</sub> layers deposited on magnesium oxide substrates [4] indicate that BaTiO<sub>3</sub> thin films do not suffer intrinsically from high propagation losses. In this work, we carefully studied various contributions to the propagation losses in hybrid BaTiO<sub>3</sub>/Si waveguides to ultimately identify and eliminate the reason for the losses. In particular, we used various waveguide geometries, process conditions, and post-fabrication annealing treatments to separate loss channels arising from scattering and absorption in the different materials and at their interfaces. We measured the propagation losses at various steps during the fabrication of the slot waveguides, using SiO<sub>2</sub> strip-loaded waveguides (Fig. 1b).

We identified a strong optical absorption of more than 10,000 dB/cm in the thin SrTiO<sub>3</sub> seed layer as the major source of these large propagation losses. When manufacturing slot-waveguide structures, the BaTiO<sub>3</sub>/SrTiO<sub>3</sub> layer stack is typically exposed to

hydrogen during integration of the top silicon layer, which is done by either direct wafer bonding or chemical vapor deposition. Control experiments together with X-ray photoelectron spectroscopy confirm that the hydrogen is incorporated in the SrTiO<sub>3</sub>-layer making it absorbing. In contrast, absorption effects in the BaTiO<sub>3</sub> layer are negligible. We demonstrate that a low-temperature anneal is sufficient to remove hydrogen and to achieve low propagation losses in waveguides. This annealing process allowed us to fabricate BaTiO<sub>3</sub>-Si waveguides with only 6 dB/cm propagation losses. Low-loss ring resonators with a radius of 75 μm with well-defined resonances and a quality factor of Q > 20,000 (Fig. 1c) demonstrate the usability of the BaTiO<sub>3</sub>-Si hybrid waveguides. Thus, we found a way to eliminate the previously observed showstopper for incorporating functional and highly nonlinear BaTiO<sub>3</sub> films in silicon photonic structures, ultimately enabling ultra-high-speed switches and novel nonvolatile optical devices.

## References

- [1] C. Xiong et al., Nano Letters, vol. 14(2014), pp. 1419–1425.
- [2] S. Abel, Ph.D. dissertation, Univ. Grenoble, France, 2014.
- [3] S. Abel et al., J. Light. Technol. 2015, 34 (8), 1688–1693.
- [4] D. M. Gill et al., Appl. Phys. Lett. 1996, 69 (20), 2968–2970.

## Figures

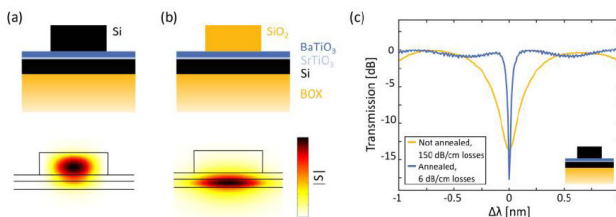


**Figure 1:** Schematics of (a) the cross section of the target slot-waveguide geometry, and (b) the SiO<sub>2</sub> strip-loaded waveguide geometry that was used to investigate partially processed structures. For comparison, the magnitude of the Poynting vector of the optical modes is shown. (c) Comparison of ring resonator (ø 75 μm) spectra before and after annealing. The inset shows the waveguide cross section.

# Experimental and numerical demonstration of a plasmonic nanoantenna embedded in a silicon waveguide gap

Alba Espinosa-Soria, Amadeu Griol, Alejandro Martínez

Nanophotonics Technology Center, Universitat Politècnica de València, Spain

alesso@ntc.upv.es

Plasmonic nanoantennas have been integrated in dielectric waveguides in recent experiments. If the metallic nanostructure is placed on top of the waveguide [1], the excitation of the nanostructure by the evanescent tail of the waveguide mode is enabled, that results in small interaction efficiencies (<10%) and low power contrasts (< 2) between maxima and minima at the waveguide output. Moreover, the output power depends on the response of the waveguide-nanostructure system, since the evanescent field of the waveguide top boundary contains a remarkable longitudinal component [2] and this prevents to properly identify the performance of the isolated nanostructure.

In this work, we present and demonstrate a new strategy to illuminate and measure the response of isolated subwavelength metallic nanostructures integrated in a silicon photonics circuit. Our concept is schematically described in Fig. 1. A very small gap separates two silicon waveguides with rectangular cross-section, being the plasmonic nanostructure placed in the middle of it, that ensures a maximum interaction of the propagating light field with the nanostructure [3]. When illuminated, part of the light scattered by the nanostructure will be emitted towards the input port (backscattering) or towards the output port (forward scattering), being the rest of scattered field radiated out of the waveguide. Besides, the metallic nanostructure can also absorb a large amount of the incoming power, especially when an LSP resonance is excited. Additionally, the nanostructure response is characterized by a crossing between the transmission and reflection spectra in the wavelength region close to the LSPR, that can be considered as a signature of the excitation of the LSP resonance.

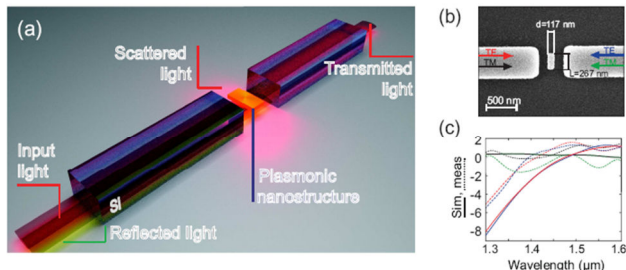
In summary, we demonstrate numerically and experimentally

[4] that embedding a plasmonic nanoantenna in a silicon waveguide gap enables the full excitation of the nanostructure, rising a high interaction efficiency and achieving a contrast beyond 10 dB in transmission (50 dB in numerical simulations). This results pave the way for exploiting the properties of isolated nanoantennas and plasmonic resonators in applications including biosensing or switching.

## References

- [1] I. Alepuz-Benache, C. García-Meca, F. J. Rodríguez-Fortuño, R. Ortuño, M. Lorente-Crespo, A. Griol, and A. Martínez, "Strong magnetic resonance of coupled aluminum nanodisks on top of a silicon waveguide," Proc. SPIE 8424, Nanophotonics IV (2012) 84242J.
- [2] A. Espinosa-Soria and A. Martínez, "Transverse spin and spin-orbit coupling in silicon waveguides," <http://arxiv.org/abs/1507.04859>
- [3] M. Castro-Lopez, N. de Sousa, A. Garcia-Martin, F. Y. Gardes, and R. Sapienza, "Scattering of a plasmonic nanoantenna embedded in a silicon waveguide.," Opt. Express, 23 (2015) 28108–18.
- [4] A. Espinosa-Soria, A. Griol, and A. Martínez, "Experimental measurement of plasmonic nanostructures embedded in silicon waveguide gaps," Opt. Express, 24 (2016) 9592-9601.

**Figure 1:** (a) Scheme of the proposed structure. (b) SEM image of the fabricated structure. (c) Simulated and measured transmission spectra.



## Beam polarimetry using silicon nanoantennas

alesso@ntc.upv.es

Polarization is a fundamental property of electromagnetic waves. Knowing the state of polarization (SoP) is an essential requirement in several disciplines as chemistry, astronomy and optical communications. It has been recently shown that the polarization of the source exciting a guided wave via near-field coupling plays a key role in determining the propagation direction of the guided wave. This behaviour can be useful to characterize the state of polarization of an incoming light beam using, for instance, dielectric scatterers (acting as nanoantennas) coupled to silicon waveguides. In [1,2] we exploit this concept to create two types of nanoantenna, first type is used to characterize linear polarization and the second type can resolve the handedness (or spin) of a circularly polarized light.

Using these tools, we present a silicon on-chip polarization analyzer working at telecom wavelengths that allows for a direct measurement of the state of polarization of an incoming light beam. This polarization analyzer obtains the SoP on the basis of the Stokes parameters. Taking advantage of the polarization-dependent characteristics of the nanoantennas described above, only three nanoantennas (two for lineal polarization and one for circular polarization) are required for full description of the four Stokes parameters defining the SoP of the incident light beam.

We have a six outputs device, where direct combination of the power at each output result in

the four Stokes parameters. However, we also present a method to reduce this scheme, achieving the same result with only four outputs. This system is based on the same principle, we need a scatterer for coupling the incoming light into the four waveguides as a result of the spin-orbit interaction taking place in the evanescent region of the silicon waveguides, and a proper study of the scatterer shape and position to be polarization-dependent is needed to. Ensuring these conditions, we achieved a universal approach, valid for any wavelength range and technological platform.

The proposed technology allows high level of integration, and the methodology outlined allows a quick analysis of the incoming SoP in real time and over an ultrabroad bandwidth, and due to the small scattering losses, it could be used in an in-line configuration. Due to all this properties, our device could find application in polarimetry, spectrometry or high speed optical communications.

### References

- [1] F. J. Rodríguez-Fortuno, I. Barber-Sanz, D. Puerto, A. Griol, and A. Martínez, *ACS Photonics*, 9 (2014) 762–767.
- [2] F. J. Rodríguez-Fortuno, D. Puerto, A. Griol, L. Bellieres, J. Martí, and A. Martínez, *Opt. Lett.*, 6 (2014) 1394–1397.

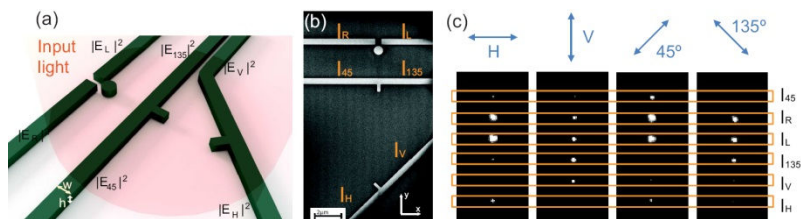


Figure 1: (a) Scheme of the proposed structure. (b) SEM image of the fabricated sample. (d) Experimental measurements verifying the performance of the device for linear input polarizations.

# Theoretical prediction of levitation due to Casimir force of plane-parallel systems made of realistic materials

V. Esteso, S. Carretero-Palacios, H. Míguez

Multifunctional Optical Materials Group, Instituto de Ciencia de Materiales de Sevilla, Consejo Superior de Investigaciones Científicas - Universidad de Sevilla, Spain

victoria.esto@csic.es

As Lifshitz predicted [1, 2], Casimir force ( $F_C$ ) may be repulsive between two materials spaced by another one at nanoscale. Taking into account the influence of gravity ( $F_g$ ) and the buoyancy forces ( $F_B$ ), the balance of the three forces may lead to levitation phenomena which is extremely relevant in micro- and nano- electromechanical devices for controlling friction, stiction and adhesion [3]. Although the geometry sphere-plane has been widely studied [4], we consider the less analysed plane-parallel system, consisting of a thin film immersed in a fluid over a substrate.

Herein, we theoretically predict that, in thermal equilibrium at room temperature, thin films of realistic materials such as teflon, silica ( $SiO_2$ ), and polystyrene (PS) immersed in glycerol, stands over a substrate of silicon at stable or unstable equilibrium distance ( $d_{eq}$ ), i.e.  $\vec{F}_C(d_{eq}) + \vec{F}_g + \vec{F}_B = 0$ . (See Fig. 1). In addition, we analyse how that ( $d_{eq}$ ) is affected by slight variations of temperature ( $T$ ) around room temperature due to the dependence of  $F_C$  on  $T$  [5, 6].

Moreover, since the magnitude and nature of Casimir force depends on the dielectric permittivity of all the materials in the system, it is able to control the equilibrium distance by mean of the optical properties of materials that compound the system. Because of that, we studied the magnitude and stability of the equilibrium distances in two plane-parallel systems where the thin film is replaced by a film made of a hybrid material whose components present Casimir forces and equilibrium distances of

opposite nature. In the first one, the hybrid material is made up of two individual thin films of different materials (bilayer system), and in the second one, it is a slab that comprise a homogeneous matrix with small inclusions inside occupying a volume fraction ( $f$ ) (composite system [7]).

All these plane-parallel systems show equilibrium distances of few hundreds of nanometres that can be controlled through the thickness of each thin film and the volume fraction. The possibility of tuning the equilibrium distances makes these kind of systems a potential ones for controlling friction, stiction and adhesion in plane-parallel geometry at nanoscale.

## References

- [1] I. E. Dzyaloshinskii, E. M. Lifshitz, L. P. Pitaevskii, Adv. Phys. 10 (1961) 165-209.
- [2] E. M. Lifshitz, Sov. Phys. JETP, 2 (1956) 73.
- [3] H. B. Chan, V. A. Aksyuk, R. N. Kleiman, D. J. Bishop, F. Capasso, Science, 291 (2001) 1941.
- [4] J. N. Munday, F. Capasso V.A. Parsegian, Nature, 457 (2009) 170.
- [5] V. Esteso, S. Carretero-Palacios, H. Miguez, J. Phys. Chem. C, 119 (2015) 5663-5670.
- [6] V. Esteso, S. Carretero-Palacios, H. Miguez, J. Appl. Phys. 119 (2016) 144301.
- [7] R. Esquivel-Sirvent, C. G. Schatz, Phys. Rev. A, 83 (2011) 042512.

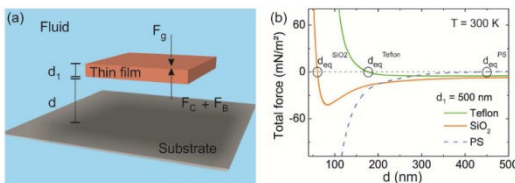


**Figure 1:** (a) Schematic of the plane-parallel system where  $d$  is the distance between the thin film and the substrate and  $d_1$  the thickness of the thin film.  $F_C$ ,  $F_g$  and  $F_B$  are the Casimir, the gravity, and the buoyancy forces, respectively. (b) Force balance as function of  $d$  for a thin film of 500 nm of thickness made of three different materials: Teflon (green),  $SiO_2$  (orange), and PS (blue). The substrate and the fluid are considered to be silicon and glycerol, respectively.  $d_{eq}$  is the value of  $d$  at which the balance of the forces is zero.



# The influence of the internal structure in the resonant properties of poly-crystalline silicon microspheres

R. Fenollosa<sup>1</sup>, M. Garín<sup>2</sup>, F. Meseguer<sup>1</sup>

<sup>1</sup>Instituto de Tecnología Química (CSIC-UPV), Universidad Politécnica de Valencia, Spain

<sup>2</sup>Universitat Politècnica de Catalunya, Dep. D'Enginyeria Electrònica, Spain.

rfenollo@ter.upv.es

Silicon microspheres are promising technological platforms for developing applications in different fields of technology, such as metamaterials and opto-electronics [1,2]. The strength of this material resides in its capability of confining light thanks to its high refractive index, which yields the possibility of achieving high Q Mie resonances. Recently, a technological application consisting of a silicon spherical Mie resonator photodiode has been developed [3] ([Fig. 1 (a)]. Such photodiode can absorb infrared light efficiently at the band-gap edge of silicon, at wavelengths above 1200 nm, thanks to the resonance phenomenon in the spherical microcavity. The richly peaked spectra of the photocurrent confirms this fact [Fig. 1 (b)]. However, such spectra could not be precisely fitted to Mie theory. We have found that the internal structure of the microspheres is the reason of this discrepancy. The HRTEM image of Fig. 1 (c) shows that poly-crystalline silicon microspheres contain in fact an onion-like distributed porous structure, surrounded by a non-porous shell. This makes that although high Q modes could in principle resonate at the non-porous shell, other modes whose electromagnetic field distribution overlaps the porous structure, such as mode  $b_{13,5}$  for instance [superimposed in Fig. 1 (c)], are expected to be killed. This fact was confirmed by optical scattering measurements performed at 90°. Based on these results, different crystallization procedures for avoiding the porous structure have been developed.

## References

- [1] F. Meseguer, R. Fenollosa, I. Rodríguez, E. Xifré-Pérez, F. Ramiro-Manzano, M. Garín, M. Tymczenko, *J. Appl. Phys.*, 109 (2011) 102424.
- [2] I. Kuznetsov, A. E. Miroshnichenko, Y. H. Fu, J. Zhang, B. Luk'yanchuk, *Sci. Rep.*, 2 (2012) 492.
- [3] M. Garín, R. Fenollosa, R. Alcubilla, L. Shi, L.F. Marsal, F. Meseguer, *Nat. Comm.*, 5 (2014) 3440.

## Figures

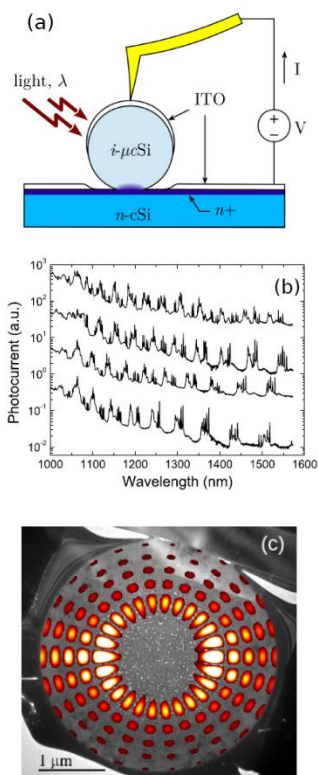


**Figure 1:** (a) Scheme of a photodiode based on a silicon microsphere, (b) measured spectral response (short circuit current) of several devices corresponding to different sphere diameters. The sharp peaks correspond to Mie resonances, (c) HRTEM image of the internal surface of a poly-crystalline silicon microsphere showing the porous structure at the core. The electric field intensity distribution of mode  $b_{13,5}$  has been superimposed.

# Photonics and applications with semiconductor nanowires

anna.fontcuberta-morral@epfl.ch

Semiconductor nanowires are filamentary crystals with a tailored diameter in the range between few and ~100 nm. Thanks to their special shape and size they have shown to exhibit extremely special properties, including anisotropic light absorption and emission, and resonant absorption phenomena depending on the nanowire diameter and position with respect to the excitation source [1-4].

In this talk I will start reviewing what optical properties of nanowires render them ideal building blocks for next generation solar cells [4,5]. I will then show how these properties can also be suppressed or modified by associating the nanowires with tailored metallic nanostructures [6,7]. Finally, I will show how NW systems can certainly bring progress to the use of nanowires for next generation solar cells and proposed a new concept for a spectral-splitting and multi-junction solar cells [8].

## References

- [1] J. Wang, M.S. Gudiksen, X.F. Duan, Y. Cui, C. M. Lieber, Highly polarized photoluminescence and photodetection from single indium phosphide nanowires *Science* 293, 1455 (2001).
- [2] L.Y. Cao, J.S. White, J.S. Park, J.A. Schuller, B.M. Clemens, M.L. Brongersma, Engineering light absorption in semiconductor nanowire devices, *Nature Mater.*, 8, 643-637, (2009).
- [3] G. Grzela, R. Paniagua-Dominguez, T. Barten, Y. Fontana, J.A. Sanchez-Gil, J.G. Rivas Nano Nanowire antenna emission *Letts.* 12, 5481 (2012).
- [4] P. Krogstrup, H.I. Jorgensen, M. Heiss, O. Demichel, J.V. Holm, M. Aagesen, J. Nygard, A. Fontcuberta i Morral, Single-nanowire solar cells beyond the Shockley-Queisser limit. *Nat. Photonics* 7 306-310 (2013).
- [5] M. Heiss, et al, III-V nanowire arrays: growth and light interaction *Nanotech* 25, 0140015 (2014).
- [6] A. Casadei, E. Alarcon-Llado, F. Amaduzzi, E. Russo, D. Ruffer, M. Heiss, L. Dal Negro and A. Fontcuberta i Morral, Polarization response of nanowires à la carte. *Scientific Reports*, 5, 7651 (2015).
- [7] M. Ramezani, A. Casadei, G. Grzela, F. Matteini, G. Tütüncüoğlu, A. Fontcuberta i Morral, J. Gomez-Rivas Hybrid semiconductor nanowire-metallic Yagi-Uda antennas, *Nano Letters*, 15, asap (2015).
- [8] A. Dorodnyy, E. Alarcon-Lladó, V. Shklover, C. Hafner, A. Fontcuberta i Morral, J. Leuthold, Efficient multi-terminal spectrum splitting via a nanowire array solar cell, 2, 1284 (2015).

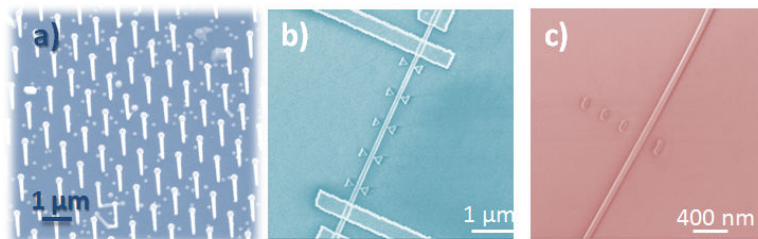


**Figure 1:** Scanning electron micrographs of a) an array of GaAs nanowires; a nanowire device with embedded bow-tie antennae (b) and a Yagi-Uda antenna (c).

# An RCE based NIR PD using a resonant cavity with dual grating mirrors

<sup>1</sup>Sami Shamoon College of Engineering, Department of Electrical and Electronics Engineering, Israel

<sup>2</sup>Ben-Gurion University of the Negev, Department of Electrical Engineering, Israel

\*moshezo@ac.sce.ac.il

Two grating mirror structures are considered for a dielectric Fabry Perot cavity within Resonant Cavity Enhanced (RCE) Near Infrared (NIR) photodetector to enhance the optical absorption in a thin semiconductor layer embedded within the cavity [1-2]. In this design, the front and back mirrors are gratings structures with Pitches comparable to subwavelength dimensions, which act as nearly perfect retroreflectors. Semi-analytical calculations, computer aided design and simulations were performed for application in a NIR wavelength band, based on a Si absorbing layer. The results indicate that this new type of cavity meets the combined challenges of significantly increasing the absorption efficiency and reducing the overall complexity of the

entire device, when compared to a conventional resonant cavity, in which both mirrors are formed from quarter-wavelength multilayer stacks (DBR mirrors). The results obtained for the graph and structures shown below:

## References

- [1] M. Zohar, M. Auslender and S. Hava, Nanoscale, 12 (2015) pp. 5476-5479.
- [2] M. S. Ünlü and S. Strite, J. Appl. Phys., 2 (1995) pp. 607-639.

Structure Type	$t_{gB}$	$d_b$	$t_a$	$d_f$	$d_{Si_3N_4}$	$t_{gF}$	$\Lambda$	W	Absorbance $A(\lambda_0)$ peak	Structure Thickness
RCE-1	-	0.069	<b>0.150</b>	0.030	-	-	-	-	<b>0.529</b>	3.065
2G-RCE-TE-1	0.120	0.130	<b>0.150</b>	1.710	0.792	0.305	0.439	0.252	<b>0.999</b>	3.307

## Figures

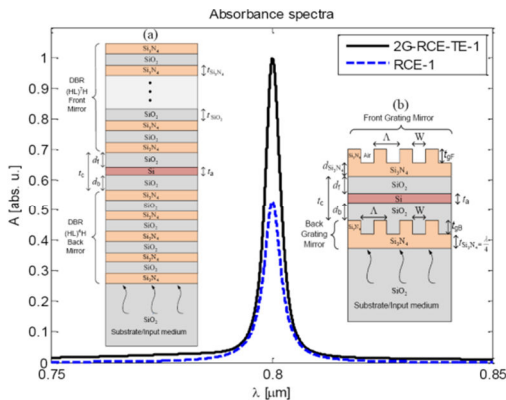


**Figure 1:** The scheme describes the RCE detector structure of (a) conventional structure designed to operate in the NIR range; (b) RCE detector structure with two Si<sub>3</sub>N<sub>4</sub> based grating mirrors in place of the DBR mirrors. The full line represents the absorption spectrum of an optimized conventional detector design RCE-1; the dashed line represents the absorption spectrum of our proposed structure 2G-RCE-TE-1, both structures having an active layer thickness of 150 nm ( $\lambda_0 = 0.8 \mu\text{m}$ ).

# Photonic colloidal crystals as nano-sand: lab-on-a-chip to study water in granular media

**Francisco Gallego-Gómez,**  
Alvaro Blanco, Cefe López

Instituto de Ciencia de Materiales de Madrid,  
CSIC, Madrid, Spain

francisco.gallego@icmm.csic.es

Solid particles ensembles inherently contain water adsorbed from the ambient moisture. This water, confined in the interstices between the building grains, greatly affects the ensemble properties. Inversely, one can benefit from such influence on collective features to explore the water behavior in such confinements. However, little is known about the behavior of water in small environments, in spite of its relevance in many areas of materials science nowadays. We have developed novel approaches to investigate in-depth where and how water is placed in the nanometric pores of self-assembled colloidal crystals [1]. Above all, their photonic properties are significantly affected by the water, not only by its content but also by its distribution. This fact renders the colloidal crystal a suitable *'lab-on-a-chip'* to study the water morphology within the porous network, and provides a simple but powerful tool to address fundamental aspects of nanoconfined water [2-5]. I summarize these advances, which are linked to general interfacial water phenomena like adsorption, capillary forces and surface flow, and, importantly, to the interplay between nanoconfined water and solid fine particles that determines the behavior of ensembles. I describe how the knowledge gained on water in colloidal crystals provides new opportunities for multidisciplinary study of interfacial and nanoconfined liquids and their essential role in the physics of utmost relevant systems such as particulate media [6]. A latest project searches for original links to granular materials, from powders to soils, for which colloidal crystals are proposed as a novel model system, in particular, through their micromechanical properties [7]: a kind of *'nano-sand'* with promising utilities.

---

## References

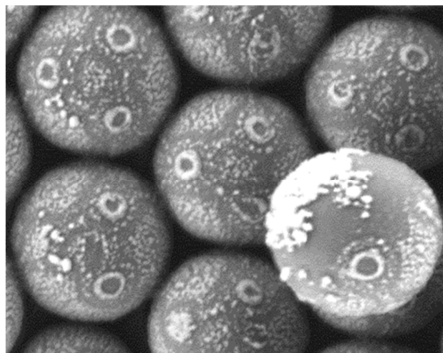
---

- [1] Gallego-Gómez F, Blanco A, López C. Adv. Mater. (Progress Report) 7 (2015), 2686–2714.
- [2] Gallego-Gómez F, Blanco A, Canalejas-Tejero V, López C. Small 7 (2011), 1838-1845.
- [3] Gallego-Gómez F, Blanco A, López C. Adv. Mater. 24 (2012), 6204–6209.
- [4] Gallego-Gómez F, Blanco A, López C. J Phys Chem. C 116 (2012), 18222-18229.
- [5] Blanco A, Gallego-Gómez F, López C. J. Phys. Chem. Lett.. 4 (2013), 1136–1142.
- [6] Gallego-Gómez F, Morales-Flórez V, Morales M, Blanco A, López C. Adv. Colloid Interface Sci. (2016),1-23 (to be published).
- [7] Gallego-Gómez F, Morales-Flórez V, Blanco A, de la Rosa-Fox N, López C. Nano Lett. 12 (2012), 4920-4924.

---

## Figures

---



# High-index contrast waveguides in potassium double tungstates: towards rare-earth ion doped on-chip integrated photonics

Mustafa A. Sefunc, Jinfeng Mu, Meindert Dijkstra, Frans Segerink,  
**Sonia M. García-Blanco**

Optical Sciences Group, MESA+ Institute for Nanotechnology, University of Twente, The Netherlands

s.m.garciablanco@utwente.nl

In recent years, low-contrast waveguides in rare-earth ion doped potassium double tungstate crystalline material have enabled the demonstration of very efficient (>80%)[1] waveguide lasers exhibiting high output power (1.6 W in a  $\text{Tm}^{3+}$  doped waveguide[1] and >650 mW in an  $\text{Yb}^{3+}$  doped device) [2]. Tunability over 55 nm bandwidth was demonstrated by the use of an external grating [3]. The wavelength of Er [3] doping is currently being studied for on-chip amplification in the C-band [4]. Ytterbium ( $\text{Yb}^{3+}$ ) and thulium ( $\text{Tm}^{3+}$ ) have been studied in recent years for laser operation wavelengths around 1 and 2  $\mu\text{m}$  respectively. The great performance of these devices is due to the combination of material properties, such as the high absorption and emission cross-sections of the rare-earth ions doped into this crystalline host material, the high dopant concentration that can be utilized due to the large ( $\sim 0.5$  nm) interionic spacing defined by the crystal lattice and a long excited state lifetime (from >260  $\mu\text{s}$  in  $\text{Yb}^{3+}$  to a few milliseconds in  $\text{Er}^{3+}$ ), with waveguide configuration, which increases the field intensity inside the waveguide core. Those factors increase the achievable modal gain, permitting the realization of low threshold high slope efficiency devices.

However, the aforementioned demonstrations utilized doped  $\text{RE:KY(WO}_4)_2$  layers epitaxially grown onto undoped  $\text{KY(WO}_4)_2$  substrates, leading to relatively large waveguide cross-sections. The large mode supported by those waveguides increases the power requirement for both the inversion of the gain material and the observation of non-linear effects. Furthermore, the size of the devices is large (i.e., centimeter range), not being suitable for on-chip integration onto passive photonic platforms such as silicon-on-insulator (SOI) and  $\text{Si}_3\text{N}_4/\text{SiO}_2$ .

In this presentation, the recent advances towards the realization of high-index contrast waveguides [5] in rare-earth ion doped  $\text{KY(WO}_4)_2$  will be given as

well as two potential integration schemes to SOI and  $\text{Si}_3\text{N}_4/\text{SiO}_2$  platforms [6]. These realizations represent the first milestones towards the demonstration of very efficient on-chip active devices in this material, which will permit the realization of novel integrated devices exploiting its excellent gain and non-linear properties.

---

## References

---

- [1] K. van Dalfsen, S. Aravazhi, C. Grivas, S. M. García-Blanco, M. Pollnau, "Thulium channel waveguide laser with 1.6 W of output power and  $\sim 80\%$  slope efficiency," *Opt. Lett.* 39, 4380-4383 (2014).
- [2] D. Gekus, E. H. Bernhardt, K. van Dalfsen, S. Aravazhi, M. Pollnau, "Highly efficient  $\text{Yb}^{3+}$ -doped channel waveguide laser at 981 nm," *Opt. Express* 21, 13773-13778 (2013).
- [3] D. Gekus, S. Aravazhi, K. Wörhoff, M. Pollnau, "High-power, broadly tunable, and low-quantum-defect  $\text{KGd}_{1-x}\text{Lu}_x(\text{WO}_4)_2:\text{Yb}^{3+}$  channel waveguide lasers," *Opt. Express* 18, 26107-26112 (2010).
- [4] S. A. Vázquez-Córdova, M. Dijkstra, E. H. Bernhardt, F. Ay, K. Wörhoff, J. L. Herek, S. M. García-Blanco, M. Pollnau, "Erbium-doped spiral amplifiers with 20 dB of net gain on silicon," *Opt. Express* 22, 25993-26004 (2014).
- [5] M.A. Sefunc, F.B. Segerink, S.M. García-Blanco, "High index contrast potassium double tungstate waveguides towards efficient rare-earth ion amplification on-chip," *Proc. SPIE* 9365, 93650P (2015).
- [6] J. Mu, M. A. Sefunc, M. Dijkstra, S. M. García-Blanco, "Design and fabrication of adiabatic vertical couplers for hybrid integration by flip-chip bonding," *Proc. SPIE* 9750, 975012 (2016).

# Silicon Photonic Integrated Mode Converter and Multiplexer for Few-Mode Fiber at 1550 nm

David García-Rodríguez, Juan L. Corral, Amadeu Griol and Roberto Llorente

Valencia Nanophotonics Technology Center, Universitat Politècnica de València, Spain

dgarciarodriguez@ntc.upv.es

Recently, significant research efforts have been focused on increasing optical fiber transmission capacity due to the rising demand of information transmission. The standard single mode fiber (SSMF) worldwide deployed operates exclusively in the infra-red band (1.3  $\mu\text{m}$ -1.6  $\mu\text{m}$ ). Although the exploitable capacity in the infra-red band is substantial, it is showing signs of exhaustion even when using modern modulation schemes [1].

Mode-division multiplexing (MDM) is a good solution to overcome the limit on the fiber optics capacity. A mode (de)multiplexer to combine and split the modes at a certain wavelength is needed [1-2]. Different techniques have been proposed to convert and (de)multiplex the modes; for example, free space optics, liquid crystal on silicon (LCOS), directional couplers (DC), asymmetrical directional couplers (ADC) and long-period fiber Bragg gratings (LPFBG).

ADCs are a compact solution that allow to excite the higher order mode from the fundamental one. Different devices have been reported operating at wavelengths around 1550 nm [3,4] employing fibre-waveguide coupling. Mode conversion is induced by matching the effective index of the  $\text{TE}_1$  mode in the waveguide 2 and the effective index of the  $\text{TE}_0$  mode in the waveguide 1[5], as depicted in Fig. 1.

Depending on the selected fabrication technology, different options for the waveguide-fiber coupling have been considered. In Silicon-On-Insulator (SOI) technology, vertical coupling through a grating coupler or lateral coupling can be used. In this case, the grating coupler offers low losses [6] and the light coupling is less difficult compared with the horizontal case due to the huge difference between the dimensions of the fiber and the waveguide. Planar Lightwave Circuit (PLC) offers a lateral coupling with lower losses but at the expenses of a higher size and less compatibility with active photonic and electronic devices.

Grating couplers based on SOI are an interesting option to efficiently couple the  $\text{TE}_0$  and  $\text{TE}_1$  waveguide modes to the different modes of a Few Mode Fiber (FMF) [7]. Different techniques have been proposed to excite the  $\text{LP}_{11}$  mode in the FMF, like exciting one or several grating couplers with different copies of the  $\text{TE}_0$  signal with the appropriate phases [8].

We propose and demonstrate a mode converter and multiplexer based on an asymmetrical directional coupler (ADC) fabricated in SOI technology, to couple simultaneously the  $\text{TE}_0$  and  $\text{TE}_1$  modes to the  $\text{LP}_{01}$  and  $\text{LP}_{11}$  modes directly in a Two Mode Fiber (TMF) through one single grating coupler.

Acknowledgments: This work has been partially supported by Spanish Ministerio de Economía y Competitividad under Project RTC-2014-2232-3 HIDRASENSE and Spain National Plan project XCORE TEC2015-70858-C2-1-R.

## References

- [1] J.J. Benson Jr et al., "Striding Optical Transport Technologies to mitigate a Cyclical Capacity Crunch," Proc. OFC, OTh4B.7, Anaheim (2013).
- [2] T. Uematsu et al., "Low-loss and broadband PLC-type mode (de)multiplexer for mode-division multiplexing transmission", Proc. OFC, OTh1B.5, Anaheim (2013).
- [3] J. Wang et al., "On-chip silicon 8-channel hybrid (de)multiplexer enabling simultaneous mode and polarization-division-multiplexing", Laser Photonics Rev. 8, No. 2, L18-L22 (2014).
- [4] D. Dai et al., "Silicon mode (de)multiplexer enabling high capacity photonic networks-on-chip with a single-wavelength-carrier light", Optics Letters, Vol. 38, no. 9, pp. 1422-1424 (2013).
- [5] N. Hanzawa et al., "Mode multi/demultiplexing with parallel waveguide for mode division multiplexed transmission", Optics Express, Vol. 22, no. 24, pp. 29321-29330 (2014).
- [6] D. Dai et al., "Multi-channel Silicon Mode (de)multiplexer based on Asymmetrical Directional Couplers for on-chip Optical Interconnects", IEEE Photonics Society, vol. 28, no. 2, (2014).
- [7] A. Li et al., "Fabrication of Low Loss Fused Fiber Spatial-Mode Coupler for Few-Mode Transmission", Photon. Technol. Lett., Vol. 25, no. 20, pp. 1985-1988 (2013).
- [8] B. Wohlfei et al., "Compact Fiber Grating Coupler on SOI for Coupling of Higher Order Fiber Modes", Proc. OFC, OTh1B.2 (2013).

**Figures**

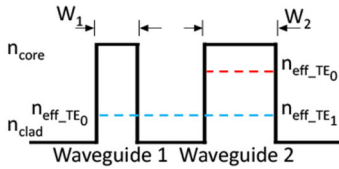


**Figure 1:** Refractive index profile for mode coupling between  $TE_0$  and  $TE_1$  modes.

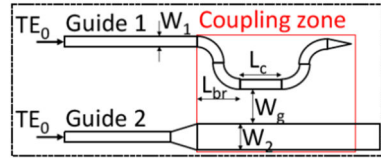


**Figure 2:** Schematic structure of a mode multiplexer based on Asymmetrical Directional Coupler (ADC).

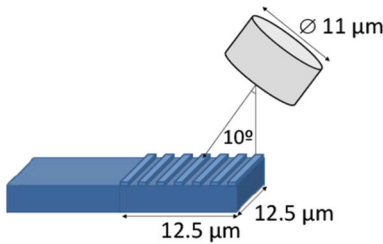


**Figure 3:** Output grating designed to couple the  $LP_{01}$  and  $LP_{11}$  modes in the few-mode fiber (FMF)

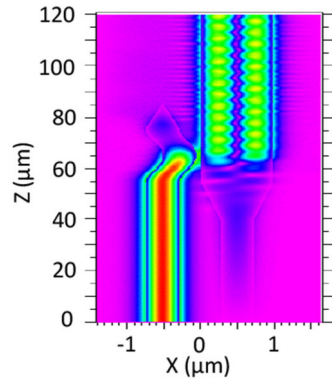


**Figure 4:** BPM simulation of a mode multiplexer based on Asymmetrical Directional Coupler (ADC).

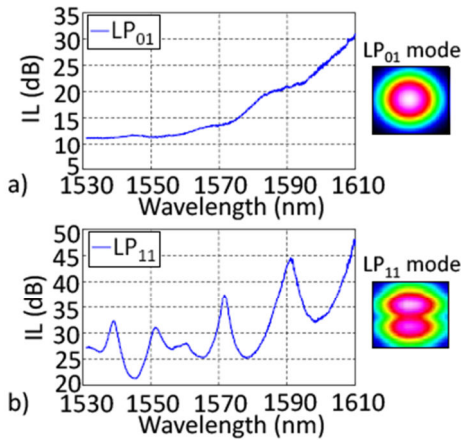


**Figure 5:** Insertion losses for  $LP_{01}$  and  $LP_{11}$  modes. The insets show the field coupled to the few mode fiber (FMF)

# Optical response of PMMA+Au<sub>2</sub> nanostructured metasurface composite over Silicon substrate

J.J. Gonzalez-Murillo<sup>1</sup>, Mauricio Moreno<sup>1</sup>, Albert Romano-Rodriguez<sup>1</sup>, Angel Rodriguez<sup>2</sup>, Carlos Calaza<sup>3</sup>

<sup>1</sup>Universitat de Barcelona, Spain

<sup>2</sup>Universitat Politècnica de Catalunya, Spain

<sup>3</sup>Institute of Microelectronics of Barcelona - CNM-CSIC, Spain

jjgonzalez@el.uib.edu

A nano-structured metasurface composite over a silicon substrate has been fabricated and experimentally tested as plasmonic device. The subwavelength building block was made in a 150nm SiO<sub>2</sub> layer on a silicon substrate coated with different thickness of PMMA. Through nanoimprint hot embossing, a 700nm square lattice of 500nm square patterns structure was imprinted in the PMMA coated Si+SiO<sub>2</sub> substrate. After the process, a layer of gold was sputtered over the embossed PMMA to achieve a metallic-dielectric surface. Optical reflection experiments were done, showing that the peak wavelength of the plasmonic device can be tuned by adjusting the thickness of the coated PMMA [1][2][3][4].

## References

- [1] A.Nemiroski, M. Gonidec, J. M. Fox, P. Jean-Remy, E. Turnage, and G. M. Whitesides, "Engineering shadows to fabricate optical metasurfaces" ACS Nano, vol. 8, no. 11, pp. 11061–70, Nov. 2014.
- [2] A. V Kildishev, A. Boltasseva, and V. M. Shalaev, "Planar photonics with metasurfaces.," Science, vol. 339, no. 6125, p. 1232009, Mar. 2013.
- [3] E. Cortes, L. Mochán, B. S. Mendoza, and G. P. Ortiz, "Optical properties of nanostructured metamaterials," Phys. status solidi, vol. 247, no. 8, pp. 2102–2107, Jun. 2010.
- [4] S. Collin, C. Sauvan, C. Billaudeau, F. Pardo, J. C. Rodier, J. L. Pelouard, and P. Lalanne, "Surface modes on nanostructured metallic surfaces" Phys. Rev. B, vol. 79, no. 16, p. 165405, Apr. 2009.

## Figures

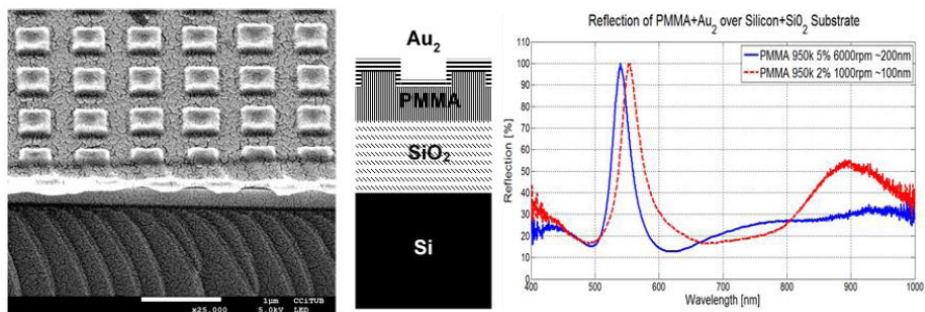


**Figure 1:** Structured metamaterial composite and its optical reflection response in the visible spectrum. SEM micrograph picture at 45° of the metamaterial (left), layer by layer building block (center) and Reflection of visible light of two different composites(right).



## Rhodium Nanocubes for plasmonics in the UV range

X. Zhang<sup>2</sup>, Y. Gutiérrez<sup>1</sup>, P. Li<sup>2</sup>, A. I. Barreda<sup>1</sup>, A. M. Watson<sup>3</sup>, R. Alcaraz de la Osa<sup>1</sup>, G. Finkelstein<sup>3</sup>, F. González<sup>1</sup>, D. Ortiz<sup>1</sup>, J. M. Saiz<sup>1</sup>, J. M. Sanz<sup>1</sup>, H. Everitt<sup>3,4</sup>, J. Liu<sup>2</sup> and F. Moreno<sup>1\*</sup>

<sup>1</sup>Departamento de Física Aplicada, Universidad de Cantabria, Spain

<sup>2</sup>Department of Chemistry, Duke University, USA

<sup>3</sup>Department of Physics, Duke University, USA

<sup>4</sup>Army Aviation and Missile RD&E Center, USA

\*morenof@unican.es

Extending nanoplasmonics to the UV-range constitutes a new challenge due to the increasing demand to recognize, detect and destroy biological toxins [1], to increase the efficiency of photocatalytic processes [2] or enhance biological imaging [3]. A study by J. M. Sanz et al. [4] analyzed several metals in order to find those more promising for UV-plasmonics. This work pointed out that those most promising were aluminum (Al), gallium (Ga) and rhodium (Rh). Aluminum has a bulk plasma frequency around 13 eV and a strong plasmonic response. However, nanoparticles made of this material suffer from oxidation [5], so it is difficult to manufacture effective and stable Al nanodevices. As a promising alternative, Ga nanoparticles have been recently proposed for Surface Enhancement Raman Scattering (SERS) experiments [6]. However, this metal presents a solid-liquid phase transition at room temperature that hinders its manipulation for other kind of applications. More recently, a numerical study has presented Rh [7] as one of the most promising metals, not only for its plasmonics behavior in the near UV, but also because it presents a low tendency to oxidation. Moreover, its easy fabrication through chemical means [7–9] (with sizes smaller than 10 nm), and its potential for photocatalysis applications, makes this material very attractive for building plasmonic tools for the UV.

In this contribution, we will show an overview of our collaborative research with rhodium nanocubes (NC) in the UV-range [9]. The electromagnetic behavior of Rh nanocubes of different sizes (ranging from 10 to 60 nm) has been numerically analyzed and compared with experimental measurements made by UV-VIS extinction spectroscopy. Because the chemical process does not produce perfect cubic shapes, other Rh cubic-based geometries have also been numerically studied, and their effect on the

LSPRs spectra of these deviations have been analyzed. In addition, for many applications it is interesting to use arrays of nanoparticles located on substrates because of the appearance of cooperative and coupling effects between particles. LSPRs spectra for these types of geometries have been also studied for different experimental configurations.

### References

- [1] Anker, J. N.; Hall, W. P.; Lyandres, O.; Shah, N. C.; Zhao, J.; Van Duyne, R. P.. *Nat. Mater.*, 7 (2008), 442–453.
- [2] Honda, M.; Kumamoto, Y.; Taguchi, A.; Saito, Y.; Kawata, S.. *J. Phys. D. Appl. Phys.*, 48 (2015), 184006.
- [3] Sharma, P.; Brown, S.; Walter, G.; Santra, S.; Moudgil, B.. *Adv. Colloid Interface Sci.*, 123-126 (2006), 471–485.
- [4] Sanz, J. M.; Ortiz, D.; Alcaraz de la Osa, R.; Saiz, J. M.; González, F.; Brown, a. S.; Losurdo, M.; Everitt, H. O.; Moreno, F.. *J. Phys. Chem. C*, 117 (2013), 19606–19615.
- [5] Knight, M. W.; King, N. S.; Liu, L.; Everitt, H. O.; Nordlander, P.; Halas, N. J.. *ACS Nano*, 8 (2014), 834–840.
- [6] Wu, P. C.; Khoury, C. G.; Kim, T.-H.; Yang, Y.; Losurdo, M.; Bianco, G. V.; Vo-Dinh, T.; Brown, A. S.; Everitt, H. O.. *J. Am. Chem. Soc.*, 131 (2009), 12032–12033.
- [7] Alcaraz de la Osa, R.; Sanz, J. M.; Barreda, a. I.; Saiz, J. M.; González, F.; Everitt, H. O.; Moreno, F.. *J. Phys. Chem. C*, 119 (2015), 12572–12580.
- [8] Watson, A. M.; Zhang, X.; Alcaraz de la Osa, R.; Marcos Sanz, J.; González, F.; Moreno, F.; Finkelstein, G.; Liu, J.; Everitt, H. O.. *Nano Lett.* 15 (2015), 1095–1100.
- [9] Zhang, X.; Li, P.; Barreda, Á.; Gutiérrez, Y.; González, F.; Moreno, F.; Everitt, H. O.; Liu, J.. *Nanoscale Horiz.* 1 (2016), 75–80.

# Synthesis and optical trapping of colloidal quantum dot-based structures

Maria Acebrón<sup>1</sup>, Héctor Rodríguez-Rodríguez<sup>1</sup>, J. Ricardo Arias-González<sup>2</sup> and **Beatriz H. Juárez**<sup>1,2</sup>

<sup>1</sup>Department of Applied Physical-Chemistry, Universidad Autónoma de Madrid, Spain  
<sup>2</sup>IMDEA Nanoscience Foundation, Spain

beatriz.hernandez@imdea.org

Colloidal quantum dots (QDs) have an increasing role in bio-imaging and other diagnostic techniques due to their unique optical properties. In this talk the synthesis of several nanostructures combining QDs, metallic nanoparticles, and thermoresponsive organic or inorganic platforms will be presented [1,2]. These platforms can be manipulated in an optical trap, where plasmon-exciton interactions and photoinduced effects including light-assisted activation and bleaching are observed and characterized [3,4]. These studies emphasize the importance of surface chemistry in QDs. These systems combine the ability for thermal sensing and labeling, representing very interesting platforms for the design of thermal sensors in biological studies.

## References

- [1] A. Salcher, M. Nikolic, S. Casado, M. Velez, H. Weller and B. H. Juárez, "CdSe/CdS nanoparticles immobilized on pNIPAM-based microspheres" *Journal of Materials Chemistry*, 20, 1367–1374, (2010).
- [2] M. Acebrón et al. *ACS Appl. Mater. Interfaces*, 7, 12, 6935–6945, (2015).
- [3] S. Hormeño, N. G. Bastús, A. Pietsch, H. Weller, R. Arias-Gonzalez, B. H. Juárez, "Plasmon-Exciton interactions demonstrated by Optical Tweezers", *Nano Letters*, 11, 4742–4747, (2011).
- [4] S. Hormeño et al. "Laser Heating Tunability by Off-Resonant Irradiation of Gold Nanoparticles" *Small*, 10, 2, 376–384, (2014).

## Figures

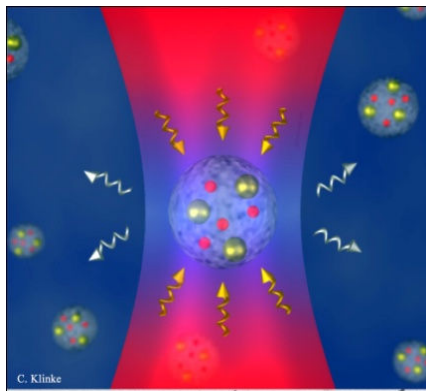


**Figure 1:** Sketch of a polymer bead decorated with colloidal quantum dots and gold nanoparticles trapped by optical tweezers.

Porous periodic multilayers have demonstrated their potential in several fields, from photovoltaics [1] to sensing [2], representing an ideal platform for large-scale devices. When applications dealing with light emission are considered, knowledge on how the local density of states (LDOS) is distributed within the multilayers is mandatory [3] in order to realize a judicious design which maximizes light matter interaction.

Using a combination of spin and dip-casting deposition techniques we report a detail study of how dyed polystyrene nanospheres ( $d=30\text{nm}$ ) constitute an effective LDOS probe to study its distribution within nanostructured photonic media [4].

This full solution process approach allows covering large areas with photonic coatings of outstanding optical quality. Further it permits incorporation of nanospheres with a diameter of 25 nm at well defined positions within nanostructured multilayers (Fig. 1a). In this manner we have placed a monolayer of such emitters at several positions of the structured sample (Fig. 1b). A combined use of photoluminescence (PL) spectroscopy and time resolved measurements are used to optically

characterize the multilayers. While the former shows how depending on the probe position its PL intensity can be enhanced or suppressed, the latter allows to probe the LDOS changes within the sample, monitored via changes in its lifetime. We demonstrate how information on the local photonic environment can be retrieved with a spatial resolution of 30 nm (provided by the probe size) and relative changes in the decay rates as small as ca. 1% (Fig. 1c), evidencing the possibility of exerting a fine deterministic control on the photonic surroundings of an emitter.

## References

- [1] C. López-López, S. Colodrero, M. E. Calvo and H. Míguez, *Energy Environ. Sci.*, **23**, 2805 (2013).
- [2] A. Jiménez-Solano, C. López-López, O. Sánchez-Sobrado, J. M. Luque, M. E. Calvo, C. Fernández-López, A. Sánchez-Iglesias, L. M. Liz-Marzán and H. Míguez. *Langmuir*, **28**, 9161 (2012).
- [3] N. Danz, R. Waldhäusl, A. Bräuer and R. Kowarschik, *J. Opt. Soc. Am. B*, **19**, 412 (2010).
- [4] A. Jiménez-Solano, J. F. Galisteo-López and H. Míguez, *Small*, **11**, 2727 (2015).

## Figures

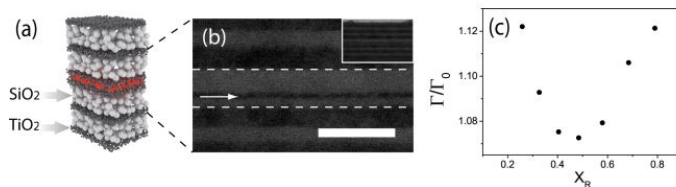


**Figure 1:** (a) Diagram of the fabricated samples. (b) SEM images obtained with backscattered electrons of a sample with a monolayer of spheres. (c) Evolution of the decay rate of the dye doped spheres (normalized to a reference sample) as their position is changed across the resonator.

# The Ultimate Limit of Photonic Scaling

**Juerg Leuthold**, Alexandros Emboras, Claudia Hoessbacher, Christian Haffner, Yuriy Fedoryshyn, Ueli Koch, Yannick Salamin, Christian Hafner

Institute of Electromagnetic Fields (IEF), ETH Zurich, 8092 Zurich, Switzerland

JuergLeuthold@ethz.ch

*Half a century of photonic research has led to a remarkable scaling of photonic footprint. We will review current state-of-the-art photonic devices and discuss recent advances in the field, including novel plasmonic devices and the emergence of new class of atomic scale devices.*

Scaling photonics devices towards a smaller footprint is a technological challenge. A challenge however, that might pay off with devices operating at higher speed, lower power consumption and with devices at an unmatched density.

Photonics has come a long way. In the early days of photonics - and to this very day - photonics often relies on assembling free space optical components into a larger system. Yet, only integrated optics offers optical devices with stable operation and economics of costs. And indeed, by now, integrated optics is dominating the communications, the sensing and entertainment markets, i.e. the markets where cost and scaling matter. And despite of the success integrated optical elements are not yet at the same scale as electronic components. As an example we will review the optical modulator. The optical modulator is a key element in every high-speed communications link. It is used to encode electrical signals onto an optical carrier. So far, the majority of optical modulators rely on the proven LiNO<sub>3</sub> technology. These modulators have footprints in the order of cm<sup>2</sup>. Fortunately, a few years ago, more compact silicon, InP and GaAs based modulators have emerged. These devices feature footprints in the order of mm<sup>2</sup> [1-3]. Yet, complementary metal-oxide semiconductor electronics (CMOS) house hundreds of transistors on a single μm<sup>2</sup>, making a co-integration of today's silicon MZMs with CMOS electronics impractical [4]. In pursuit of more compact silicon modulators, various approaches have been demonstrated. E.g. resonant ring modulators [5, 6] – which, however only work at discrete frequencies. Recently, plasmonics has drawn significant interest as an

alternative solution [7, 8]. And indeed, novel plasmonic-organic hybrid modulators have demonstrated modulators with footprints in the order of μm<sup>2</sup>, electrical bandwidths way above 100 GHz with power consumption in the fJ/bit that operate across all optical wavelengths [9], see Fig. Most recently, a new generation of atomic scale switches has been introduced [10]. These devices depend on relocating a single atom or at most a few atom and thereby switching a plasmonic switch from the on- to the off-state and the other way round [10, 11]. We will conclude our talk by reviewing this new technology.

Acknowledgements: Partial funding through the ERC Plasilor, the FF-Photon and SNF project preCoR is acknowledged.

---

## References

---

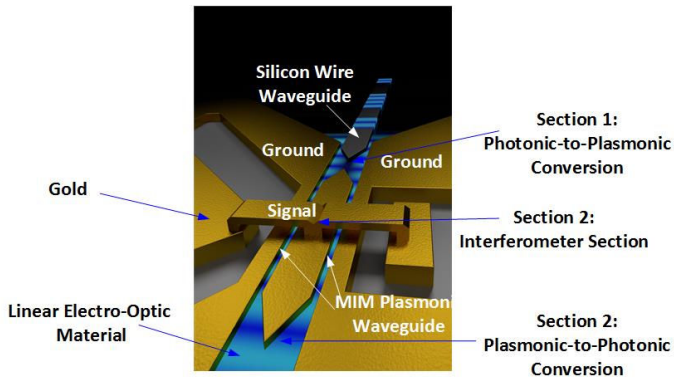
- [1] G. T. Reed, G. Mashanovich, F. Y. Gardes, and D. J. Thomson, "Silicon optical modulators," *Nature Photonics*, vol. 4, pp. 518-526, 2010.
- [2] J. Leuthold, C. Koos, W. Freude, L. Alloatti, R. Palmer, D. Korn, et al., "Silicon-Organic Hybrid Electro-Optical Devices," *IEEE Journal of Selected Topics in Quantum Electronics*, vol. 19, pp. 114-126, 2013.
- [3] P. Dong, X. Liu, C. Sethumadhavan, L. L. Buhl, R. Aroca, Y. Baeyens, et al., "224-Gb/s PDM-16-QAM Modulator and Receiver based on Silicon Photonic Integrated Circuits," in *Optical Fiber Communication Conference, Anaheim, California, 2013*.
- [4] N. Kinsey, M. Ferrera, V. M. Shalaev, and A. Boltasseva, "Examining nanophotonics for integrated hybrid systems: a review of plasmonic interconnects and modulators using traditional and alternative materials," *J. of the Opt. Society of America B*, vol. 32, pp. 121-142, Jan. 2015.
- [5] Q. Xu, B. Schmidt, S. Pradhan, and M. Lipson, "Micrometre-scale silicon electro-optic

- modulator," *Nature*, vol. 435, pp. 325-327, 05/19/print 2005.
- [6] E. Timurdogan, C. M. Sorace-Agaskar, J. Sun, E. S. Hosseini, A. Biberman, and M. R. Watts, "An ultralow power athermal silicon modulator," *Nature Communications*, vol. 5, p. 11, Jun 2014.
- [7] S. A. Maier, M. L. Brongersma, P. G. Kik, S. Meltzer, A. A. G. Requicha, and H. A. Atwater, "Plasmonics—A Route to Nanoscale Optical Devices," *Advanced Materials*, vol. 13, pp. 1501-1505, 2001.
- [8] M. L. Brongersma and V. M. Shalaev, "The Case for Plasmonics," *Science*, vol. 328, pp. 440-441, April 2010.
- [9] C. Haffner, W. Heni, Y. Fedoryshyn, J. Niegemann, A. Melikyan, D. L. Elder, et al., "All-plasmonic Mach–Zehnder modulator enabling optical high-speed communication at the microscale," *Nature Photonics*, vol. 9, pp. 525-528, Aug. 2015.
- [10] A. Emboras, J. Niegemann, P. Ma, C. Haffner, A. Pedersen, M. Luisier, et al., "Atomic Scale Plasmonic Switch," *Nano Letters*, vol. 16, pp. 709-714, Jan. 2016.
- [11] M. Barbry, P. Koval, F. Marchesin, R. Esteban, A. G. Borisov, J. Aizpurua, et al., "Atomistic Near-Field Nanoplasmonics: Reaching Atomic-Scale Resolution in Nanooptics," *Nano Letters*, vol. 15, pp. 3410-3419, May 2015.

---

## Figures

---




---

**Figure 1:** Plasmonic Mach-Zehnder modulator with 10  $\mu\text{m}$  length. The plasmonic interferometer is formed by the metallic island and the metallic contact pads. An electrical signal can be applied to the island via a suspended bridge [9].

---

The homogenous slab system plays a central role in the design of opto-electronic devices, like for example solar cells, where the active region is constituted by a single layer. In the case of a slab comprising a non-dispersive material, the reflection and transmission spectra exhibit a series of maxima and minima which can be exactly described by the Fabry-Perot (FP) resonances. If the material presents losses, these are described by a complex refractive index. The absorption spectra result in a series of peaks, where their maxima are coincident with those of the transmission spectra. The exact position of this maxima is well predicted by the real part of the complex frequencies of the quasinormal modes [1]. It is possible to identify a maximum appearing at smaller frequencies than the fundamental FP mode, whose position has no correspondence with the real part of any quasinormal mode frequency, but with the imaginary part of the zero-frequency one (see Fig. 1). This is a consequence of its over-damped character, given that the real part is very close to the absolute zero frequency. The small frequency regime is equivalent to the ultra-thin film one, i.e. the wavelength is much larger than the thickness of the slab. Even at thicknesses of just a few nanometers, it is possible to observe an absorption peak at visible frequencies. If the surrounding refractive index is non-absorbing, the absorption of the zero-th FP mode amounts a 5% of the incoming light. However, if the layer sits on top of an absorbing substrate, the zero-th order mode red-shifts, increase its absorption and becomes a regular weakly damped resonance. This interpretation is compatible with the experimental observation of a peak in a 25 nm GaAs layer over a gold substrate [2] and in nanometer films of germanium also over a gold substrate [3].

## References

- [1] J. M. Llorens, J. Buencuerpo, and P. A. Postigo, "Absorption features of the zero frequency mode in an ultra-thin slab," *Appl. Phys. Lett.* 105, 231115 (2014).
- [2] I. Massiot, N. Vandamme, N. Bardou, C. Dupuis, A. Lemaitre, J.-F. Guillemoles, and S. Collin, "Metal Nanogrid for Broadband Multiresonant Light-Harvesting in Ultrathin GaAs Layers," *ACS Photonics* 1, 878 (2014).
- [3] M. A. Kats, R. Blanchard, P. Genevet, and F. Capasso, "Nanometre optical coatings based on strong interference effects in highly absorbing media," *Nat. Mater.* 12, 20 (2013).

## Figures

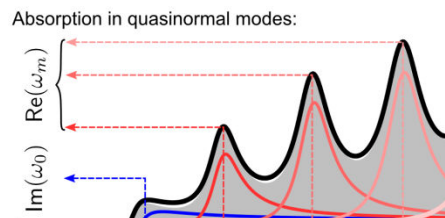


Figure 1: Modal decomposition of the absorption spectrum of a non-dispersive homogeneous slab.

# Arrested dimer's diffusion by self-induced back-action optical forces

Jorge Luis-Hita<sup>1,2\*</sup>, Juan José Sáenz<sup>2,3†</sup>,  
Manuel I. Marqués<sup>4‡</sup>

<sup>1</sup>Departamento de Física de la Materia Condensada, Universidad Autónoma de Madrid, Spain

<sup>2</sup>Donostia International Physics Center (DIPC), Spain

<sup>3</sup>IKERBASQUE, Basque Foundation for Science, Spain

<sup>4</sup>Departamento de Física de Materiales, Condensed Matter Physics Center (IFIMAC) and Instituto Nicolás Cabrera, Universidad Autónoma de Madrid, Spain

\*jluishita@gmail.com

†juanjo.saenz@dipc.org

‡manuel.marques@uam.es

The diffusion of a dimer made out of two resonant dipolar scatterers in an optical lattice is theoretically analyzed. When a small particle diffuses through an optically induced potential landscape, its Brownian motion can be strongly suppressed by gradient forces, proportional to the particle's polarizability [1]. For a single lossless monomer at resonance, the gradient force vanishes and the particle diffuses as in absence of external fields. However, we show that when two monomers link in a dimer, the multiple scattering among the monomers induces both a torque and a net force on the dimer's center of mass [2]. The "self-induced back-action" force leads to an effective potential energy landscape, entirely dominated by the mutual interaction between

monomers, which strongly influences the dynamics of the dimer. Under appropriate illumination, single monomers in a colloidal suspension freely diffuse while dimers become trapped. Our theoretical predictions are tested against extensive Langevin molecular dynamics simulations.

## References

- [1] S. Albaladejo, M.I. Marqués, F. Scheffold, J.J. Sáenz, *Nano Letters*, 9 (2009) 3527-3531.
- [2] J. Luis-Hita, J.J. Sáenz, M.I. Marqués (to be published).

## Figures

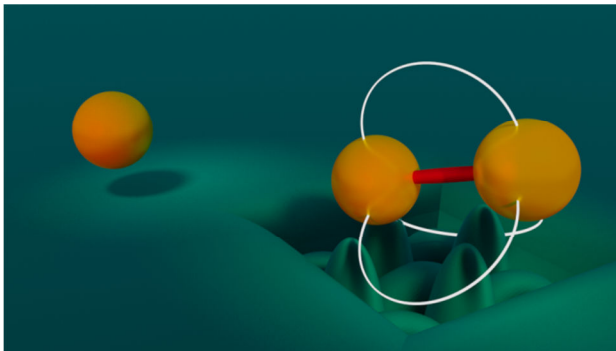


**Figure 1:** A single monomer at resonance, moving through an optical lattice, will not see its motion affected by any optical force. However, the diffusion of two monomers at resonance forming a dimer will be arrested via multiple scattering between the particles.

# Enhanced and tunable magneto-optical activity in magnetoplasmonic crystals

N. Maccaferri<sup>1\*</sup>, L. Bergamini<sup>2,3</sup>, M. Pancaldi<sup>1</sup>, X. Inchausti<sup>1</sup>, M. K. Schmidt<sup>3</sup>, N. Zabala<sup>2,3</sup>, A. O. Adeyeye<sup>4</sup>, A. Garcia-Martin<sup>5</sup>, J. C. Cuevas<sup>6</sup>, J. Aizpuru<sup>3</sup> and P. Vavassori<sup>1,7†</sup>

<sup>1</sup>CIC nanoGUNE, Spain

<sup>2</sup>Dept. of Electricity and Electronics, Faculty of Science and Technology, UPV/EHU, Spain

<sup>3</sup>Materials Physics Center CSIC-UPV/EHU and DIPC, Spain

<sup>4</sup>Information Storage Materials Laboratory, Department of Electrical and Computer Engineering, National University of Singapore, Singapore

<sup>5</sup>IMM-Instituto de Microelectrónica de Madrid (CNM-CSIC), Spain

<sup>6</sup>Departamento de Física Teórica de la Materia Condensada and Condensed Matter Physics Center (IFIMAC), UAM, Spain

<sup>7</sup>Kerbasque, Basque Foundation for Science Spain

\*n.maccaferri@nanogune.eu

†p.vavassori@nanogune.eu

We present a novel concept of a magnetically tunable plasmonic crystal based on the excitation of Fano lattice surface modes in periodic arrays of magnetic and optically anisotropic nanoantennas [1]. Due to the intrinsic magneto-optical activity of the system, two perpendicular lattice surface resonances can be induced in the crystal plane in the spectral range explored (visible/near-infrared): one directly excited by the incident light and perpendicular to its oscillation direction, and the other one, which is parallel to the oscillation direction of the incoming radiation, induced by the application of an external magnetic field perpendicular to the crystal plane (polar Kerr effect configuration). We show how the coherent diffractive far-field coupling between elliptical nickel nanoantennas is governed by the two in-plane, orthogonal and spectrally detuned localized plasmonic resonances of the individual building blocks, one directly induced by the incident radiation and oscillating parallel to it, and the other induced by the applied magnetic field and oscillating orthogonally to the directly excited localized resonance. The consequent excitation of these two Fano-like lattice surface modes leads to highly tunable and amplified magneto-optical effects as compared to a continuous magnetic film or metasurfaces made of disordered non-interacting magnetoplasmonic anisotropic nanoantennas. We demonstrate how, by tuning the pitch of the array and the shape of the individual building blocks, it is possible to design magnetoplasmonic crystals with huge and engineered optical and magneto-optical anisotropies.

We also study magnetoplasmonic crystals made of periodic nanostructured magnetic surfaces combining the features of surface plasma-polaritons

excitation and magneto-optical tunability [3]. While in continuous metallic film surfaces plasma-polaritons can be excited only by a p-polarized incident radiation, a periodic modulation of the surface enables the coupling of free space radiation either p- or s-polarized to certain surface plasma-polariton modes, so called “non-collinear plasmonic modes”. Here we demonstrate that in this kind of magnetoplasmonic crystals this property, in conjunction with the intrinsic polarization conversion due to the inherent magneto-optical activity, enable coupling of non-collinear propagating surface plasmon polariton modes. We observe that the magneto-optical spectral response arises from all the excitable plasmonic modes, conventional and non-collinear, in the magnetoplasmonic crystal irrespective of the incoming light polarization. Moreover, we demonstrate that a large resonant enhancement of the longitudinal Kerr effect is induced when those special non-collinear plasmonic modes are excited. Our findings besides unveiling the fascinating underlying physics that governs the peculiar magneto-optical properties of magnetoplasmonic crystals, open a clear path to the design of novel active metamaterials with tailored and enhanced magneto-optical activity. The concepts presented here can be exploited to design novel and ultrasensitive magnetoplasmonic sensors [3] and nanoscale metamaterials for precise control and magnetically-driven tunability of light polarization states.

## References

- [1] N. Maccaferri et al. Nano Letters 14 (2016), 2533-2542.
- [2] N. Maccaferri et al. ACS Photonics 2 (2015) 1769-1779.
- [3] B. Caballero et al. ACS Photonics, 3 (2016) 203-208.



# Dynamics of electric dipoles in fluctuating random electromagnetic fields

<sup>1</sup>Departamento de Física de Materiales, IFIMAC & Instituto Nicolás Cabrera, UAM, Spain

<sup>2</sup>Departamento de Física de la Materia Condensada, UAM, Spain

<sup>3</sup>Department of Physics, University of Fribourg, Fribourg, Switzerland

<sup>4</sup>Donostia International Physics Center (DIPC), Spain

manuel.marques@uam.es

In this work, we analyze the dynamics of single and coupled electric dipoles in a light field consisting on electromagnetic plane waves with polarizations randomly distributed and fluctuating phases.

For the particular case of an isolated dipole, the expressions for the optical random force fluctuations, the optical drag force, the equilibrium kinetic energy and the diffusion constant are derived [1]. Numerical simulations for the dynamics of a resonant dipole, initially at rest, show a crossover between super diffusive and diffusive regimens (see Figure 1).

For the case of two dipolar particles in a random electromagnetic field an isotropic interaction between the two particles emerges [2,3,4]. The value of the interaction strongly depends on fields and particle's properties [5] and, for some particular situations, gravitational like dynamics with interactions showing a  $1/r^2$  dependence are expected [2,3,4].

## References

- [1] Marqués M.I. Dynamics of a small particle in a fluctuating random light field. *Opt. Lett.* 41, 796 (2016).
- [2] Thirunamachandran, T. Intermolecular interactions in the presence of an intense radiation field. *Mol. Phys.* 40, 393 (1980).
- [3] Sukhov, S., Douglass, K. M. & Dogariu, A. Dipole-dipole interaction in random electromagnetic fields. *Opt. Lett.* 38, 2385 (2013).
- [4] Brügger G., Froufe-Pérez L.S., Scheffold F., Sáenz J.J., Controlling dispersion forces between small particles with artificially created random light fields. *Nature Comm.* 6:7460 (2015).
- [5] Luis-Hita J., Marqués M.I., Sáenz J.J., to be published.

## Figures

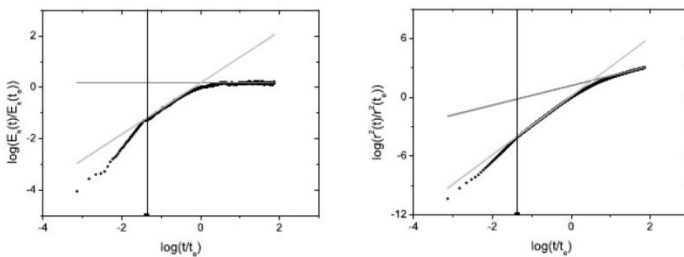


**Figure 1:** Log-Log plot of the molecular dynamics simulation results for the mean kinetic energy and the mean square displacement of a resonant electric dipole in a fluctuating random field (black dots). The dark gray line is the expected diffusive behavior. The gray line is the expected super diffusive behavior.

---

# Quantum nanophotonics in waveguides

**Luis Martín-Moreno**

Instituto de Ciencia de Materiales de Aragón,  
Spain

[lm@unizar.es](mailto:lm@unizar.es)

It is nowadays possible to place both natural and artificial few-level systems in the proximity of waveguides. This allows, for instance, the creation of quasiparticles with mixed exciton-photon characteristics, the modification (via the photons) of the emitter-emitter interaction and the generation (via the emitters) of photon-photon interactions.

In this talk I will (i) present a general numerical framework to investigate this kind of systems and (ii) use to study how to generate non-linear optical effects at the few-photon level, (iii) analyze the existence and properties of bound states that appear in this system.

Random lasers are characterized by the absence of a cavity as such and rely on multiple scattering for feedback.[1] The latter has been customarily provided by a diffusive material mixed with the gain material, but it does not constitute a necessary requirement and the two functionalities can be embodied by different components.[2] In trying to customize the active regions and mirrors in this kind of lasers we propose a new way to prepare the devices with high control over the size and position of individual *mirrors* and characteristics of the gain material.

Here we report on the preparation of random laser consisting of two or more titania powder clusters embedded in a film of DNA-CTMA complex doped with DCM dye. The device is made by laser-drilling several holes in the polymeric film (for subsequent use as template). In a second step the holes are filled with a  $\text{TiO}_2$  nanoparticles solution and allowed to dry. Next, the template is removed leaving only the clusters on the substrate. Finally, the clusters are covered again with dye-doped polymer film to get the final device. An SLM-shaped laser beam profile is used to optically pump the device establishing interactions between clusters involved in forming the *cavity*. Not only the length of the pumped segments and the roughness of the clusters play a role in selecting the modes involved in the laser action [3] but the film thickness determines the wavelength range where they appear.

## References

- [1] Wiersma, D. S. The physics and applications of random lasers. *Nat. Phys.* 4, 359–367 (2008).
- [2] Consoli, A. & López, C. Decoupling gain and feedback in coherent random lasers: experiments and simulations. *Sci. Rep.* 5, 16848 (2015).
- [3] Consoli, A & López, C; Emission regimes of random lasers with spatially localized feedback, *Opt. Express* in press (2016).

## Figures

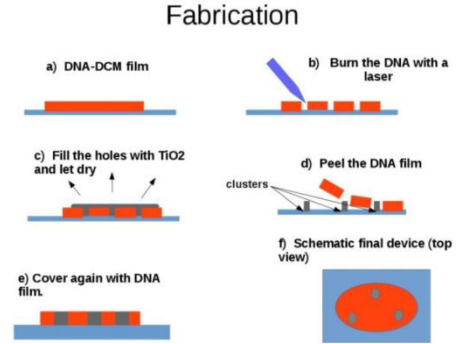


Figure 1: Fabrication process. See text.

### a) Real device. We can see the 3 cluster embeded in a DCM-DNA film.



### b) Pumped device with a shaped laser beam profile



Figure 2: a) Clusters size are around 100 microns and the distance between them is around 1.2 mm. b) Optical pump made with a Spatial light Modulator.

# Solution-Processed QD Solid by Doctor Blading Based on PbS QD Nanoinks for the Fabrication of Photodetectors at Telecom Wavelengths

**Alberto Maulu**<sup>1</sup>, Pedro J. Rodríguez-Cantó<sup>2†</sup>, Juan Navarro-Arenas<sup>1</sup>, Rafael Abargues<sup>2</sup>, Juan F. Sánchez-Royo<sup>1</sup>, Raúl García-Calzada<sup>1</sup>, Juan P. Martínez Pastor<sup>1\*</sup>

<sup>1</sup>Instituto de Ciencia de Materiales, Universidad de Valencia, Spain

<sup>2</sup>INTENANOMAT S.L., Spain

†pedro.j.rodriguez@uv.es

\*Juan.Mtnez.Pastor@uv.es

Solution-processed QD solids are emerging as a novel concept for high-performance optoelectronic devices [1]. In this work, doctor blading is proposed for the realization of closed-packed QD solids from a PbS nanoink for the fabrication of photodetectors at telecom wavelengths. The key step of this procedure is the solid-state ligand exchange, which reduces the interparticle distance and increases the carrier mobility in the QD solid [2]. This is accomplished by replacing the original long oleylamine molecules by shorter molecules such as 3-Mercaptopropionic acid, as confirmed by FTIR, TGA and XPS. XPS surface analysis of the QD solid shows a decrease of undesired oxidation products, like PbSO<sub>3</sub>, as result of an optimized ligand exchange procedure. XPS also reveal the presence of an oxidized shell around the PbS core, mainly composed by Pb(OH)<sub>2</sub>, that does not affect the structural quality of the PbS core and effectively passivates the QD surface [3]. Finally, the QD solid was tested as active layer for the fabrication of a Schottky NIR photodetector. The device performances are among the most appealing so far reported [2], with a maximum responsivity of 0.26 A/W that corresponds to an internal quantum efficiency higher than 30 % at 1500 nm and detectivity around 10<sup>11</sup> Jones.

## References

- [1] M. P. Hansen and D. S. Malchow, Proc. SPIE, vol. 6939, "Overview of SWIR detectors, cameras, and applications," pp. 69390I-1–69390I-11, Mar. 2008.
- [2] Ruili Wang, Yuequn Shang, Pongsakorn Kanjanaboos, Wenjia Zhou, Zhijun Ning and Edward H. Sargent, Energy Environ. Sci., vol. 9, "Colloidal quantum dot ligand engineering for high performance solar cells" pp. 1130–1143, 2016.
- [3] G. Konstantatos and E. H. Sargent, Proc. IEEE vol. 9, Solution-processed quantum dot photodetectors, pp. 1666-1683, 2009.

Nanostructured dielectric and metallic photonic architectures can concentrate the electric field through resonances, increase the light optical path by strong diffraction and exhibit many other interesting optical phenomena that cannot be achieved with traditional lenses and mirrors. The use of these structures within actual devices will be most beneficial for enhanced light absorption in thin solar cells, photodetectors and to develop new sensors and light emitters. However, emerging optoelectronic devices rely on large area and low cost fabrication routes such as roll to roll or solution processing, to cut manufacturing costs and increase the production throughput. If the exciting properties exhibited photonic structures are to be implemented in these devices then, they too have to be processed in a similar fashion as the devices they intend to improve. In this presentation, I will describe different low cost and large area photonic architectures that coupled to solution processed solar cells, photodetectors and SERS sensors facilitate enhanced light matter interaction within the active layer and are fully compatible with current manufacturing processes.

## Figures

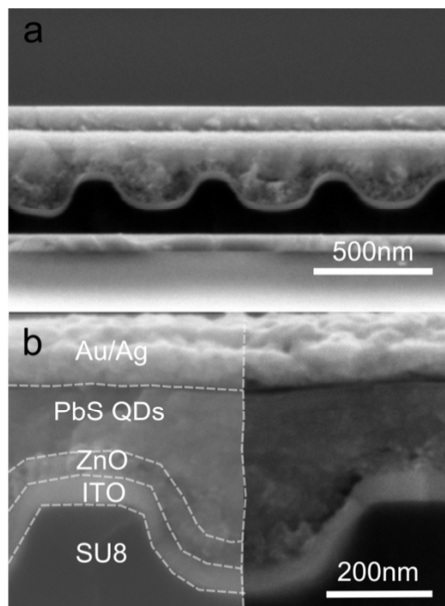


**Figure 1:** Cross-sectional SEM image of a ZnO-PbS solar cell built on top of an photonic electrode.

# Tailoring disorder for absorption enhancement in bifacial dye-sensitized solar cells

**José M. Miranda-Muñoz**, Sol Carretero-Palacios, Alberto Jiménez-Solano, Yuelong Li, Gabriel Lozano and Hernán Míguez

Multifunctional Optical Materials Group, Institute of Materials Science of Sevilla, Consejo Superior de Investigaciones Científicas - Universidad de Sevilla (CSIC-US), Spain

jm.miranda@csic.es

Great interest is devoted toward the fabrication of photonic devices with enhanced performance, for which the ability to control light transport is highly relevant. Optically disordered media appear as a means for the control of light propagation through interference inside the material. They combine appealing light scattering and characteristic resonance effects with ease of fabrication, which provide them with beneficial features for the integration in dye-sensitized solar cells (DSSCs). Bifacial dye solar cells presenting operation under front and rear illumination have been proposed as an effective means toward cost reduction, as a same area cell is able to harvest a higher amount of light [1].

In this work, an optically disordered medium offering control over the light scattering has been fabricated and integrated in a bifacial DSSC after theoretical design by means of a model. This yielded an optimized device with enhanced performance without modification of any of the commonly employed components. Such optically random medium comprises a mesoporous  $\text{TiO}_2$  matrix, in which monodisperse crystalline  $\text{TiO}_2$  nanospheres are dispersed in a random manner. The random distribution of submicron particles of high refractive index in the electrode of DSSCs has been previously proposed as a means toward enhancement of their absorption [2,3]. Due to the effects of multiple scattering, the path length of the light can be effectively enlarged, so that the residence time of the photons can be increased inside the sensitized film and, thus, their probability to interact with a dye molecule. Owing to the features of the scattering centres herein used and the possibility of tailoring disorder, the presented procedure offers unprecedented control over the scattering taking place inside the active film of the device. The optimized design is calculated from a model based on a Monte Carlo approach in which the multiple scattering of the light within the cell is fully

accounted for. We identify as key parameter for the control of the angular distribution of the scattered light the spherical shape of the inclusions.

The optically disordered system including scattering centres in diverse conditions has been optically characterized and successfully integrated in bifacial DSSCs after sensitization by a dye. Power conversion efficiencies (PCE) as high as 6.72% and 5.38% have been attained for devices operating under front and rear illumination, respectively. This represents a 25% and a 33% PCE enhancement with respect to an 8  $\mu\text{m}$ -thick standard dye-solar cell using platinum as catalytic material. The remarkable bifacial character our approach grants the devices is proved by the high rear/front efficiency ratio attained, around 80%, which is among the largest reported for this sort of devices [4].

## References

- [1] S. Ito et al., *Nat. Photonics*, 2 (2008), 693.
- [2] F. E. Gálvez et al., *J. Phys. Chem. C*, 116 (2012), 11426.
- [3] F. E. Gálvez et al., *Energy Environ. Sci.*, 7 (2013), 689.
- [4] J. M. Miranda-Muñoz et al., *J. Mater. Chem. A*, 4 (2016), 1953.

## Figures

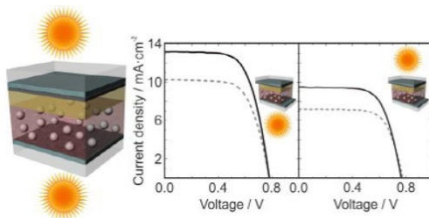


**Figure 1:** Schematic of the solar cell architecture and Current density/Voltage characteristic for the optimized configuration under front and rear illumination.

# Supramolecular mediated self-assembly of gold nanoparticles for selective SERS detection

Verónica Montes-García<sup>1</sup>, Borja Gómez<sup>2</sup>, Luis García-Río<sup>2</sup>, Isabel Pastoriza-Santos<sup>1</sup> and Jorge Pérez-Juste<sup>1</sup>

<sup>1</sup>Departamento de Química Física, Universidade de Vigo, Spain

<sup>2</sup>Departamento de Química Física, Universidade de Santiago de Compostela, Spain

veronicamontes@uvigo.es

Pillar[5]arenes are a new class of macrocycles, first synthesized in 2008 by Ogoshi [1], with interesting host-guest capabilities [2]. On the other hand, Au nanoparticles based systems are powerful SERS sensing platforms for the detection and identification of a wide range of analytes [3]. As recently reported, the combination of Au nanoparticles and pillar[5]arene can give rise to synergistic effects with great potential in selective SERS based detection of molecules [4]. Herein, we propose the fabrication of a novel sensing plasmonic platform through the assembly of Au nanoparticles directed by pillar[5]arene through electrostatics (see Figure 1). Since the assembly is a multistep process the optical properties, localized surface plasmon resonance (LSPR), can be easily modulated along the VIS-NIR range by varying the amount of Au deposited. Finally we analyze the SERS efficiency with a wide range of laser lines (532, 633, 785, 830 and 1064nm) demonstrating the importance of LSPR

frequency on the SERS activity. We also demonstrate the dependence of the SERS response on the refractive index of the surrounding media. This kind of studies, not usually accomplished, provides accurate information of plasmonic platform which contributes to elucidate the relationship between optical properties and SERS efficiency in hot-spot containing systems.

## References

- [1] T. Ogoshi, et al., *J. Am. Chem. Soc.*, 130 (2008) 5022.
- [2] X. Hu, et al., *Chem. Commun.*, 47 (2011) 469.
- [3] R. A. Álvarez-Puebla and L. M. Liz-Marzán, *Small*, 6 (2010) 604.
- [4] V. Montes-García, et al., *Chem. Eur. J.*, 20 (2014) 8404.

## Figures

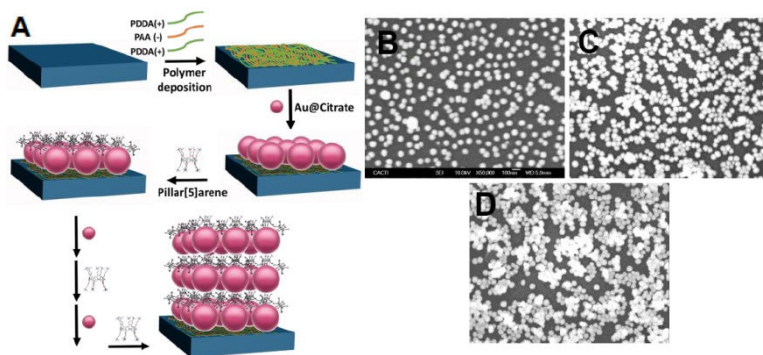


**Figure 1:** a) Schematic representation of the synthetic route where Au nanoparticles are deposited through electrostatic interactions in a multistep process. b-d) SEM images of the plasmonic substrate with 1, b); 2, c) or 3, d) additions of Au nanoparticles.

# Self-sustained coherent phonon generation in optomechanical crystals

D. Navarro-Urrios<sup>1</sup>, N. E. Capuj<sup>2</sup>, J. Gomis-Bresco<sup>3</sup>, M. F. Colomano<sup>1</sup>, P. D. García<sup>1</sup>, M. Sledzinska<sup>1</sup>, F. Alzina<sup>1</sup>, A. Griol<sup>4</sup>, A. Martínez<sup>4</sup>, C. M. Sotomayor-Torres<sup>1,5</sup>

<sup>1</sup>ICN2, CSIC and The Barcelona Institute of Science and Technology, Spain

<sup>2</sup>Depto. Física, Universidad de la Laguna, Spain

<sup>3</sup>ICFO and Universitat Politècnica de Catalunya, Spain

<sup>4</sup>Nanophotonics Technology Center, Universitat Politècnica de València, Spain

<sup>5</sup>Catalan Institute for Research and Advances Studies ICREA, Spain

daniel.navarro@icn2.cat

Miniaturized self-sustained coherent phonon sources, also known as “phonon lasers”, are interesting for applications such as mass-force sensing, intra-chip metrology and intra-chip time-keeping among others. We will review several mechanisms and techniques that can drive a mechanical mode into the lasing regime by exploiting the radiation pressure force in optomechanical cavities. We will specifically focus on a novel and efficient strategy for achieving the “phonon lasing” regime in optomechanical (OM) crystals [1] using the radiation pressure as the driving force of the motion. The mechanism is based on a self-pulsing limit cycle, which is a spontaneous process triggered within the optical cavity that modulate the intracavity radiation pressure force in resonance with a mechanical mode [2]. Self-sustained mechanical oscillations of modes up to 0,2 GHz are achieved if one of the low harmonics of the modulated force is resonant with a mechanical eigenstate (see Figure 1). We will discuss how it will be possible to further speeding up of the self-pulsing dynamics to reach the GHz regime, where the lack of good quality and miniaturized sources is a severe issue.

## References

- [1] J. Gomis-Bresco, D. Navarro-Urrios, M. Oudich, S. El-Jallal, A. Griol, D. Puerto, E. Chavez, Y. Pennec, B. Djafari-Rouhani, F. Alzina, A. Martínez, and C. S. Torres, Nat. Commun. 5, 4452 (2014).
- [2] D. Navarro-Urrios, N. E. Capuj, J. Gomis-Bresco, F. Alzina, A. Pitanti, A. Griol, A. Martínez and C. M. Sotomayor Torres, Sci. Rep. 5, 15733 (2015).

## Figures

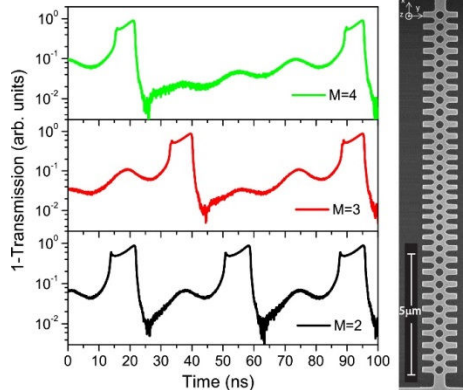


**Figure 1:** Dynamic behavior of the inverted transmitted optical signal for three different values of the self-pulsing frequency. In the three cases, the self-pulsing is frequency-entrained with the coherent mechanical oscillation of a flexural mode at  $\Omega_m=54$  MHz, which was activated by the anharmonic modulation of the intracavity radiation pressure force. The bottom, medium and top panels correspond to  $M=2$ ,  $M=3$  and  $M=4$  situations,  $M$  being the order of the harmonic used to pump the mechanics. The sinusoidal-like oscillations correspond to the mechanical coherent oscillation while the strongly asymmetric peaks are dominated by the self-pulsing. On the right, we show a SEM picture of one of our optomechanical crystals.



ITO has since long been used for transparent electrodes in opto-electronic applications such as photovoltaics and display technology because of its transparency to visible and near-IR light. This transparency can also be exploited to integrate ITO on silicon waveguides for modulation and switching at the 1550 nm telecom wavelength. For wavelengths beyond 1  $\mu\text{m}$ , ITO's permittivity can be described using a Drude model [1]. Since the plasma frequency of ITO is in the near-IR range, changes in the carrier density can lead to a refractive index shift greater than unity [2]. This strong manifestation of the plasma dispersion effect makes ITO so interesting for modulation. Until now, most proposed ITO-based absorption modulators used a MOS structure to accumulate charges capacitively and change the permittivity drastically in this layer. Since this layer is only a few nanometers long, very high confinement of the optical mode is needed to increase their interaction and reduce the structure's footprint. We have simulated structures for absorption modulation under the assumption that the bulk carrier density in the ITO can be tuned, for instance using P-N or N<sup>+</sup>-N junctions. For P-N junctions, a transparent, degenerate p-type semiconductor is needed. Degenerately doped silicon and the new promising p-type transparent conducting oxide LaCuOSe are candidates. Mg-doped LaCuOSe is reported to reach a hole density of  $2 \cdot 10^{20} \text{ cm}^{-3}$  with a relatively high hole mobility [3]. Under the assumption of complete depletion in the junctions, the absorption contrasts of our simulated absorptive modulators reach 200 for both polarizations. Refractive modulators based on P-N junctions have already been explored for silicon. However, the index shift due to the plasma

dispersion effect can be up to two orders of magnitude larger in ITO than in silicon. Integration of ITO near the waveguide can lead to higher modal index modulation with a smaller device footprint. ITO's conducting properties also suggest its use as an efficient heater for thermo-optic switching. However, experiments have shown that dissipating power in the deposited ITO layers leads to nonlinear and irreversible changes in the optical properties of the waveguides (figure 1a: power through the ITO strip on the long arm of the MZI). A resonance shift has been observed when applying a voltage over the ITO (figure 1b). This shift is not reversed completely when the voltage returns to zero and thus a permanent change is induced. In contrast, the insertion losses of the structure are more reversible in this experiment (figure 1c: maximal and minimal signal value around the resonance). Although the optical properties of the waveguide are changed, the electrical properties of the ITO remain the same. Understanding the origin of this behaviour and controlling it would lead to ITO enabling non-volatile switching and furthermore might allow the tuning of the ITO integrated structures' optical response after deposition.

## References

- [1] F. Michelotti, L. Dominici, E. Descrovi, N. Danz and F. Menchini, *Opt. Lett.*, 34 (2009) 839-841.
- [2] E. Feigenbaum, K. Diest and H.A. Atwater, *NanoLetter.*, 10 (2010) 2111-2116.
- [3] D. O. Scanlon, J. Buckeridge, C. Richard, A. Catlow and G. W. Watson, *J. Mater. Chem. C*, 2 (2014) 3429-3438.

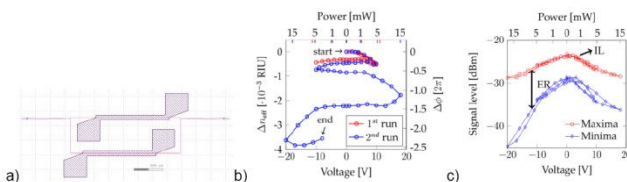


**Figure 1:** (a) ITO deposited onto an asymmetric MZI structure with TE gratings. Experimental change in (b) modal index, phase shift, (c) insertion loss and extinction ratio as function of the dissipated power in the ITO strip on the long arm of the MZI. Each measurement took 3 minutes to complete and was immediately followed by the next measurement.

## Fano resonance reveals Percolation in photonic crystals

<sup>1</sup>Instituto de Ciencia de Materiales de Madrid (ICMM); Consejo Superior de Investigaciones Científicas (CSIC), Spain

<sup>2</sup>Research Institute for Applied Physics and Astronomy, University of Tabriz, Iran

<sup>3</sup>Universidad Autónoma de Madrid, Spain

<sup>4</sup>Instituto de Microelectrónica de Madrid (IMM, CSIC), Spain

[jpariente@icmm.csic.es](mailto:jpariente@icmm.csic.es)

Percolation is a geometrical concept concerning end-to-end connectivity of a minority phase across a system which has brought new understanding to several areas of physics, mathematics and other areas of science. Percolation can have tremendous impact on the physical response of the system [1]. Although this effect is well understood for some systems (e.g. transition from insulating to conducting) the effects of percolation in the optical response (transport) of photonic structures is still a matter of study. Here we show how by using photonic crystals where precise amounts of random vacancies can be easily incorporated it is possible to reach the percolation threshold for an *fcc* while recording its optical response. We have found that these vacancies introduce a background of diffuse scattering which couples with the photonic band gap and give rise to asymmetric resonances in the optical spectra that follow the *Fano* line shape [2]. A fine control of the vacancies density [3] permits to prepare the systems so that different asymmetric profiles, characterized by the parameter  $q$ . We found that at the percolation threshold, probably due to the divergence of cluster size and subsequent enhanced diffuse scattering,  $q$  changes sign as signaled by the photonic band gap collapse.

### References

- [1] J. C. Miller, "Percolation in clustered networks," *Networks*, Apr. 2009.
- [2] U. Fano, "Effects of configuration interaction on intensities and phase shifts," *Phys. Rev.*, vol. 124, no. 6, pp. 1866–1878, 1961.
- [3] P. D. García, R. Sapienza, C. Toninelli, C. López, and D. S. Wiersma, "Photonic crystals with controlled disorder," *Phys. Rev. A - At. Mol. Opt. Phys.*, vol. 84, no. 2, pp. 1–7, 2011.

### Figures

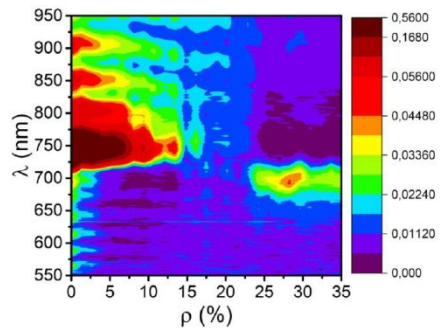


**Figure 1:** Vacancy concentration dependence of the reflectance.

Specular reflectance spectra evolution for a PMMA opal formed by 20 layers of 330 nm spheres as the density of vacancies increases. At percolation threshold ( $\rho_c = 15\text{-}22\%$ ), the band gap disappears and beyond the peak becomes a dip.

## Near thresholdless laser operation at room temperature

<sup>1</sup>IMM-Instituto de Microelectrónica de Madrid (CNM-CSIC), Spain

<sup>2</sup>Laboratory for Solid State Physics, ETH Zurich, Switzerland

<sup>3</sup>UMDO (Unidad asociada al CSIC), Spain

<sup>4</sup>Optics and Quantum Communications Group, ITEAM, UPV, Spain

pabloaitor.postigo@imm.cnm.csic.es

Laser emission using photonic crystal microcavities (PCM) [1] has opened new ways towards very low threshold and highly efficient solid state lasers with also very small size [2,3]. Recently, the term "thresholdless" has been used in the literature [4] to identify lasers presenting two main features: a spontaneous emission coupling factor ( $\beta$ ) close to 1 and low non radiative losses. Non radiative losses are reduced by several orders of magnitude at cryogenic temperatures, although they can never be completely suppressed. When the spontaneous emission factor  $\beta$  is equal to 1 every photon emitted by the device is emitted in the lasing mode. Such "thresholdless" lasers were proposed by Noda [4] to be realized by combining QDs as light emitters and PCMs as high quality resonators. Using that recipe, ultra-low threshold lasing has been achieved at cryogenic temperatures using an ever-decreasing number of QDs within PCMs.[2,5-7] That strategy was adopted by Strauf et al. to demonstrate near thresholdless lasing at low temperature (4.5 K) by using few QDs (between 2 to 4) as active emitters

and a high  $\beta = 0.85$  with power threshold values of 124 nW.[5] Khajavikhan et al. recently demonstrated thresholdless operation at low temperature (4 K) using metallic microcavities instead PCMs.[8] In this work we report a RT continuous wave (c.w.) laser with emission characteristics close to those of an deal thresholdless laser.[6]

### References

- [1] O. Painter, et al. Science, 284, no. 5421, pp. 1819–1821, (1999).
- [2] M. Nomura et al., Nat. Phys., 6, no. 4, pp. 279–283, (2010).
- [3] L. J. Martinez, et al. J. Vac. Sci. Technol. B Mic. Nanometer Struct., 27, no. 4, pp. 1801, (2009)
- [4] S. Noda, Science 314, 260-261 (2006).
- [5] S. Strauf, et al. Phys. Rev. Lett., 96, no. 12, p. 127404, (2006).
- [6] I. Prieto et al. Optica 2, 66 (2105).

### Figures

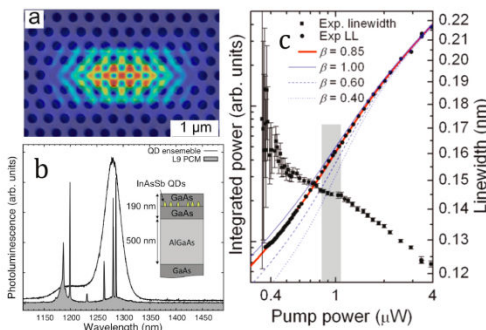


**Figure 1:** (a) shows the calculated spectral distribution of the lasing mode superimposed to a SEM image of the photonic crystal microcavity (PCM). (b) shows the photoluminescence spectrum at RT of the ensemble of QDs outside (black line) and inside (grey) of the PCM; the inset describes the layers that compose the device. (c) shows the integrated power emitted by the laser versus the pump power and the theoretical fittings performed for different values of  $\beta$ .

# Optical coupling of double L7 photonic crystal microcavities for applications in quantum photonics

P. A. Postigo, J.M. Llorens,  
L. E. Muñoz-Camuñez, I. Prieto

IMM–Instituto de Microelectrónica de Madrid  
(CNM–CSIC), Spain

pabloaitor.postigo@imm.cnm.csic.es

Coupled photonic crystal microcavities have been considered when exploring platforms for quantum photonic effects like quantum-optical Josephson interferometers, [1] single photon emitters and coupled-cavity single-photon emitters [2] and many others [3]. Arrays of photonic cavities are relevant structures for developing large-scale photonic integrated circuits, single mode coupled-cavity lasers [4] and for investigating basic quantum electrodynamics phenomena due to the photon hopping between interacting nanoresonators [5]. In this work we have measured the emission of two L7 microcavities when the distance between them (the number of rows of holes) is varied (Figure 1). We have found optical shared modes (“supermodes”) that appear more clearly at a certain distance of separation. Finally we have simulated the optical mode distribution of the coupled system using the GME method, finding a good agreement between experiment and theory.

## References

- [1] D. Gerace et al., Nature Physics 5, 281 - 284 (2009).
- [2] M. Maragkou et al. Physical Review B, 86 (7), 085316 (2012).
- [3] J.L. O’Brien et al. Nature Photonics 3, 687 - 695 (2009).
- [4] J. Huang et al. APL 99 (2011).
- [5] N. Caselli et al. ACS Photonics, 2015, 2 (5), pp 565–571.

## Figures

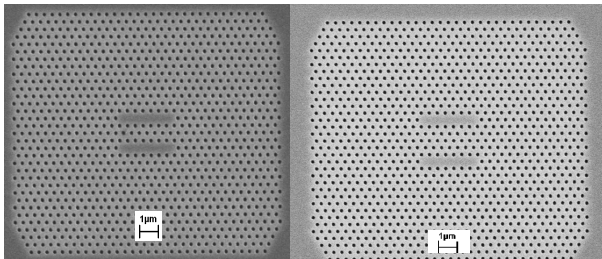


**Figure 1:** Two L7 photonic crystal microcavities separated by 3 and 5 rows of holes.

# Finite-difference time-domain optimization of organic thin-film solar cells using photonic crystal gratings

P. A. Postigo<sup>1</sup>, J.M. Llorens<sup>1\*</sup>, P. Romero<sup>2</sup> and J. Martorell<sup>2</sup>

<sup>1</sup>Instituto de Microelectrónica de Madrid, CSIC, Spain

<sup>2</sup>FCO - Institut de Ciències Fotòniques, Parc Mediterrani de la Tecnologia, Spain

\*jose.llorens@imm.cnm.csic.es

Organic photovoltaics (OPV) has taken off with the promise of low materials costs and fast, scalable manufacturing. However, an important factor limiting the efficiency of current OPV cells is the length-scale mismatch between the electronic carrier extraction, and optical absorption of the organic semiconductors used. While organic semiconductors are typically strong optical absorbers, it is difficult to efficiently extract photogenerated charge carriers from them. For example, in solar cells using recently developed organic bulk heterojunctions, the active layer needs to have a thickness of less than 100 nm for efficient carrier extraction. These thin layers leave many photons unharvested, and have thus motivated much recent interest in optical design and light trapping for organic solar cells. In contrast to most inorganic cells, the active layers in organic cells have thicknesses that are far smaller than the wavelength, thereby placing them in the nanophotonic regime, where the 'conventional'  $4n^2$  limit on light trapping could be easily surpassed. In

this work we present detailed finite-difference time-domain calculations for light trapping nanostructures (photonic crystal gratings) introduced in organic solar cells using P3HT, MoO<sub>3</sub>, Ag and ZnO/ITO on glass as substrate. We have simulated the effect of the minimum and maximum thicknesses of each layer and founded the optimal values. Next, we have simulated the light trapping effect by using a grating in an ITO/glass substrate with different thicknesses of ITO, founding the best values for the grating geometry. The dependence with the angle of incidence and polarization of the light has been also simulated for different grating periods and thicknesses of ITO, founding enhancements in the absorption ( $J_{sc}$ ) from 1.3% to 1.7%. Finally, contour maps of  $J_{sc}$  versus the height of the grating and for several filling factors have been calculated, which show total enhancement values for  $J_{sc}$  around 3% compared to the structures without grating.

## Figures

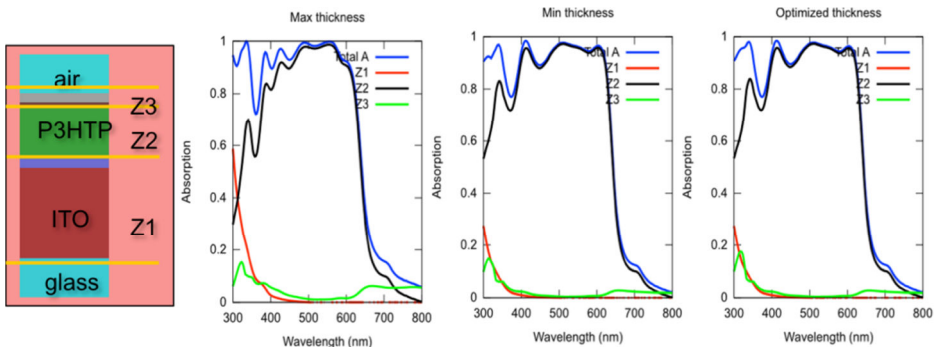


Figure 1: Dependence of the absorption on the wavelength for minimum, maximum and optimized thicknesses of the organic solar cell.

## Enlargement of free spectral range by selective suppression of optical cavity modes

The free spectral range (FSR) of a cavity mode is an important parameter on the design of photonic cavities, and relates the spectral distance between two consecutive modes. The design of a high quality factor (Q), small mode volumen (V) and large FSR cavity mode is required for cavity quantum electrodynamics effects to be effective [1]. The combination of quantum light sources operating at room temperature (RT) in the 1.3-1.7  $\mu\text{m}$ , integrated on a photonic cavity is key in several fields such as telecommunications or biosensing.

A procedure to increase the FSR while preserving the high-Q of a L7 photonic crystal cavity is presented. We designed and fabricated suspended L7 cavities on slabs 237 nm thick of InP embedding a single layer of quantum wires (QWRs), operating at 1.67  $\mu\text{m}$  at RT. The corresponding near field profiles of the first and second mode of the L7 gives us the hint to selectively filter the second mode by the design and fabrication of tiny stripes on the field maxima of the second mode. The L7m (Fig. 1a-b) consists of the regular L7 with two nano-strips within the cavity defect. The first and second modes of the L7 cavities are observed in a photoluminescence spectra at RT (Fig. 1c—red line), whereas the L7m (Fig. 1c—blue line) shows a

suppression of the corresponding second mode. The FSR of the first mode of the L7m is enlarged by more than a factor of 2 while preserving the Q. Therefore, the approach constitutes an alternative to engineer the mode structure of a photonic crystal microcavity. The enhancement of the FSR might improve the potential of PCMs embedding quantum nanostructures in the realization of low threshold lasers [2,3] or efficient gas and biological sensors [4].

### References

- [1] G. Bjork and Y. Yamamoto. IEEE J. Quantum Electron. 27 (1991) 2386.
- [2] I. Prieto, J. M. Llorens, L. E. Muñoz-Camúñez, A. G. Taboada, J. Canet-Ferrer, J. M. Ripalda, C. Robles, G. Muñoz-Matutano, J. P. Martínez-Pastor, and P. A. Postigo, *Optica*, 2 (2015) 66.
- [3] S. -H. Kim, H.-Y. Ryu, H.-G. Park, G. -H. Kim, Y. -S. Choi, Y. -H. Lee, and J. -S. Kim, *Appl. Phys. Lett.* 81 (2002) 2499.
- [4] J. Huang, S-H Kim, J. Gardner, P. Regreny, C. Seassal, P. A. Postigo, A. Scherer, *Appl. Phys. Lett.* 99 (2011) 091110.

### Figures

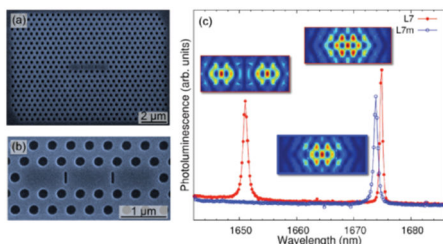


**Figure 1:** (a) SEM view of a L7m, (b) close-up showing two nano-strips in specific sites within the defect region, (c) PL spectra at room temperature from a L7 and a L7m; the insets show the  $|E|^2$  plots of the different modes simulated by finite difference time.

# Ultra-Fast Spectral Optical Analysis of Nanophotonic Structures

F. Prats, R. Caroselli, D. Zurita, Á. Ruiz-Tortola, J. García-Rupérez

Nanophotonics Technology Center, Universitat Politècnica de València, Spain

frapraq@ntc.upv.es

An ultra-fast spectral interrogation platform for nanophotonic structures is presented in this work. This platform allows the simultaneous interrogation of all the photonic structures in a photonic chip using a tunable laser and an IR camera as main elements, which will be controlled by a LabVIEW application.

Light from the tunable laser, with a continuous sweeping speed of 10 nm/s, is vertically injected with an aspheric collimator to the input grating couplers in the chip. After the light goes through the photonic chip, output light from all the output gratings couplers is simultaneously measured using an IR camera working at a frame rate of up to 2000 fps. This parameter allows the spectral interrogation of a region of 100 nm in 10 seconds with a very high resolution (up to 5 pm). The left figure shows the interrogation platform.

This ultra-fast interrogation has been pursued in order to carry out a continuous interrogation of nanophotonic sensing structures, where we need to acquire the response of all the sensing structures within a chip in a time as short as possible. These structures are designed to have certain characteristic spectral features (e.g., resonances in ring resonators or guided band edge in photonic bandgap structures (PBG)) which will be shifted when a change of the refractive index is produced

on their upper cladding. Typically, these spectral features have bandwidths ranging from few hundreds of pm (e.g., resonances) to few nm (e.g., a PBG edge), so our interrogation platform will allow us to monitor those features with a temporal resolution of only 1-2 seconds (approximately).

With these temporal and spectral resolutions, we have been able to characterize the sensing performance of photonic sensors based on ring resonators and on PBG structures, reaching detection limit values in the range of  $10^{-6}$  RIU (right figure) for the simultaneous interrogation of several sensing structures in the chip. We expect to reduce this detection limit value to the range of  $10^{-7}$  RIU by implementing several improvements targeting a reduction of the platform noise (e.g., referencing, averaging, temperature control, etc.).

A LabVIEW software application is used in order to control the different instruments of the platform. A Graphical User Interface (GUI) (right figure) allows the user to control different aspects related with the experiments and monitor the results.

This work has been supported by the European Commission through the projects H2020-644242-SAPHELY and H2020-634013-PHOCNOSIS, as well as by the Generalitat Valenciana through the grant PPC/2015/032.

## Figures

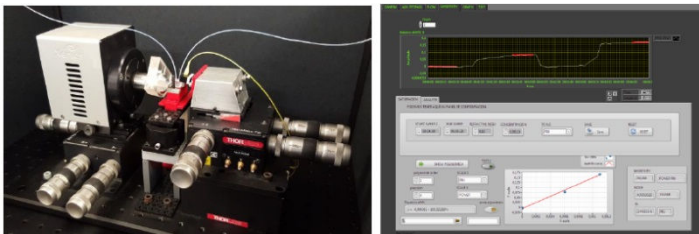


**Figure 1:** (Left) Picture of the interrogation platform where the light is coupled from the right side using a collimator and an IR camera is used in the left side to collect the output light. White tubes are the input and output channels of the microfluidic cell placed over the chip. (Right) Sensing performance of the system for a refractive index sensing experiment when the spectral response at the edge of a PBG is fitted using a combination of 2 Gaussian functions.

# Heterogeneous nanoplasmonics for quantum optics and biosensing

Romain Quidant<sup>1,2</sup>

<sup>1</sup>ICFO-Institut de Ciències Fotoniques, The Barcelona Institute of Science and Technology, 08860 Castelldefels (Barcelona), Spain

<sup>2</sup>ICREA-Institució Catalana de Recerca i Estudis Avançats, 08010 Barcelona, Spain

romain.quidant@icfo.es

Extensive research in Nano-optics over the last decade has made possible controlling optical fields on the nanometer scale. Such concentration of light, well below the limit of diffraction, opens plenty of new opportunities towards enhanced interaction with tiny amounts of matter down to the single molecule/atom level. In this talk we will present our recent advances in enhanced light-matter interaction on the nanometer scale and their applications to both quantum optics and biosensing.

The first part of the talk focuses on the controlled interaction of single quantum emitters with optical nanostructures. We first discuss different strategies to deliver a single quantum emitter in the hot spot of a plasmonic nanostructure. Next we show how these techniques are applied to deterministically locate single nano-diamonds in the hot spot of plasmonic antennas and waveguides [1,2]. In particular, we discuss the possibility to build on-chip single photon sources [3] as well as nanolasers [4].

In the second part of the talk, we change gear and present our latest advances in the optical, label free detection of biomarkers based on gold nanoantennas integrated into a state-of-the-art microfluidic platform. We first demonstrate the capability of our platform to detect low concentrations (<1ng/ml) of protein cancer markers in human serum [5] with low unspecific binding and high repeatability. In a second step we present a novel design that enables to simultaneously determine the absolute concentration of four different target molecules from an unknown sample. The system is validated in the context of breast cancer, as a strategy to assess the risk for brain metastasis [6]. Our research demonstrates the high potential of optical nanoresonators for the detection of different biomarkers in real biological samples and thus gets us closer to future nano-optical point-of-care devices.

---

## References

---

- [1] M. Geiselmann et al, Nature Nanotechnol. 8, 175-179 (2013).
- [2] M. Geiselmann et al, Nano Lett. 14, 1520-1525 (2014).
- [3] E. Bermúdez et al, Nature Commun. 6, 7883 (2015).
- [4] E. Bermúdez et al, submitted (2016).
- [5] S. S. Acimovic et al, Nano Lett. 14, 2636–2641 (2014).
- [6] O. Yavas et al, submitted (2016).



# Towards a high degree of uniformity in the diameter and length of self-catalyzed GaAs nanowires on silicon by adjusting the growth temperature

A. M. Raya, D. Fuster, J. M. Llorens, J. Buencuerpo and J. M. Ripalda

Instituto de Microelectrónica de Madrid, CSIC, Spain

andres.raya@csic.es

Nanowire-based devices are promising candidates for next generation solar cells. Lattice matching enforces a significant restriction on material choices for multijunction solar cells. However, the strain relaxation through the nanowire sidewall allows the growth of lattice-mismatched III-V compounds on inexpensive silicon substrates. Our theoretical calculations based on the detailed balance limit [1,2] indicate that an optimal tandem cell based on GaAs nanowires on Si can achieve an efficiency of 38.8%. The efficiency reaches a maximum value of 44.9% if an  $\text{Al}_{0.24}\text{Ga}_{0.76}\text{As}$  compound ( $E_g = 1.72$  eV) is used for the nanowire top cell, making III-V nanowire on Si tandem cells a promising candidate to compete with current three- and four-junction solar cells.

Many parameters need to be tuned for an optimum growth of the nanowires by molecular beam epitaxy (MBE). The understanding and control of the nanowire growth process is necessary in order to design and build a high efficiency device. The thickness of the  $\text{SiO}_2$  layer formed on the silicon substrate plays a critical role in the density and yield of self-catalyzed GaAs nanowires [3], whereas the length and diameter of the nanowires have to be optimized because they affect the current matching [4]. In the present work we investigate the influence of the growth temperature on the final characteristics of the nanowires. We report that the optimization of the substrate temperature used during the Ga droplet formation step leads to a significant narrowing of the diameter and length distributions of the nanowires.

Series of samples consisting of GaAs nanowires on Si (111) substrates were grown using standard growth parameters, whereas the growth temperature was set to different values in the interval between 555 and 630 °C. We have used scanning electron micrographs of the samples to measure the density, yield, diameter and length of a wide number of nanowires as functions of the oxide thickness and growth temperature. The results reveal that

lowering the growth temperature leads to a higher degree of uniformity in the length and diameter of the GaAs nanowires, as can be seen in Fig. 1. This tendency is observed regardless of whether we are using an optimum value of the native  $\text{SiO}_2$  layer or a thicker one. Optical microscopy and reflectivity results are also correlated with electron microscopy images.

## References

- [1] W. Shockley and H. J. Queisser, *J. Appl. Phys.*, 32, 510 (1961).
- [2] A. De Vos, *J. Phys. D.( Appl. Phys.)*, 13, 839 (1980).
- [3] F. Matteini, G. Tütüncüoğlu, H. Potts, F. Jabeen and A. Fontcuberta i Morral, *Cryst. Growth Des.*, 15, 3105 (2015).
- [4] N. Huang, C. Lin and M. L. Povinelli, *J. Appl. Phys.*, 112, 064321 (2012).

## Figures

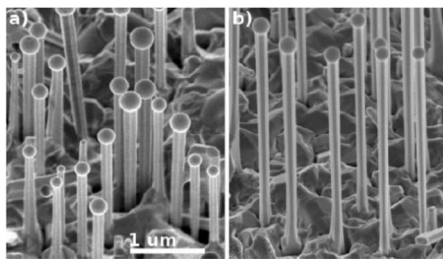


**Figure 1:** SEM images of GaAs nanowires grown on Si (111) substrate using a)  $T_{\text{growth}} = 630^\circ\text{C}$  and b)  $T_{\text{growth}} = 580^\circ\text{C}$ . Scale bar corresponds to 1  $\mu\text{m}$ .

# Kamikaze Silicon colloids as cancer cells killers

I. Rodríguez<sup>1</sup>, R. Fenollosa<sup>1</sup>, E. García-Rico<sup>2</sup>, S. Alvarez<sup>3</sup>, R. Alvarez<sup>3</sup>, X. Yu<sup>4</sup>, S. Carregal-Romero<sup>4</sup>, C. Villanueva<sup>5</sup>, M. García-Algar<sup>6</sup>, P. Rivera-Gil<sup>5</sup>, A. R de Lera<sup>3</sup>, W. J Parak<sup>4</sup>, F. Meseguer<sup>1</sup> and R. A Álvarez-Puebla<sup>6,7</sup>

<sup>1</sup>Instituto de Tecnología Química and Centro de Tecnologías Físicas. CSIC/UPV, Spain

<sup>2</sup>Servicio de Oncología, Hospital Universitario Madrid-Torrelodones, Spain.

<sup>3</sup>Departamento de Química Orgánica, Universidade deVigo, Spain

<sup>4</sup>Fachbereich Physik, Philipps Universität Marburg, Germany

<sup>5</sup>Medcomtech SA, Spain

<sup>6</sup>Departamento de Química Física e Inorgánica, Universitat Rovira i Virgili and Centro de Tecnología Química de Catalunya, Spain

<sup>7</sup>ICREA, Spain

mirodrig@upvnet.upv.es

Nanoparticles have shown a great potential in nanomedicine [1]. In most approaches, surface functionalization of nanoparticles by antibodies, allows them to be directed to the target cells for drug delivery or also for heating treatment through magnetothermia [2] or photothermia [3]. A drawback of such techniques is the large and expensive facilities required and/or the limited efficiency. Porous silicon particles represent a promising platform for cancer therapies due to their good biocompatibility and biodegradability [4]. They have been largely employed as vehicle for drug administration. However, if one takes into account the well-known violent reaction of oxidation and degradation that silicon undergoes in aqueous medium [5], it appears that silicon nanoparticles themselves can constitute a lethal weapon if they could be introduced inside the target cells using a Trojan horse-like subterfuge. Here we present the demonstration of this concept through tests in vitro of viability of cancerous cells (SK-BR3). The strategy consists coating silicon nanoparticles with sugars to avoid the extracellular solubilization, followed by a functionalization with the appropriated antibody to target the desired cells. Once the functionalized silicon nanoparticles reach the target, the enzymatic machinery of Eukaryotic cells begin the degradation of particles into excretable elements. It can be seen in Figure 1 the decrease of the viability of cancerous cells after contact with silicon particles functionalized with the directing vector HER-2-positive breast cancer [6].

## References

- [1] Prasad, P.N. Introduction to Nanomedicine and Nanobioengineering. (Wiley, New York; 2012).
- [2] Gomella, L.G. Nat Clin Pract Urol 1(2004)72; Maier-Hauff, K. et al. J Neurooncol 103(2011)317.
- [3] Hong, C., et al. Anti-Cancer Drugs 22(2011)971; Lal, S., et al., Accounts of Chemical Research 41, 1(2008)842; Lee, C. et al. Journal of Materials Chemistry 18(2008)4790; Osminkina, L.A., et al., Appl. Phys. B 105(2011)665; Jain, P.K., et al., Accounts of Chemical Research 41(2008)578.
- [4] Park, J.-H. et al. Nat Mater 8 (2009) 331; Popplewell, J.F. et al. J. Inorg. Biochem. 69(1998)177; Shabir, Q. et al. Silicon 3(2011)173.
- [5] Mikulec, F.V., et al., Adv Mater. 14(2002)38; Clement, D., et al., Phys Stat Sol A 202(2005)1357.
- [6] Fenollosa, R., et al. Journal of Nanobiotechnology 12(2014)35.

## Figures

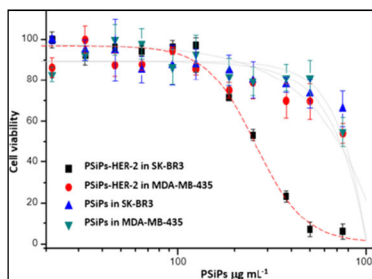


**Figure 1:** Cell viability. Relative cell viability after incubation of SK-BR-3 and MDA-MB-435 cells with PSiPs and PSiPs-HER-2 for 48 h.

## 3D Printing Sets New Standards in Microfabrication

rodriguez@nanoscribe.com

The technique of two-photon polymerization (TPP) allows for high precision additive manufacturing based on 3D digital models with sub-micrometer feature sizes and resolution. In addition, 2D and 2.5D topologies can be fabricated with ultra-high aspect ratios and outstanding design freedom with a resolution between electron beam and UV lithography. This talk gives an overview on the technology and its performance and highlights both scientific disruptive breakthroughs and enabled applications in industry.

The benefits of 3D printing are now fully available on the micrometer scale. While TPP was previously known for ultra-fine yet small objects mostly viewed under the scanning electron microscope, now mm<sup>3</sup>-scale fabrication has become the novel standard in 3D microfabrication with still sub-micrometer features. This closes the gap to conventional stereolithography formerly considered as highest resolution 3D printing technique.

Unique designs and precision open new applications in multiple fields such as photonics, micro-optics, microfluidics, micro robotics, mechanical metamaterials, and life sciences. In optics and photonics, TPP is - among others - used for the fabrication of photonic crystals, metamaterials [1,2], optical cloaks [3], photonic colours or high-precision micro-optics [4]. Industrial application examples such as wafer-level micro-optics and photonic multi-chip integration [5] will be discussed.

Filters, mixers, complex nozzles, micro-robots or micro-needles for painless drug delivery exemplify the challenges that can be overcome by 3D printing on the micro- to mesoscale. Design freedom, resolution, processing speed and a wide range of materials allow to easily produce tailored 3D scaffolds and matrices for mimicking in vivo 3D physiological environments for cell studies. And mechanical engineers are enabled to design unique mechanical properties previously unachievable by shaping complex microtrusses. Ultra-light yet strong [6, 7] or auxetic [8] materials as well as unfeelability cloaks [9] have been reported.

---

### References

- [1] N. Muller, J. Haberko, C. Marichy, and F. Scheffold, "Silicon Hyperuniform Disordered Photonic Materials with a Pronounced Gap in the Shortwave Infrared", *Advanced Optical Materials* 2, 115–119 (2014).
- [2] J.K. Gansel, M. Thiel, M.S. Rill, M. Decker, K. Bade, V. Saile, G. von Freymann, S. Linden, and M. Wegener, "Gold helix photonic metamaterial as broadband circular polarizer", *Science* 325, 1513-1515 (2009).
- [3] T. Ergin, N. Stenger, P. Brenner, J. B. Pendry and M. Wegener, "Three-dimensional invisibility cloak at optical wavelengths", *Science* 328, 337-339 (2010).
- [4] M. Nawrot, Ł. Zinkiewicz, B. Włodarczyk, and P. Wasylczyk, "Transmission phase gratings fabricated with direct laser writing as color filters in the visible", *Optics Express*, 21, 31919 (2013).
- [5] N. Lindenmann, G. Balthasar, D. Hillerkuss, R. Schmogrow, M. Jordan, J. Leuthold, W. Freude, and C. Koos, "Photonic wire bonding: a novel concept for chip-scale interconnects", *Optics Express* 20, 17667 (2012).
- [6] D. Jang, L.R. Meza, F. Greer, and J.R. Greer, "Fabrication and Deformation of Three-Dimensional Hollow Ceramic Nanostructures", *Nature Materials* 12, 893 (2013).
- [7] J. Bauer, S. Hengsbach, I. Tesari, R. Schwaiger, and O. Kraft, "High-strength cellular ceramic composites with 3D microarchitecture", *PNAS* 111 no. 7, 2453-2458 (2014).
- [8] T. Bückmann, N. Stenger, M. Kadic, J. Kaschke, A. Frölich, T. Kennerknecht, C. Eberl, M. Thiel, and M. Wegener, "Tailored 3D mechanical metamaterials made by Dip-in Direct-Laser-Writing Optical Lithography", *Advanced Materials* 24, 2710 (2012).
- [9] T. Bückmann, M. Thiel, M. Kadic, R. Schittny & M. Wegener, "An elasto-mechanical unfeelability cloak made of pentamode metamaterials", *Nature Communications* 5, 4130 (2014).

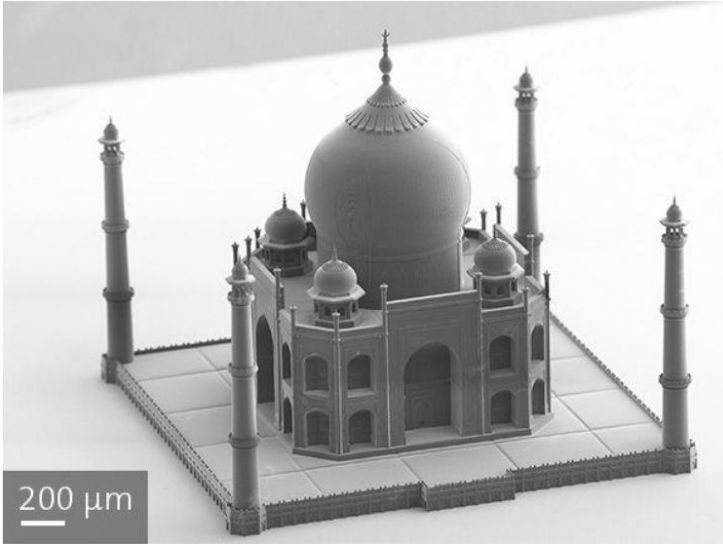


Figure 1: SEM image of the Taj Mahal demonstrating the fine features enabled by Nanoscribe's high-resolution 3D microprinting.

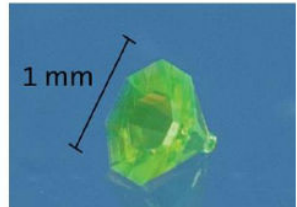
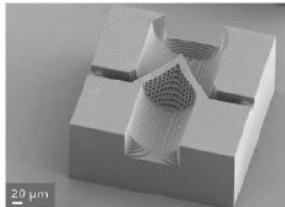
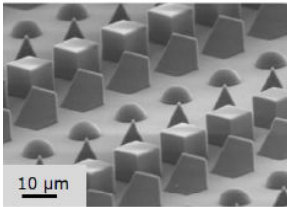


Figure 2: Application examples: (left) wafer-level micro-optics, (middle) microfluidic filter (design provided by IMSAS) and (right) microfluidic nozzle.

In quantum physics it is well known that the spin of a particle can determine its motion: this is known as spin-orbit interaction. It is not so well known that Maxwell's equations can show the same effect with electromagnetic radiation. Contrary to the approximate assumptions of ray optics, in which rays propagate independently of light polarization, Maxwell's equations tell us that the spin of photons (their polarization) can affect their motion, under certain conditions [1]. Although these spin-orbit effects of light are usually small, recent advances in nanotechnology have found ways to enhance them dramatically. This opens up very interesting applications in nanophotonics for light generation and switching of light through the control of its polarization.

In this work we will summarize a collection of relatively recent experiments that we performed based on structures that enable the unidirectional excitation of electromagnetic modes by simply controlling the incident polarization of light, exhibiting a strong spin-orbit coupling of light. These structures include slits etched on gold films [2], gold nanoparticles on plasmonic surfaces [3], radio-frequency antennas emitting near two dimensional hyperbolic metamaterial circuits [4] and silicon nanoantennas [5]. All these different scenarios can be explained using the same unified fundamental explanation of spin-momentum locking of evanescent waves [1,2,6,7]: evanescent near fields are characterised by elliptically polarized fields whose rotation sense is directly determined by their propagation direction. Therefore, any electromagnetic mode which possesses an "evanescent tail" can be excited unidirectionally if the appropriate polarization is used for its excitation.

We also describe experiments involving the reciprocal scenario, in which the direction of propagation of an electromagnetic mode can be used to determine the polarization of radiated light. We show how this can be used to design dual-input nanoantennas that synthesize arbitrary light polarizations in the radiated light [8].

---

## References

---

- [1] Bliokh, K. Y., Rodríguez-Fortuño, F. J., Nori, F. & Zayats, A. V. Spin-orbit interactions of light. *Nat. Photonics* 9, 796–808 (2015).
- [2] Rodríguez-Fortuño, F. J. et al. Near-Field Interference for the Unidirectional Excitation of Electromagnetic Guided Modes. *Science* 340, 328–330 (2013).
- [3] O'Connor, D., Ginzburg, P., Rodríguez-Fortuño, F. J., Wurtz, G. A. & Zayats, A. V. Spin-orbit coupling in surface plasmon scattering by nanostructures. *Nat. Commun.* 5, 5327 (2014).
- [4] Kapitanova, P. V. et al. Photonic spin Hall effect in hyperbolic metamaterials for polarization-controlled routing of subwavelength modes. *Nat. Commun.* 5, 3226 (2014).
- [5] Rodríguez-Fortuño, F. J., Barber-Sanz, I., Puerto, D., Griol, A. & Martínez, A. Resolving light handedness with an on-chip silicon microdisk. *ACS Photonics* 1, 762–767 (2014).
- [6] Bliokh, K. Y., Smirnova, D. & Nori, F. Quantum spin Hall effect of light. *Science* 348, 1448–1451 (2015).
- [7] Neugebauer, M., Bauer, T., Aiello, A. & Banzer, P. Measuring the Transverse Spin Density of Light. *Phys. Rev. Lett.* 114, 063901 (2015).
- [8] Rodríguez-Fortuño, F. J. et al. Universal method for the synthesis of arbitrary polarization states radiated by a nanoantenna. *Laser Photon. Rev.* 8, L27–L31 (2014).

# Design and characterization of plasmonic nanostructures on silicon waveguides for sensing

Ángela Ruiz-Tórtola,

A. Griol, A. Martínez

Universitat Politècnica de València,  
Nanophotonics Technology Center, Spain

anruitor@ntc.upv.es

Plasmonics and silicon photonics are two high-impact research topics. Plasmonics studies the interaction between light and subwavelength metallic nanostructures, opening the way towards light manipulation at the nanoscale. Plasmonic nanostructures display many interesting properties when illuminated with visible or NIR radiation. For instance, they can strongly confine electric and magnetic fields via localized surface plasmon resonances (LSPR) in deep subwavelength regions close to the metal surface [1]. This feature can be used to build highly sensitive plasmonic nanoresonators to tiny variations in their surroundings and very useful in sensing. It would be highly desirable to use such resonators on silicon waveguides, since they could be used for massive multiplexed biosensing in silicon photonics chips, enabling low-cost mass-manufacturing of biosensors.

In this work, we present and demonstrate experimentally a plasmonics-on-silicon biosensor based on an array five gold nanodipoles on a  $500 \times 250 \text{ nm}^2$  silicon waveguide supporting the propagation of the fundamental TE mode (Fig. 1). An exhaustive study about the variation and influence of parameters is performed by using CST Microwave Studio in order to achieve steep LSPR in the wavelength regime from 1260 to 1630 nm. We got a deep transmission dip when the nanodipoles are ellipsoidal-shaped with long axis ( $d_1=205 \text{ nm}$ )

parallel to the electric field and short axis ( $d_2=80 \text{ nm}$ ) parallel to the propagation direction of the guided wave, being both the gap and metal thickness equal to 30 nm. Figure 2 shows a numerical simulation, where the transmission dip is clearly seen. When applying a liquid with index 1.33 on top of the nanostructure, we get a strong red-shift of the response, resulting in a sensitivity of 520 nm/RIU and a figure of merit of 288.89 1/RIU. Figure 3 shows a SEM image of a fabricated sample. Preliminary results show a huge displacement of the dip when a liquid is deposited in the top of the fabricated sample.

This work opens new perspectives in the field of parallel simultaneous access to label-free biosensing arrays, where plasmonic nanostructures exhibit unprecedented values of sensitivity [2]. It would allow the development of on-chip multiplexed LSPR sensors with submicron size for highly-sensitive detection of multiple analytes in real-time.

## References

- [1] M. Lorente-Crespo et al., Nano Lett. 13 (6), (2013) 2654-2661.
- [2] A. A. Yanik et al., Proc. Natl. Acad. USA 108, (2011) 11784-11789.

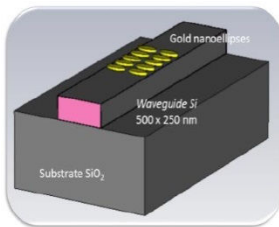


Figure 1: Plasmonics-on-silicon biosensor.

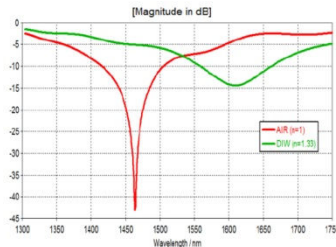


Figure 2: Normalized power transmission spectrum.

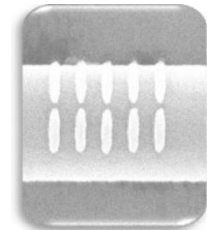


Figure 3: Image SEM (Scanning Electron Microscopy) of a fabricated sample.

Photonic technology for the development of sensing devices is currently attracting a lot of interest due to several advantages, such as high sensitivity, compactness and high integration level, shorter time to result, label-free detection and use of very low sample volumes [1]. Moreover, it has also attracted this interest due to the possibility of using CMOS-compatible materials and mass manufacturing processes to reach very high production volumes and very low costs.

In this work, we present and experimentally demonstrate several configurations of PBG (Photonic Band Gap) sensing structures, whose PBG edge is located around 1550 nm when a water upper cladding is considered. These configurations are mainly based on the periodic introduction of transversal elements and/or holes onto a single mode waveguide [2]. It is a silicon layer with a thickness of 220 nm over a lower cladding made of silicon oxide. Specifically, we will focus on 1D periodic waveguides (Fig 1). The optimal configurations for each PBG sensing structure have been determined by means of MPB simulations and then we have simulated their transmission response using CST Microwave Studio. Figure 2 shows a SEM image of a fabricated sample. Figure 3 shows experimental transmission data of two repetitions of the PBG sensing structures within the same chip. The considered dimensions are:  $a=400$  nm,  $w_i=100$  nm and  $w_e=2000$  nm. Preliminary results show a PBG being very deep and sharp, with a moderate

ripple in the pass band edge and with a good matching between two repetitions fabricated in the same chip. Finally, we monitor the spectral shift of the PBG when applying a solution on top of the nanostructure with different refractive index and we get a sensitivity of 205.4 nm/RIU.

In conclusion, this work represents an experimental demonstration of refractive index variation detection using a PBG-based sensor. These nanostructures would allow proteins or DNA detection, as it is proposed in Saphely project, under the framework that this work is done. In order to perform multiplexed analyses for the simultaneous detection of several target miRNA biomarkers, several sensing structures will be included in the photonic chip, being each of them bio-functionalized.

The authors acknowledge the received funding from the European Commission through the H2020-644242 - SAPHELY project and the Generalitat Valenciana through the help PPC / 2015/ 032.

## References

- [1] J.G. Catelló et al., Optics Letters, 37 (17) (2012) 3684-3686.
- [2] J.G. Catelló et al., Optics Letters, 36 (14) (2011) 2707-2709.

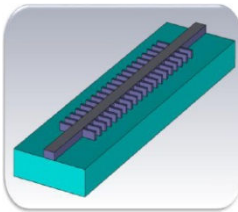


Figure 1: 1D SOI periodic structure used as biosensor: corrugated waveguide.

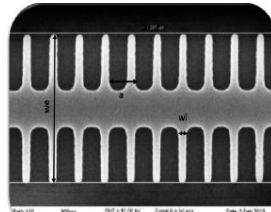


Figure 2: Scanning electron microscope image of corrugated waveguide.

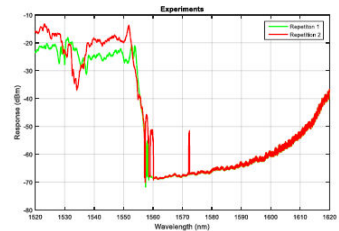


Figure 3: Normalized transmission spectra of two identical corrugated waveguide.

# Inverted BHJ solar cells based on PTB7:PC<sub>70</sub>BM using TiO<sub>x</sub> as electron transport layer

J.G. Sánchez<sup>1</sup>, V.S. Balderrama<sup>2</sup>, M. Estrada<sup>1</sup>, J. Ferrè-Borrull<sup>1</sup>, L.F. Marsal<sup>1</sup> and J. Pallarès<sup>1\*</sup>

<sup>1</sup>Departament d'Enginyeria Elèctrica, Electrònica i Automàtica, ETSE, Univ. Rovira i Virgili, Spain  
<sup>2</sup>Centro de Investigación y de Estudios Avanzados (CINVESTAV-I.P.N.), México

\*josep.pallares@urv.cat

In recent years, bulk-heterojunction (BHJ) polymer solar cells (PSCs) have been widely studied because they offer low-cost, easy manufacture process, the possibility to be fabricated and deposited on flexible substrates and obtained large areas, which it is opposite case for the conventional silicon solar cells. It well know, that the calcium (Ca) and poly(3,4-ethylene dioxythiophene):poly-(styrenesulfonate) (PEDOT:PSS) are use as electron and hole transport layers in PSCs, respectively [1]. Nevertheless, the high reactivity of calcium with oxygen and the hygroscopical and acidic nature of PEDOT:PSS in environmental air can lead degradation of the active layer and the indium tin oxide (ITO) electrode resulting in poor stability [2]. In order to improve the stability, buffer layers and new inverted architecture structures have been developed for the PSCs [3]. In this work, we present the fabrication of PSCs based on thieno[3,4-b]-thiophene/ benzodithiophene (PTB7) and [6,6]-phenyl-C71-butyric acid methyl ester (PC<sub>70</sub>BM) using an inverted structure. Titanium sub oxide (TiO<sub>x</sub>) film is used as electron transport layer, and this one was processed by via sol-gel method [4]. The inverted PSC was manufactured with the stack: ITO (120 nm) / TiO<sub>x</sub> (20 nm)/ PTB7:PC<sub>70</sub>BM (~100 nm) / V<sub>2</sub>O<sub>5</sub> (5 nm) / Ag (100 nm) as is shown in figure 1a. In order to compare the performance of the cell, standard PSCs were manufactured. The performance parameters obtained for standard and inverted PSC were V<sub>OC</sub>= 710 and 720 mV; J<sub>SC</sub>= 14.7 and 16.4 mA/cm<sup>2</sup>; FF= 0.71 and 0.68 and PCE= 7.3 and 7.9 %, respectively. Figure 1 shows the J-V curves under illumination at 1 sun (AM 1.5G spectrum), and under darkness for both structures manufactured.

**Acknowledgements:** This work was supported by the Spanish Ministry of Economy and competitiveness (MINECO) under grant number, TEC2015-71324-R by the ICREA under the ICREA Academia Award, by Catalan authority under project AGAUR 2014 SGR 1344 and CONACYT Project 237213 in Mexico.

## References

- [1] Krebs, F. C., Sol. Energy Mater. Sol. Cells, 4, (2009), 394.
- [2] Z. B. Wang, M. G. Helander, M. T. Greiner, J. Qiu, and Z. H. Lu, Phys. Rev. B: Condens. Matter Mater. Phys., 23, (2009), 235325.
- [3] H. Choi, J. S. Park, E. Jeong, G. H. Kim, B. R. Lee, S. O. Kim, M. H. Song, H. Y. Woo, and J. Y. Kim, Adv. Mater., 24, (2011), 2759.
- [4] C. Meneses, J.G. Sánchez, M. Estrada, A. Cerdeira, J. Pallarès, B. Iñiguez. L.F. Marsal, Microelectronics Reliability, 5, (2014), 893.

## Figures

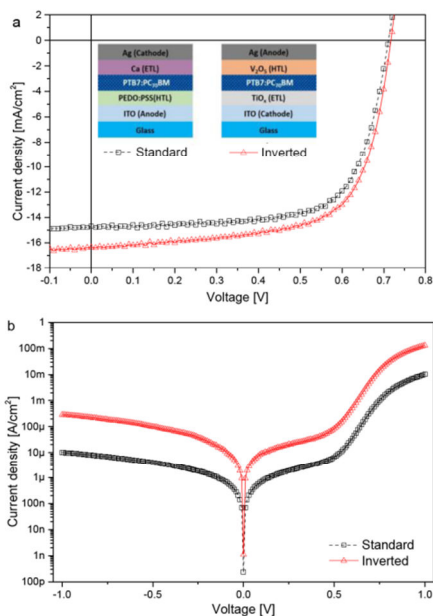


**Figure 1:** Current density – voltage characteristics under a) illumination AM 1.5G spectrum and b) darkness of both structures manufactured.



# Light Emission Statistics as a Local Probe for Structural Phase Switching

N. de Sousa<sup>1</sup>, J.J. Saenz<sup>2</sup>, F. Scheffold<sup>3</sup>, A. García-Martín<sup>4</sup> and L.S. Froufe-Pérez<sup>3</sup>

<sup>1</sup>Departamento de Física de la Materia Condensada, UAM, Spain

<sup>2</sup>Donostia International Physics Center, Spain

<sup>3</sup>Physics Department, Univ. of Fribourg, Switzerland

<sup>4</sup>Instituto de Microelectrónica de Madrid, CSIC, Spain

nuno.teixeira@uam.es

The sensitivity of the spontaneous emission rate of an excited dipolar emitter to the local environment makes single-molecule spectroscopy a unique tool to sense optical and structural properties in its surrounding on the nanoscale. Modification of the emission rate has been reported in literature using well-defined structures, such as metal surfaces [1] or photonic crystals [2]. The increasing interest in the statistical properties of the spontaneous emission rates in complex media [3-6] is justified by their importance for many applications, such as molecular imaging or solar cells.

From a fundamental point of view, the emission rate is proportional to the number of available optical modes at the position of the emitter, i.e. proportional to the electromagnetic local density of states (LDOS)[7]. In random uncorrelated media, the LDOS fluctuations can be explained to some extent by a single scattering statistical model and are dominated by the near-field interaction with the nearest scatterer at the scale of the excluded volume [4]. Temporal lifetime fluctuations can then be correlated to fluctuations in the position of the nearest scatterer and provide a suitable probe for the dynamics of the structure around the emitter. The observed variance of experimental spatial fluctuations of LDOS in random photonic media and lifetime measurements in dense colloidal suspensions of weak scattering particles seem to be consistent with this single-scattering regime. However, the experimental distributions of emission rates in disordered highly scattering dielectrics can present disparate results ranging from non-Gaussian long-tailed statistics with very large decay rates [5], to nearly Gaussian distributions [6]. It can be argued that the differences in the experimentally retrieved decay rate distributions are attributed to effect of multiple scattering between nearby scatterers or long-range spatial correlations between scatterers. In this work we show that the statistics of emission rates in correlated disordered media is extremely sensitive to the details of the radial distribution function around the emitter. We analyze the emission statistics for single emitter embedded in a finite cluster of resonant particles. However, instead of generate random configurations of scatterers, we

compute the emission rates as the system evolves with time under equilibrium conditions. Assuming a standard Lennard-Jones (L-J) interaction between particles, this system is known to present a peculiar solid-liquid-like phase transition at finite temperature: Due to finite-size effects, the two phases cannot coexist at the melting temperature and the whole cluster presents an interesting dynamical behavior, switching between an amorphous solid-like phase and liquid-like phases [8]. This makes it an ideal model system to analyze the effects of local order on the emission rates. In the solid phase at low temperatures, the equilibrium positions are close to those corresponding to a face-centred-cubic (FCC) lattice, and the spectrum of emission rates present a strong chromatic dispersion reminiscent of the band structure of an infinite crystal of resonant dipoles, including spectral windows where the emission is enhanced and pseudo-gaps where it is dramatically inhibited. At the melting temperature, the total scattering cross section of the system does not present significant differences between the two phases while the emission rate jumps following the dynamics of the system. While light scattering measurements would be blind to such dynamical changes, the lifetime statistics would then provide a direct signature of a phase switching behavior.

---

## References

---

- [1] R. Chance, et al. *Adv. Chem. Phys.* 37, 65 (1978).
- [2] P. Lodahl, et al. *Nature* 430, 654 (2004).
- [3] J. Martorell et al. *Phys. Rev. Lett.* 65, 1877 (1990); L. Sapienza et al. *Science* 327, 1352 (2010).
- [4] L.S. Froufe-Pérez, et al. *physica status solidi (a)* 205 (2008).
- [5] R. Sapienza, et al. *Phys. Rev. Lett.* 106, 163902 (2011).
- [6] M. D. Birowosuto, et al. *Phys. Rev. Lett.* 105, 013904 (2010).
- [7] R. Carminati, et al. *Surf. Sci. Rep.* 70, 1 (2015).
- [8] N. de Sousa, et al. *J. of Phys.: Cond. Matt.* 28 (13), 135101.

# Magneto-optical activity in high-index dielectric materials

N. de Sousa<sup>1,2</sup>, L.S. Froufe-Pérez<sup>3</sup>, J.J. Sáenz<sup>2,4</sup>, A. García-Martin<sup>5</sup>

<sup>1</sup>Departamento de Física de la Materia Condensada, UAM, Spain

<sup>2</sup>Donostia International Physics Center, Spain

<sup>3</sup>Physics Department, Univ. of Fribourg, Switzerland

<sup>4</sup>IKERBASQUE, Basque Foundation for Science, Spain

<sup>5</sup>Instituto de Microelectrónica de Madrid, (CNM-CSIC), Spain

nuno.teixeira@uam.es

The magneto-optical response of high-index, non-absorbing dielectric nanospheres is theoretically analyzed. We will show that in these systems the magneto-optical response is fully governed by the magnetic resonances with little effect of the electric ones.

The control of light propagation in the visible and near-infrared domain using resonant systems such as optical nanoantennas has been a matter of intense research during the last decades. The possibility to create and manipulate nanostructured materials encouraged the exploration of new strategies to control the electromagnetic properties with an external agent. A possible approach is combining magnetic and plasmonic materials, where it is feasible to control the optical properties with magnetic fields in connection to the excitation of plasmon resonances [1].

These nanoantennas have been traditionally made of metallic entities, which have the important drawback of a sizeable absorption. In the case of magnetic resonances based on Babinet inverted magnetoplasmonic structures, it has already been demonstrated that the magneto-optical effect has the ability to manipulate magnetic dipole-like resonances [2].

In the last years, there has been a quest for the so-called magnetic resonances in the visible domain [3]. Linked to it, there has been an increasing interest in the use of high index dielectric nanospheres as optical antennas, in particular for their ability to sustain magnetic resonances and the absence of absorption [4-6].

In this work we introduce the magneto-optical effect in the context of those high index dielectric nanospheres, i.e. a silicon nanosphere with a non-negligible of diagonal element in the dielectric

tensor. We will show how the magneto-optical effect is controlled by the internal resonances of the nanosphere, and that the magnetic resonances dominate the spectral dependence of the magneto-optical response, having the electric dipolar resonance a very weak effect. We will establish a clear correlation of the spectral magneto-optical response with the spatial field profile at the interior of the nanosphere that is, in turn, linked to each type of resonance [7].

## References

- [1] Armelles, G., Cebollada, A., García-Martín, A. and González, M. U. "Magnetoplasmonics: combining magnetic and plasmonic functionalities", *Adv. Opt. Materials*, Vol. 1, 10–35, 2013.
- [2] Armelles, G., Caballero, B., Cebollada, A., García-Martin, A. and Meneses-Rodríguez, D., "Magnetic field modification of optical magnetic dipoles" *Nano Lett.*, Vol. 15, 2045–2049, 2015.
- [3] Alu, A. and Engheta, N., "The quest for magnetic plasmons at optical frequencies", *Opt. Express*, Vol. 17, 5723–5730, 2009.
- [4] García-Etxarri, A. et al. "Strong magnetic response of submicron silicon particles in the infrared", *Opt. Express*, Vol. 19, 4815–4826, 2011.
- [5] Schmidt, M. K., Esteban, R., Sáenz, J. J., Suárez-Lacalle, I., Mackowski, S., and Aizpurua, J., "Dielectric antennas - a suitable platform for controlling magnetic dipolar emission," in *Opt. Express*, Vol. 19, 13636- 13650, 2012.
- [6] Person, S., et al., "Demonstration of Zero Optical Backscattering from Single Nanoparticles", *Nano. Lett.* 13, 1806-1809, 2013.
- [7] de Sousa, N., Sáenz, J.J., and Garcia-Martin, A., submitted, 2016.

# Photonic sensors based on molecular gates and plasmonic structures

Biological sensors have been applied in a wide range of applications such as food safety control, medical diagnostics, environmental control or drug discovery. A biosensor consists of a recognition element used to interact with a specific target and a transducer (in our case an optical transducer based on index and colour intensity changes) that can convert this interaction into a quantifiable signal.

This paper presents the development of a low-cost and compact biosensing device. The proposed system combines the advantages of gated porous materials and localized surface plasmons resonances (LSPR). Firstly, arrays of gold nanoparticles are fabricated by e-beam lithography and lift-off process on a glass or silicon substrate in order to create LSPR structure. After that, a porous silica film is dip-coated by a surfactant template method on the LSPR structures. Finally, molecular gates are attached to the porous support: they are capable of being 'opened' or 'closed' when certain external stimuli are applied allowing the release of previously entrapped cargo (colored or fluorescent materials) in the porous. [1]. The sensing scheme in Fig 1 is based on detecting the change of color/fluorescence of the device. For this purpose, Rhodamine B was

introduced in the porous substrate. The pores were grafted with a suitable hapten able to recognize antibodies prepared for the recognition of finasteride, capping the pores and inhibiting dye release. Fig. 2 shows the shift of the resonance of the plasmonic structure when surrounding environment indices change due to the colorant realizing. Sensitivity values of 500-800 nm per refractive index unit has been obtained by using plasmonic dimer resonant structures, which give rise to very large field enhancement in their gap region [2] [3].

## References

- [1] F. Sancenón, L.Pascual, M.Oroval, E.Aznar, R.Martínez-Mañez, Chemistry Open, 4 (2015) 418-437.
- [2] G.Bi, W.Xiong, L.Wang, K.Ueno, H.Misawa, J.Qiu, Optics Communications, 285 (2012) 2472-2477.
- [3] C. Tsai, J. Lin, C. Wu, P. Lin, T. Lu, P. Lee, Nano Letters, 12 (2012) 1648-1654.

## Figures

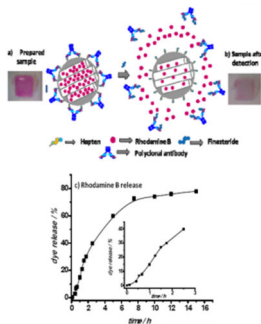


**Figure 1:** Representation of a gated porous support and its behavior for finasteride sensing.

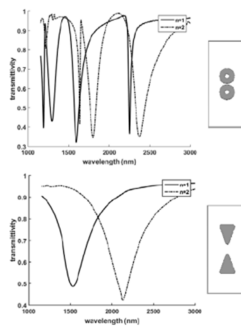


**Figure 2:** LSPR structures and numerical simulations of the transmission spectra for different surrounding medium indices.

# Integration of metal nanoparticles in polymer waveguides: enhancement and redirection of light in photonic structures

**M. Signoretto**<sup>1</sup>, I. Suárez<sup>1</sup>, N. Zink-Lorre<sup>2</sup>, E. Font-Sanchis<sup>2</sup>, A. Sastre-Santos<sup>2</sup>, Fernando Fernandez-Lázaro<sup>2</sup>, R. Abargues<sup>3</sup>, P. Rodríguez-Cantó<sup>3</sup>, V. Chirvony<sup>1</sup> and J. Martínez-Pastor<sup>1</sup>

<sup>1</sup>ICMUV, University of Valencia, Spain

<sup>2</sup>Área de Química Orgánica, Instituto de Bioingeniería, Universidad Miguel Hernández de Elche, Spain

<sup>3</sup>Intenanomat S.L, Spain

sigmatt@uv.es

Metal nanoparticles (MNPs) are potential candidates to provide novel functionalities in photonic devices [1]. Their exotic optical properties, derived from the highly localized surface plasmon polariton (LR-SPP), can be applied in unusual optical applications, such as the redirection photons or the confinement of the electromagnetic energy in the nanoscale. In this way, these nanostructures have been successfully exploited in several optoelectronic devices, like solar cells [2], optical sensors [3] or subwavelength waveguides [4]. Here we propose suitable technologies to incorporate MNPs in optical architectures compatible with planar organic polymer photonics. Then, their interesting optical properties were used to construct integrated light coupler, or to demonstrate the enhancement of light by a photon-plasmon coupling effect.

In a first approach we propose a novel technology able to grow in situ Au MNPs embedded in the commercially available resist Novolak (NV) [5]. As a consequence, the intensity and position of the plasmonic resonance can be easily tuned in a controllable way by the size of the nanostructures and their concentration into the host matrix. In addition, since NV is a commercially available resist suitable for e-beam or UV lithography, the nanocomposite can be easily patterned facilitating its incorporation in photonic structures. A second approximation consisted of depositing pre-prepared MNPs (ex-site growth) into the polymer waveguide by a simple drop casting technique. Fabrication parameters were carefully controlled to obtain a good homogeneity and to control the concentration of nanostructures on the surface.

Once these technologies were optimized, layers (or patterns) of MNPs were integrated in optical waveguides by depositing the nanostructures on a SiO<sub>2</sub>/Si substrate, and then capping with a PMMA

layer [5]. Then, optical properties of the MNPs were successfully applied for different purposes. For example, high scattering cross section of MNPs was exploited to demonstrate coupling of normally incident light into the PMMA waveguide. The couplers exhibited a broad wavelength range (400-780 nm) and efficiencies larger than 1 % measured at the output edge of the waveguide structure [5].

In addition, the interaction of MNPs with organic dyes embedded in the PMMA waveguide was studied in order to enhance their emission of photoluminescence (PL) by a photon-plasmon coupling effect [6]. When the gap between the optical emitters and the MNPs was carefully optimized, the high intensity near electromagnetic field of the MNP induced a tenfold enhancement of the light emitted by the dye.

## References

- [1] P. Mulvaney, *MRS Bull* (2001) 1009-1014.
- [2] Y.A. Akimov, Koh W. S. and Ostrikov K., *Opt. Express*, 17, no. 12 (2009) 10195-10205.
- [3] R. Abargues, P. J. Rodríguez-Cantó, S. Albert, I. Suárez and J.P. Martínez-Pastor, *Journal of Materials Chemistry C*, 2 (2014) 908-915.
- [4] Maier S. A., Kik P. G., Atwater H. A., Meltzer S., Harel E., Koel B. E. and Requicha A. A., *Nature*, 2 (2003) 229-232.
- [5] Signoretto M., Suárez I., Chirvony V. S., Abargues R., Rodríguez-Cantó P. J., and Martínez-Pastor J., *Nanotechnology*, 26, no. 47 (2015) 475201-475210.
- [6] Yeechi Chen, Keiko Munechika, and David S. Ginger, *Nano Lett.* 7, No. 3 2007 (2007) 690.
- [7] R. R. Chance, A. Prock, and R. Silbey, *J. Chem. Physics* 60, No.7 (1974) 2744.

# Periodic arrangements of Si quasi-spheres

**Magdalena Solà**, Ramón Alcubilla,  
Moisés Garín\*

Departament d'Enginyeria Electrònica,  
Universitat Politècnica de Catalunya, Spain

\*moises.garin@upc.edu

Silicon photonics has gained increasing interest in recent years as it promises high performance, cost-effective integrated optical devices. The advent of Si fabrication techniques at the micro and nano-scales, in conjunction with the interesting optical properties of this material, such as its high refractive index, has enabled the development of new methods of light confinement, which allows them to behave as excellent resonators with ultra-high quality factors.

In particular, Si microspheres offer a great potential for sunlight harvesting applications [1,2] since they can exhibit absorption cross sections higher than one in the visible, and boost absorption at the bandgap edge at wavelengths above 1200 nm. Indeed, a PV device was recently reported in single  $\mu\text{-Si}$  microspheres, with diameters in the range 1–3  $\mu\text{m}$ , showing experimentally the band-to-band resonant absorption enhancement in the NIR frequencies up to  $\lambda=1600$  nm.

There are already a few methods that allow to produce silicon microspheres with sizes in the micrometer range. One of the most promising methods is the synthesis in gas phase by CVD [3]. This method, which can be potentially scaled for mass production, allows for the production of amorphous and polycrystalline Si particles in the size range 0.5–8  $\mu\text{m}$  and with exceptional spherical and surface quality. However, the fabrication of monocrystalline particles with controlled size, and the ability to precisely control the distribution over a surface still remains a challenge. In this poster we present a material consisting of high-quality monocrystalline silicon quasi-spheres with a controlled size and distribution over the surface. This material offers high possibilities in any field where light managing plays an important role, such as photovoltaics and photodetectors.

## References

- [1] M. Garín, R. Fenollosa, R. Alcubilla, L. Shi, L.F. Marsal, & F. Meseguer, *Nature communications* 5 (2014) 3440.
- [2] M. Garín, R. Fenollosa, P. Ortega, and F. Meseguer, *J. Appl. Phys.* 119 (2016) 033101.
- [3] R. Fenollosa, F. Meseguer, and M. Tymczenko *Adv. Mater.* 20 (2008) 95–98.

## Figures

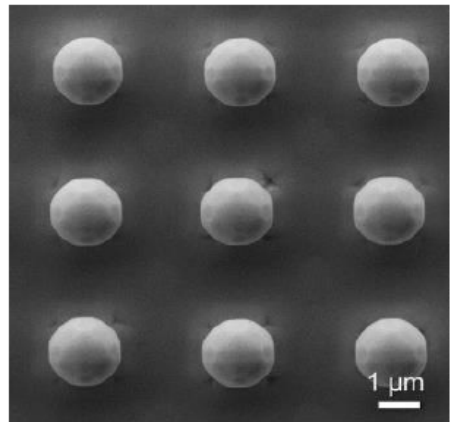


**Figure 1:** SEM image, top view, of a square array of monocrystalline silicon quasi-spheroids.

# Optical spectroscopy of metallic nanoparticles: classical versus quantum description

M. Urbieto<sup>1,2,3</sup>, M. Barbry<sup>1</sup>, Y. Zhang<sup>1</sup>, P. Koval<sup>1,2</sup>, D. Sánchez-Portal<sup>1,2</sup>, N. Zabala<sup>1,2,3</sup> and J. Aizpurua<sup>1,2</sup>

<sup>1</sup>CFM-MPC, Centro Mixto CSIC-UPV/EHU, Spain

<sup>2</sup>Donostia International Physics Center, Spain

<sup>3</sup>Department of Electricity and Electronics, FCT/ZTF, UPV/EHU, Spain

mattin.urbieto@ehu.es

Progress in nanotechnology has allowed control of metallic nanoparticles at the nanometer and even subnanometer scale. Some of the most fascinating properties and applications of plasmonic nanoparticles are based on the tunability of their optical response and their ability to localize the electromagnetic fields around tips or at inter particle gaps. The near-fields are commonly addressed theoretically within classical frameworks. However, in some situations the atomic structure needs to be considered to correctly determine the response of the nanosystem [1].

In this work we study the far- and near-field response of Na icosahedral nanoparticles and compare three different models. i) First, we use a classical modeling within a boundary element method (MNPBEM) [2-3], which considers abrupt boundaries between media and incorporates homogeneous and isotropic dielectric functions to solve Maxwell's equations. At the particle size considered (around 1.5 nm) the mean free path of the electrons is comparable to the size of the particles considered, so the billiard model is used to account for surface scattering effects [4], with the resulting increase of damping in the dielectric function. ii) Secondly, we consider a discrete dipole approximation (DDA), in which each atom of the nanoparticle is described as a dipole [5] and the atomistic structure is preserved. iii) Finally, our results are compared with atomistic ab-initio time-

dependent density functional theory (TDDFT) calculations [1].

We show that the general patterns of subnanometric localization and enhancement of fields can effectively be approached by classical means. The presence of tips and sharp endings in the geometry of the particle introduces a major enhancement and localization of the near-fields. Nevertheless, for the case of close particle dimers, differences arise due to the lack of quantum tunneling effects in the classical descriptions. In Figure 1) we show the near-field enhancement and the absorption cross section for a dimer of sodium icosahedral particles of radius 1.6 nm, as calculated in the classical BEM model.

## References

- [1] M. Barbry, P. Koval, F. Marchesin, R. Esteban, A. G. Borisov, J. Aizpurua, D. Sánchez-Portal, *Nano Lett.*, 15 (2015) 3410-3419.
- [2] U. Hohenester, A. Trügler, *Comput. Phys. Commun.*, 183 (2012) 370-381.
- [3] F. J. García de Abajo, A. Howie, *Phys. Rev. B*, 65 (2002) 115418.
- [4] A. Moroz, *J. Phys. Chem. C*, 112 (2008) 10641-10652.
- [5] L. L. Jensen, L. Jensen, *J. Phys. Chem. C* 2008 112 (40), 15697-15703; L. L. Jensen, L. Jensen *J. Phys. Chem. C* 2009 113 (34), 15182-15190.

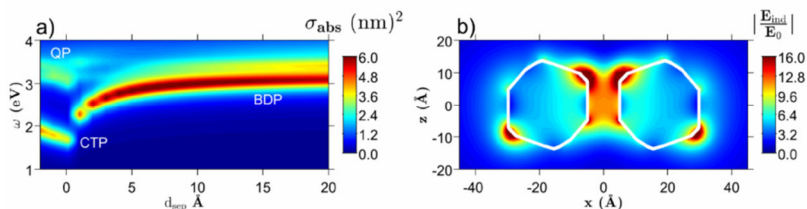


**Figure 1:** a) Absorption cross section of a facet-to-facet configuration of a Na icosahedral dimer for varying separation distances. The circumscribed radius of the icosahedral particles is  $r = 1.6$  nm and the polarization of the external field parallel to the dimer axis. b) Field enhancement for a separation distance of  $d_{sep} = 1$  nm at energy corresponding to the bonding dimer plasmon (BDP) shown in plane a).

# Femtosecond dynamics at the nanoscale: talking to antenna complexes one-by-one

Niek F. van Hulst

ICFO—Institut de Ciències Fotòniques, The Barcelona Institute of Science and Technology, ICREA—Institutió Catalana de Recerca i Estudis Avançats, Spain

Niek.vanHulst@ICFO.eu

Nature has developed photosynthesis to power life. Nanoscale networks of light harvesting antennas capture the sunlight to funnel the photonic energy towards reaction centres. Surprisingly, despite the complexity and ambient conditions, quantum coherences are observed in the energy transfer of antenna complexes, even at room temperature. Does nature exploit quantum concepts? Does the coherence help to find an optimal path for robust or efficient transfer? How are the coherences sustained? What is their spatial extent in a real light-harvesting network?

Specializing on femto-nanophotonics we aim to look ultrafast into the nanoscale, to see molecules in action. Addressing the antenna complex of purple bacteria, we have found glimpses of coherent oscillations of a single photo-synthetic complex, moreover non-classical photon emission of individual antenna complexes. These results, pave the way to address photosynthetic networks in real nano-space and on femtosecond timescale. We address the transport mechanism between adjacent light-harvesting complexes in tubular crystal sheets with few picosecond temporal resolution, to track the coherent light path in such photosynthetic networks. For spatial control, the single complexes are brought in the near field of optical resonant antennas for nanoscale excitation and enhancement of the emission with full command of rates and polarization. With state-of-the-art antenna fabrication the excitation can be confined to 10 nm scale, while the emission can be enhanced up to 1000 times for a single molecule close to an antenna hotspot.

In conclusion I hope to apprise the CEN2016 audience as to the potential of nano-femto tools

This work is supported by ERC Adv.Grants 247330-NanoAntennas and 670949-LightNet; FP7-NanoVista 288263; Marie-Curie International COFUND Fellowships; MINECO Grant FIS2012-35527; Catalan AGAUR 2014 SGR01540; Severo Ochoa grant SEV2015-0522; Fundació CELLEX Barcelona.

## References

- [1] Lukasz Piatkowski, Nicolò Accanto, Niek F van Hulst, "Ultrafast meets Ultrasmall: Controlling Nanoantennas and Molecules", ACS Photonics 3, (2016).
- [2] Emilie Wientjes, Jan Renger, Richard Cogdell, Niek van Hulst, "Pushing the Photon Limit: Nanoantennas Increase Maximal Photon Stream ", J.Phys.Chem.Lett. 7, 1604 (2016).
- [3] Lukasz Piatkowski, Esther Gellings and Niek van Hulst, "Broadband Single Molecule Excitation Spectroscopy", Nature Communications 7:10411 (2016).
- [4] Emilie Wientjes, Jan Renger, Alberto Curto, Richard Cogdell, Niek van Hulst, "Antenna-enhanced fluorescence of single LH complex shows photon anti-bunching". Nature Comm. 5: 4236 (2014).
- [5] Richard Hildner, Daan Brinks, Richard Cogdell, Niek F. van Hulst, Quantum coherent energy transfer over varying pathways in single light-harvesting complexes. Science 340, 1448-1451 (2013).

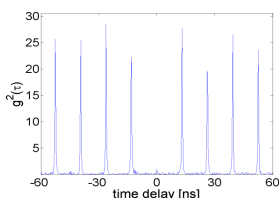


**Figure 1:** Light harvesting antenna complex (LH2) of purple bacteria shows anti-bunching ( $g^{(2)}(0)=0$ ), i.e. non classical photon statistics and single photon emission character.

# Influence of Annealing for Enhancing Second-Order Nonlinearity in Strained Silicon

Steven Van Roye, Irene Olivares,  
Pablo Sanchis\*

Nanophotonics Technology Center, Universitat  
Politécnica de València, Spain

\*pabsanki@ntc.upv.es

Second-order optical nonlinearity can be induced in silicon (Si) by breaking the crystal symmetry with a straining layer [1,2]. The influence of annealing for enhancing the nonlinearity by means of a silicon nitride (SiN) layer is investigated. The annealing process has been simulated taking into account different begin temperatures to room temperature. Furthermore, the influence of the intrinsic stress and thickness of the SiN layer has also been analyzed. To start with, SiN deposited on top of a Si substrate was considered and the stress when crossing the interface was obtained. Figure 1(a) shows that the stress in the Si ( $y > 0$ ) is zero and increases in a small layer around the interface to the intrinsic stress 1.2 GPa of the SiN ( $y < 0$ ). Whenever an annealing step is performed, both the stress in the Si and in the SiN increases, but the increase in the SiN is larger than in the Si. Therefore, a higher begin temperature of annealing leads to higher stress around the interface. Next, a figure of merit (FOM) has been defined as the normalized overlap integral over the waveguide core between the electric field intensity and partial derivatives of the strain components, since the value of this FOM will be proportionate with the induced nonlinearity. The dimensions of the waveguide (height = 220 nm, width = 400 nm) were optimized in previous work [3]. From the simulations, it was found that the FOM for TE was ten times larger than the one for TM, therefore only the TE is considered here. Figure 1(b) shows the FOM as a function of the begin temperature of

annealing for a SiN-thickness of 500 nm and 700 nm. In the latter, the FOM is slightly larger than in the former, although the difference is quite small. We also see that an annealing procedure starting from a higher temperature leads to a higher FOM and therefore to a larger non-linearity. In Figure 1(c), the FOM is plotted as a function of begin temperature of annealing for a 700 nm SiN-layer, but the intrinsic stress of this layer is changed from 1.2 GPa (as before) to 10 MPa and to -1.2 GPa. The case of 10 MPa shows the same behaviour as the case of 1.2 GPa, but the FOM is significantly smaller. For -1.2 GPa, the FOM at room temperature is equal to the 1.2 GPa case, but performing an annealing step leads to a lower FOM. As a conclusion, a combination of annealing and compressive intrinsic stress of the SiN layer will be beneficial to enhance the induced second-order optical nonlinearity in silicon.

## References

- [1] R. Jacobsen et al., Nature 441(7090), 199–202 (2006).
- [2] M. Cazzanelli et al., Nat. Mater. 11(2), 148–154 (2011).
- [3] I. Olivares, T.I. Angelova, E. P.-Cienfuegos, P. Sanchis, SPIE Photonics Europe, Brussels (Belgium), 2016.

## Figures

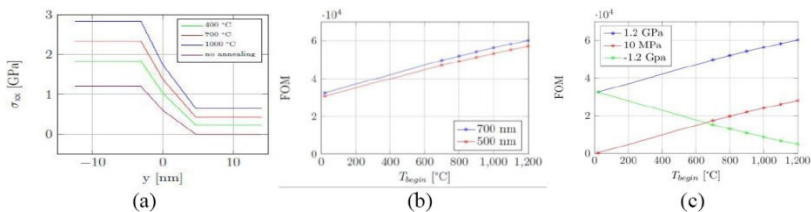


**Figure 1:** (a) Stress  $\sigma_{xx}$  as a function of distance perpendicular to the interface for no annealing, 400°C, 700°C and 1000°C (from bottom to top), (b) FOM as a function of begin temperature of annealing for 500 nm and 700 nm SiN –layer, (c) FOM as a function of begin temperature of annealing for different intrinsic stresses of the SiN.



## New Materials for Multifunctional Photonic ICs

**D. Van Thourhout**<sup>1,3</sup>, Z. Wang<sup>1,3</sup>, B. Tian<sup>1,3</sup>,  
Y. Shi<sup>1,3</sup>, M. Pantouvaki<sup>4</sup>, C. Merckling<sup>4</sup>, Y.  
Hu<sup>1,3</sup>, I. Asselberghs<sup>4</sup>, S. Brems<sup>4</sup>, L.  
Abdolahi<sup>1,3</sup>, C. Alessandri<sup>4</sup>, J.P. George<sup>2,3</sup>, J.  
Beeckman<sup>2,3</sup>, H. Min-Hsiang<sup>4</sup>, P. Absil<sup>4</sup>, J. Van  
Campenhout<sup>4</sup>

<sup>1</sup>Photonics Research Group, INTEC, Belgium

<sup>2</sup>Department of Electronics and Information  
Systems, Belgium

<sup>3</sup>Center for Nano- and Biophotonics, Ghent  
University, Belgium

<sup>4</sup>IMEC, Leuven, Belgium

dries.vanhourhout@ugent.be

In this presentation we will report on our recent work on new materials that can be monolithically integrated on high-index contrast silicon or silicon nitride photonic ICs to enhance their functionality. This includes InP and InGaAs epitaxially grown on silicon for realizing efficient lasers [1-5], graphene and other 2D-materials for realizing compact electro-absorption modulators and non-linear devices [6-7] and ferroelectric materials for realizing phase modulators [8].

---

### References

---

- [1] M. Paladugu, C. Merckling, R. Loo, O. Richard, H. Bender, J. Dekoster, W. Vandervorst, M. Caymax, and M. Heyns, "Site selective integration of III-V materials on Si for nanoscale logic and photonic devices," *Cryst. Growth Des.*, vol. 12, no. 10, pp. 4696–4702, 2012.
- [2] C. Merckling, N. Waldron, S. Jiang, W. Guo, N. Collaert, M. Caymax, E. Vancoille, K. Barla, A. Thean, M. Heyns, and W. Vandervorst, "Heteroepitaxy of InP on Si (001) by selective-area metal organic vapor-phase epitaxy in sub-50 nm width trenches: The role of the nucleation layer and the recess engineering," *J. Appl. Phys.*, vol. 115, p. 023710, 2014.
- [3] Z. Wang, B. Tian, M. Paladugu, M. Pantouvaki, N. Le Thomas, C. Merckling, W. Guo, J. Dekoster, J. Van Campenhout, P. Absil, and D. Van Thourhout, "Polytypic InP nanolaser monolithically integrated on (001) silicon," *Nano Lett.*, vol. 13, no. 11, pp. 5063–9, Nov. 2013.
- [4] B. Tian, Z. Wang, M. Pantouvaki, W. Guo, M. Clement, and J. Van Campenhout, "InP Nanowire lasers Epitaxially Grown on (001) Silicon 'V-groove' templates," in *IPRM 2014*, paper Thu-B1–4.
- [5] Z. Wang, B. Tian, M. Pantouvaki, W. Guo, P. Absil, J. Van Campenhout, C. Merckling, and D. Van Thourhout, "Room Temperature InP DFB Laser Array Directly Grown on (001) Silicon," <http://arxiv.org/abs/1501.03025>, Jan. 2015.
- [6] Y. Hu, M. Pantouvaki, J. Van Campenhout, S. Brems, I. Asselberghs, C. Huyghebaert, P. Absil, D. Van Thourhout, "Broadband 10 Gb/s operation of graphene electro-absorption modulator on silicon," *Laser & Photonics Reviews*, 10(2), p.307-316 (2016).
- [7] K. Alexander, Y. Hu, M. Pantouvaki, S. Brems, I. Asselberghs, S.-P. Gorza, C. Huyghebaert, J. Van Campenhout, B. Kuyken, D. Van Thourhout, "Electrically Controllable Saturable Absorption in Hybrid Graphene-Silicon Waveguides", accepted for publication in *Conference on Lasers and Electro-Optics (CLEO)*, United States, 2015.
- [8] J. George, J. Beeckman, W. Woestenborghs, P.F. Smet, W. Bogaerts, "Preferentially oriented BaTiO3 thin films deposited on silicon with thin intermediate buffer layers", *Nanoscale Research Letters*, 8, p.1-7 (2013).

It is well known that a light beam can be characterized by means of several dynamical properties such as energy, momentum or angular momentum (AM). The latter can be decomposed into two distinct contributions: the spin AM and the orbital AM. Whereas the orbital AM is related with the spatial field distribution, the origin of the spin AM is associated with the circular polarization of the light beam. Traditionally, spatial and intrinsic polarization features have been treated separately. However, at the subwavelength scale, it appears a broad class of phenomena dealing with the interaction between the polarization and the spatial degrees of freedom: the optical spin-orbit interaction (SOI). It has been shown that most of the basic optical processes rely on SOI, thus forcing to review all the fundamental optical phenomena by considering this new perspective [1].

In this work, we report theoretically the emergence of a pattern associated with the spin of light that arises from the superposition of two arbitrarily polarized electromagnetic planewaves [2, 3]. In particular, by assuming two light beams with the same circular polarization (helicity) state, we can

observe high correlations between the typical distribution of the energy density (bright and dark fringes) and the light spin localization pattern (fig. 1A). Furthermore, we find configurations where the main contribution of the spin is transverse out-of-plane (fig. 1B), which is independent of the wave helicity and crucial to understand plasmonic propagation, or the spin-momentum locking effect. This findings provide new avenues to gain further comprehension on the interpretation of the “double-slit experiment”.

## References

- [1] K. Y. Bliokh, F. J. Rodríguez-Fortuño, F. Nori, A. V. Zayats, Spin-orbit interaction of light, *Nature Photonics* 9, 796–808 (2015).
- [2] A. Y. Bekshaev, K. Y. Bliokh, F. Nori, Transverse Spin and Momentum in Two-Wave Interference, *Phys. Rev. X* 5, 011039 (2016).
- [3] N. F. Kubrakov, Interference of Plane Light Waves with Different Polarizations and the Jones Matrix Formalism, *Optics and Spectroscopy* 117, 814–821 (2014).

## Figures

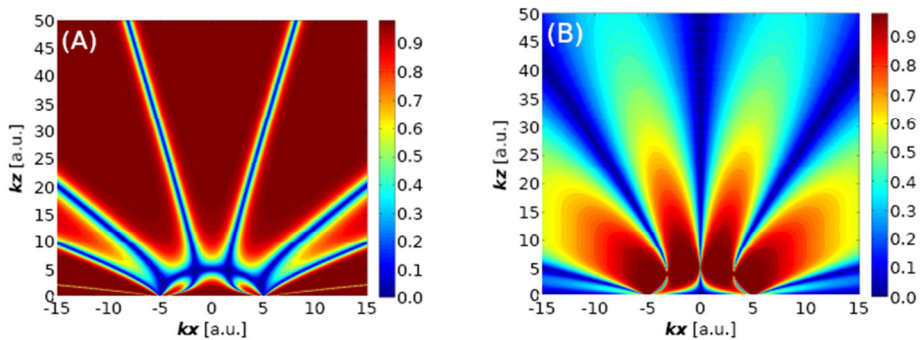


Figure 1: Spin angular momentum (SAM) of light resulting from the interference of two circularly polarized plane waves having equal (A) and mirror-symmetric (B) polarization states.

# Photoluminescent porous alumina particles for the development of label-free biomarkers

**Elisabet Xifre-Perez**, Chris Eckstein, Josep Ferré-Borrull, Josep Pallarès, Lluís F. Marsal\*

Departament d'Enginyeria Electrònica, Elèctrica i Automàtica, Universitat Rovira i Virgili, Spain

elisabet.xifre@urv.cat

\*lluís.marsal@urv.cat

Particles in the micrometric and nanometric range have attracted great interest in recent years especially because of their interesting properties for biotechnological applications [1,2]. Porous anodic alumina can be an excellent material for the formation of these particles. Porous alumina is obtained by the electrochemical etching of highly-pure aluminum and consists of nanometric pores hexagonally arranged in an alumina matrix. Its geometric characteristics, such as pore size, inter-pore distance, porosity, and thickness, can be controlled by the anodization conditions (voltage and time of anodization, temperature, and acid used as electrolyte, etc.) [3]. Therefore, we are able to tune the porous morphology of porous alumina to meet the requirements of its very diverse applications. The physical, chemical and optical properties of this material together with its nontoxicity, its highly stable morphology in buffer solutions and its cost-effective fabrication [4] makes of porous alumina an interesting material for the development of particles for biological applications. Especially remarkable is its high effective surface area, that can be chemically modified with organic compounds [5]. Furthermore, another singular characteristic distinguishes porous alumina from many other materials: its inherent photoluminescence in the visible spectrum range (Figure 1). In this work, we present porous alumina particles and evaluate their properties for the development of label-free biomarkers and also for a

wide range of applications in the biomedical and biotechnological fields.

**Acknowledgements:** This work was supported in part by the Spanish Ministry of Economy and competitiveness TEC2015-71324-R, the Catalan authority AGAUR 2014SGR1344, ICREA under the ICREA Academia Award.

## References

- [1] E. Xifre-Perez, J. Ferré-Borrull, J. Pallarès, L.F. Marsal, *Mesoporous Biomater.*, 2 (2015) 13.
- [2] M.H. El-Dakdouki, E. Puré, X. Huang, *Nanoscale*, 5 (2013) 3895.
- [3] A. Santos, M. Alba, M.M. Rahman, P. Formentin, J. Ferré-Borrull, J. Pallarès, L.F. Marsal, *Nanoscale Res. Lett.*, 7 (2012) 228.
- [4] K.E. La Flamme, K.C. Popat, L. Leoni, E. Markiewicz, T.J. La Tempa, B.B. Roman, C. A. Grimes, T. A. Desai, *Biomaterials*, 28 (2007) 2638.
- [5] K.C. Popat, G. Mor, C. A. Grimes, T. A. Desai, *Langmuir*, 20 (2004) 8035.
- [6] E. Xifre-Perez, S. Guaita-Esteruelas, M. Baranowska, J. Pallarès, L. Masana, L.F. Marsal, *ACS Appl. Mater. Interfaces*, 7 (2015) 18600.

## Figures

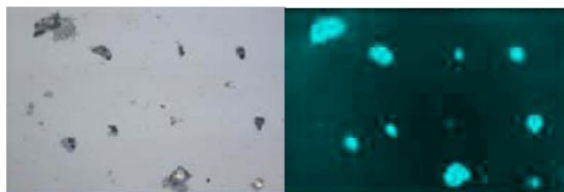


**Figure 1:** Photoluminescent porous alumina particles: white light (left), DAPI filter (right).

# Ultrafast control of plasmonic nanoantennas driven by hot-spot induced phase-transition in VO<sub>2</sub>

N. Zabala<sup>1,2</sup>, L. Bergamini<sup>1,2</sup>, Y. Wang<sup>3</sup>, J. M. Gaskell<sup>4</sup>, C. H. de Groot<sup>3</sup>, D. W. Sheel<sup>4</sup>, Otto L. Muskens<sup>3</sup> and J. Aizpurua<sup>2</sup>

<sup>1</sup> Department of Electricity and Electronics, UPV/EHU, Spain

<sup>2</sup> CFM, CSIC-UPV/EHU and DIPC, Spain

<sup>3</sup> Faculty of Physical Sciences and Engineering, University of Southampton, UK

<sup>4</sup> Materials and Physics Research Centre, University of Salford, UK

neraa.zabala@ehu.eus

Efficient and reversible switching of plasmonic modes at Vis and NIR wavelengths is one of the key desirable properties for tunable devices [1]. Phase-transition materials offer technologically relevant opportunities as they can provide notable changes in the dielectric response [2]. So far most studies have reported the effects of a global phase transition of these materials on the plasmonic response of nanoparticles and metamaterials. Unlike chalcogenide phase-transition materials which offer slow, rewritable memory functionality at relatively high temperatures, vanadium dioxide (VO<sub>2</sub>) provides an ultrafast, reversible phase-transition at only modestly elevated temperatures around 68°C [3].

In this work, we exploit for the first time resonant pumping and nanometer-scale plasmonic hot-spots to induce an optical change of the nanoantenna (NA) response through highly localized phase-transitions in the underlying substrate [4]. Multifrequency crossed gold antenna arrays were fabricated on top of high-quality VO<sub>2</sub> films (NA-VO<sub>2</sub> hybrids). Optical experiments show that fully reversible switching of antenna resonances at the picosecond timescale are possible using resonant pumping schemes. Simulations revealed that the

change in optical response of the antennas stems from the change in dielectric properties of VO<sub>2</sub> regions neighboring the NAs. Moreover, it is demonstrated that the phase transition mediated by local pumping of a plasmon resonance does not influence the resonance of a perpendicular NA positioned less than 100 nm away from the modulated antenna.

The nanoantenna-VO<sub>2</sub> hybrids enable new directions in all-optical ultrafast switching at picoJoule energy levels, and open up the possibility for plasmonic memristor-type devices exploiting nanoscale thermal memory.

## References

- [1] J. A. Schuller, et al., *Nature Mater.* 9, 193 (2010).
- [2] Z. Yang, and S. Ramanathan, *IEEE Phot. J.* 7, 0700305 (2015).
- [3] M. M. Qazilbash, et al., *Science* 318, 1750 (2007).
- [4] O. L. Muskens, et al., *Light Sci. Appl.*, submitted.

## Figures

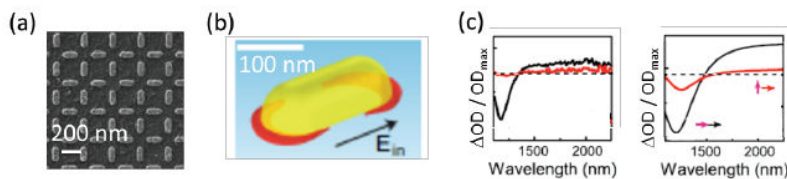


**Figure 1:** (a) Example of a fabricated NA-VO<sub>2</sub> hybrid. (b) Simulated 68°C isosurfaces showing the phase-switched hot-spots around the nanoantennas generated by resonant pumping. (c) Difference in the OD of the antennas, induced by the hot-spots of (b), for both (black curves) parallel and (red curves) perpendicular pump-probe polarization. (left) Experiments and (right) simulations.

# Optical response and electron dynamics of charged plasmonic nanoparticles

Mario Zapata Herrera<sup>1</sup>, Andrei G. Borisov<sup>2</sup>, Andrey K. Kazansky<sup>3</sup> and Javier Aizpurua<sup>1</sup>

<sup>1</sup>Materials Physics Center CSIC-UPV/EHU and Donostia International Physics Center, Spain

<sup>2</sup>Institut des Sciences Moléculaires d'Orsay, UMR 8214 CNRS-Université Paris-Sud, France

<sup>3</sup>KERBASQUE, Basque Foundation for Science, Spain

mario\_zapata001@ehu.es

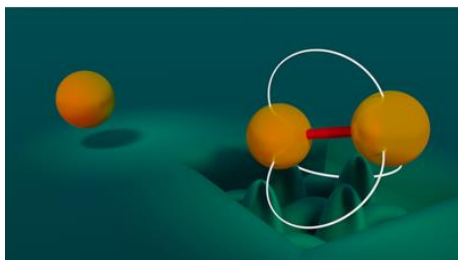
There is a continuous effort in the plasmonics community to achieve a control of the optical response of metallic nanostructures via a proper design of their morphology [1, 2]. However, in the last years there has been an increasing interest in obtaining an active control of the response by application of external bias, or polarizing fields [3]. The modulation of the plasmon resonances in this active fashion has been recently achieved in electrochemistry by adding chemical reductants to the colloidal nanoparticle solution [4-6]. Similarly to the situation in 2D materials, such as graphene [7-9], the observed shift of the plasmon frequency has been often interpreted also in 3D particles as a result of the charge doping of the nanoparticles. Based on a full quantum mechanical description, we review this long-standing misconception in electrochemistry.

In this work, we study the electron dynamics and plasmon modes of small charged metallic clusters in vacuum with use of density functional theory (DFT) and time-dependent density functional theory (TDDFT) calculations. We obtain the electronic structure and trace the dynamics of well-defined nanoparticle clusters that allow to isolate and identify the effects of pure charging in the optical response of metallic nanostructures, with respect to the action of an external polarization or chemical effects. In particular, we show that the frequency shift of the plasmon mode is generally small when a nanoparticle is charged, and this shift has an opposite sign to that expected from the arguments based on the change of bulk electron density. Our results can be well understood based on the theory of dynamical screening [10-12] to describe the dependence of the dipolar plasmon resonance on the nanoparticle size. We also demonstrate that for negatively charged clusters, as soon as the Fermi level is promoted above the vacuum level, the extra charge decays at femtosecond (fs) time scales. Despite the small size of the systems considered in our model calculations (~5 nm in diameter), our results can be generalized to the case of larger nanoparticles as those commonly treated in

electrochemistry. Counterintuitively, these results reveal that the plasmon energy shifts observed in electrochemical solutions of plasmonic nanoparticles cannot be explained without considering the effect of the dipole layer formed by the ions that screen the nanoparticle charge and the eventual modification of the surface electronic structure of the metal nanoobject by the chemisorbed species.

## References

- [1] Boardman, A. D.; Grimalsky, V. V.; Kivshar, Y. S.; Koshevaya, S. V.; Lapine, M.; Litchinitser, N.M.; Malnev, V. N.; Noginov, M.; Rapoport, Y. G. and Shalaev, V. M. *Laser. Photon. Rev.*, 10 (2010) 00012.
- [2] Liu, A. Q.; Zhu, W. M.; Tsai, D. P.; and Zheludev, N. I. *J. Opt.*, 14 (2012) 114009.
- [3] Chu, K. C.; Chao, C. Y.; Chen, Y. F.; Wu, Y. C.; Chen, C. C. *Appl. Phys. Lett.*, 89 (2006) 103107.
- [4] Dondapati, S. K.; Ludemann, M.; Müller, R.; Schwieger, S.; Schwemer, A.; Handel, B.; Kwiatkowski, D.; Djiango, M.; Runge, E.; Klar, T. A., *Nano Lett.*, 12 (2012) 1247–1252.
- [5] Mulvaney, P.; Perez-Juste, J.; Giersig, M.; Liz-Marzán, L. M.; Pecharroman, C. *Plasmonics*, 1 (2006) 61–66.
- [6] Daniels, J. K.; Chumanov, G., *J. Electroanal. Chem.*, 575 (2005) 203–209.
- [7] Ju, L.; Geng, B.; Horng, J.; Girit, C.; Martin, M.; Hao, Z.; Bechtel, H. A.; Liang, X.; Zettl, A.; Shen, Y. R.; Wang, F., *Nat. Nanotechnol.*, 6 (2011) 630–634.
- [8] Grigorenko, A. N.; Polini, M.; Novoselov, K. S. *Nat. Photonics.*, 6 (2012) 749–758.
- [9] Manjavacas, A.; García de Abajo, F. J. *Nat. Commun.*, 5 (2014) 3548.
- [10] Apell, P.; Ljungbert, Å., *Solid State Commun.*, 44 (1982) 1367–1369.
- [11] Liebisch, A, *Phys. Rev. B: Condens. Matter Mater. Phys.*, 48 (1993) 11317–11328.
- [12] Monreal, R. C.; Antosiewicz, T. J.; Apell, S. P. *New J. Phys.*, 15 (2013) 083044.



## Cover image credit

**J. Luis-Hita**, J.J. Sáenz, M.I. Marqués  
Arrested dimer's diffusion by self-induced  
back-action optical forces, *ACS Photonics*,  
DOI: [10.1021/acsp Photonics.6b00259](https://doi.org/10.1021/acsp Photonics.6b00259)



---

Edited by



Phantoms Foundation

Alfonso Gómez 17  
28037 Madrid – Spain

[info@phantomsnet.net](mailto:info@phantomsnet.net)  
[www.phantomsnet.net](http://www.phantomsnet.net)

---